Unlocking the Hidden Potential of Cobalt: Hydrodeoxygenation of Aromatic Ketones by Cobalt Clusters

by

Aukse Braziunaite

A thesis submitted in partial fulfillment of the requirements for the degree of

Master of Science

Department of Chemistry
University of Alberta

Abstract

Cobalt phosphoranimide clusters $[Co(NPPh_3)(OSiMe_3)(THF)]_2$, $[Co(NPPh_3)(O^tBu)(THF)]_2$ and $[Co(NP^iPr_3)_2]_3$ were synthesized. Salt metathesis between $CoBr_2$ and $NaNPPh_3$ and a subsequent *in situ* reaction with $KOSiMe_3$ provides a convenient and scalable preparation of $[Co(NPPh_3)(OSiMe_3)(THF)]_2$. The same synthetic route affords the analogous $[Co(NPPh_3)(O^tBu)(THF)]_2$ from a metathesis reaction with KO^tBu but the synthesis suffers from reproducibility issues. An easy, one-step reaction between $CoBr_2$ and $NaNP^iPr_3$ gives $[Co(NP^iPr_3)_2]_3$ in high yield. All complexes were characterized by Elemental Analysis and Fourier Transform – Infrared Spectroscopy.

Preliminary catalytic experiments with these clusters found that 4-acetylbiphenyl is deoxygenated overnight at 200 °C and 34 atm H_2 in the presence of excess KO^tBu as a co-catalyst and water scavenger. Aldol condensation and dimerization driven by benzylic radical intermediates occur to a significant extent. Further radical additions produce insoluble oligomers as the major product.

Mercury tests revealed that the precatalysts decompose into heterogeneous cobalt nanoparticles under harsh reaction conditions. A deliberate pre-decomposition of clusters $[Co(NPPh_3)(OSiMe_3)(THF)]_2$ and $[Co(NPPh_3)_2]_3$ at 200 °C and 34 atm H_2 yields heterogeneous catalysts that completely deoxygenate 4-acetylbiphenyl using activated 3Å molecular sieves to scavenge the resulting H_2O. Aldol condensation is suppressed in the base-free reactions; only minor, radical-driven dimerization takes place. The thermally stable phosphoranimide ligands

cause slow cluster decomposition but are eventually liberated to produce the active cobalt catalyst.

Activation of ligand-free $CoBr_2$ by alkali metal *tert*-butoxides and a subsequent *in situ* decomposition at 200 °C and 34 atm H_2 for 1 h produces the most active catalyst. At 7 atm H_2 and 200 °C, heterogeneous cobalt particles fully deoxygenate 4-acetylbiphenyl in 2.5 h using molecular sieves to scavenge water. Deoxygenation of deactivated substrates such as 4-fluoroacetophenone requires longer reaction times; the catalyst is inactive towards cleaving unactivated C–O bonds. The heterogeneous reaction exhibits a strong dependence on the reaction temperature, pressure and reaction time.

"The success or failure of your deeds does not add up to the sum of your life. Your spirit cannot be weighed. Judge yourself by the intention of your actions and by the strength of which you faced the challenges that have stood in your way."

~ Robert C. Cooper (Oma Desala in Stargate SG-1)

Acknowledgements

My sincere appreciation goes towards many people who made my journey possible.

Table of Contents

List of Tables

List of Figures

Chapter 1

Chapter 2

Chapter 3

List of Schemes

Chapter 1

Chapter 2

Chapter 3

List of Equations

Chapter 3

Abbreviations

Å	angstroms
°C	degrees Celsius
ν	Nu (frequency)
η	Eta (hapticity)
9-BBN	9-borabicyclo[3.3.1]nonyl
Ar	generic aryl substituent
at	apparent triplet
atm	atmosphere
Bu	butyl
cm^{-1}	wavenumbers
Cp	cyclopentadienyl
d	days
dd	doublet of doublets
dippe	1,2-bis(diisopropylphosphino)ethane
e	electron
DCE	1,2-dichloroethane
equiv	equivalent
Et	ethyl
FLP	Frustrated Lewis Pairs
FT-IR	Fourier Transform Infrared Spectroscopy
g	grams
h	hours
Hz	hertz

^{i}Pr	isopropyl
IR	Infrared
J	coupling constant
kcal	kilocalories
L_n	ligand
M	metal
Me	methyl
mg	milligrams
MHz	megahertz
min	minutes
mL	milliliter
mmol	millimole
mol	mole
MS	molecular sieves
NMR	Nuclear Magnetic Resonance Spectroscopy
^{n}Bu	normal Butyl
PMHS	polymethylhydrosiloxane
Ph	phenyl
ppm	part per million
R	generic alkyl substituent
rt	room temperature
^{t}Bu	*tert*-butyl
THF	tetrahydrofuran
tt	triplet of triplets

Chapter 1. Overview of ketone deoxygenation

1.1 Introduction

Scientific discoveries in disciplines such as chemistry, biology or physics have always been the driving force behind the rise and development of civilizations. The significance of chemical discoveries can be highlighted by the Haber-Bosch breakthrough that is often called the greatest discovery of mankind in the 20th century.[1] The Haber-Bosch process to synthesize ammonia, and, henceforth, the manufacture of needed fertilizers on a large scale, has allowed for a production of sufficient food supply to sustain the explosive increase in the human population. Furthermore, this process is still applied in the industry one hundred years later.[2] The discovery also emphasizes the importance of catalysis in the modern society: transition metal catalyzed processes have multiple applications ranging from manufacturing integrated circuits[3] to food production.[4-5] Due to the ability of the catalysts to mitigate harsh reaction conditions, catalysis is now an integral part of chemical synthesis.

One of the most prominent drivers of transition metal catalysis is the pharmaceutical industry due to its health impact and billion-dollar revenue.[6] Drug design, however, is a long and expensive process due to the complex nature of the molecules involved. The main challenge is introduction and modification of individual functional groups within the same molecule throughout a multi-step synthesis.[7] Often, the most convenient approach is to start from a compound that possesses a desired skeletal structure and can be readily modified using current

technology. Fine chemicals, traditionally extracted from natural products or petrochemicals, are commonly used as standard building blocks.[8]

The prevalence of aromatic compounds in nature makes their presence in fine chemicals synthesis strongly necessitated. Functionalization of aromatic rings has been extensively explored in organic chemistry and is highly dependent on the substituents already present in the structure. Among the most desired modifications is the formation of new carbon – carbon bonds, particularly alkylation. One of the oldest, most conventional and inexpensive pathways of doing so is Friedel-Crafts alkylation or acylation (Scheme **1.1**).

Scheme 1.1 Friedel-Crafts reactions.
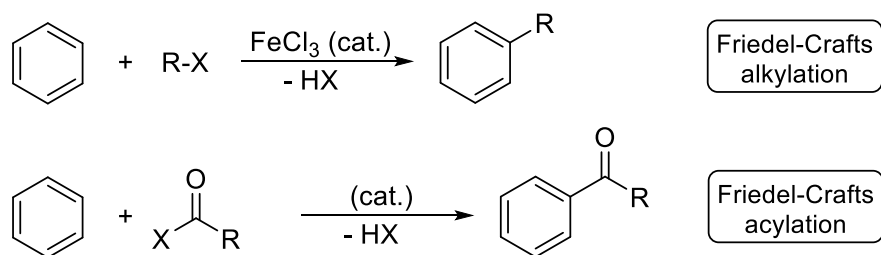
Friedel-Crafts alkylation provides a pathway for direct arene alkylation, however, it suffers severe drawbacks: 1) mixtures of products are obtained due to rearrangements of carbocation intermediates, 2) the activating nature of alkyl substituents leads to overalkylation, and 3) the reaction rarely works in the presence of deactivating groups (e.g. *nitro*, *cyano* etc.).[9] Friedel-Crafts acylation is a viable alternative, however, it requires an additional step of carbonyl deoxygenation.[10] While other methods exist (such as coupling reactions mediated by Grignard reagents or organometallic catalysts), the procedures are more challenging and costly.[11] Therefore, a mild and inexpensive method for ketone deoxygenation would provide a convenient

synthetic pathway to chemoselective synthesis or modification of fine chemicals and bioactive molecules.[12]

1.2 Properties of carbonyl group

Ketones are comprised of a carbonyl group with two aryl- or alkyl-based substituents. While ketones share similarities with aldehydes, their properties differ due to the distinctive electronic and steric nature of the alkyl/aryl substituents compared to hydrogen.

Bond	Bond energy	Bond distance, [Å]
ketone C=O	745 kJ/mol, 180 kcal/mol	1.23
alkene C=C	611 kJ/mol, 146 kcal/mol	1.34
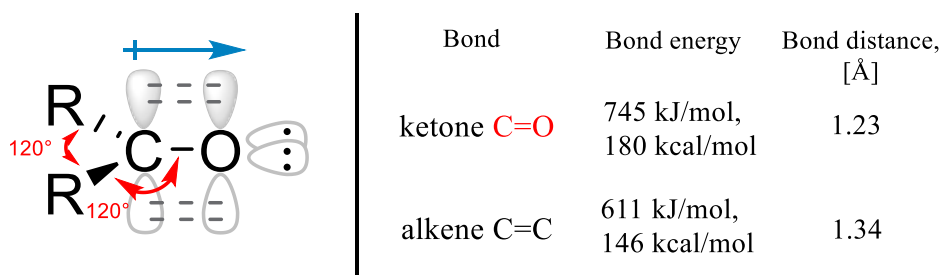
Figure 1.1 Bonding in ketones.

The carbonyl group consists of carbon and oxygen atoms in sp^2 hybridization. It lays in trigonal planar geometry with 120° bond angles. The double bond formally consists of two electrons in a σ-bond and two electrons in a π-bond. The C=O bond is commonly compared to alkene C=C bond due to the same hybridization and bonding, however, carbonyl bond is stronger and shorter than the olefin bond (Fig. **1.1**).[13-14] Therefore, additions to the C=O bond require harsh conditions or strong reducing reagents. Furthermore, the C–O σ-bond has the highest bond energy compared to other types of σ-bonds within organic molecules requiring most energy to be cleaved.[13]

Table 1.1 Bond energies of C – element bonds.

Bond	Energy, [kcal/mol]
C – O	86
C – C	83
C – N	73
C – S	65

Due to the difference in electronegativities between the constituents, the C=O bond is strongly polarized towards the oxygen. The polar character of the bond contributes to resonance structures as well as electrophilic (carbon) and nucleophilic (oxygen) sites within the same functional group (Fig. **1.2**). Therefore, the $C^{\delta+}$ can be regarded as a Lewis acid (LA) and the $O^{\delta-}$ can be considered a Lewis base (LB).
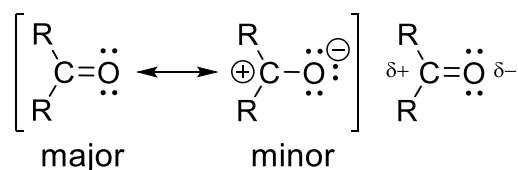
Figure 1.2 Resonance structures of ketones.

1.3 Challenges and advancements in ketone deoxygenation

Whereas catalytic carbonyl reduction to alcohols is easily achievable with multiple reductants and is widely applied in industry,[15] deoxygenation under mild conditions has been a challenge for over a century. Generally, the carbonyl group is first reduced to an alcohol followed by a successive cleavage of the C–O bond. Aliphatic ketones are stabilized by electron-releasing alkyl groups; they lack resonance stabilization in deoxygenation intermediates and are usually reduced only to the alcohols. Aryl ketones undergo C–O bond scission more readily due to the reactivity

of the benzylic position, although their reactivity is also governed by the nature of arene substituents. Activating/electron-donating substituents increase susceptibility towards deoxygenation and accelerate reaction rates while deactivating/electron-withdrawing substituents inhibit the reactivity (usually *halo* and *nitro* groups are reduced first).[16-20] Steric factors also play a role; bulky substituents on α-carbons lower deoxygenation rates and yields.

The earliest and best-known deoxygenation methods are Wolff-Kishner reduction,[21-22] Clemmensen reduction,[23-24] Mozingo (thioketal) and Raney Ni reductions,[25-26] and heterogeneous catalytic Pt or Pd systems.[27] Other stoichiometric alternatives commonly employ borohydride reductants in acidic media;[28] however, significant progress has been made in the last few decades towards deoxygenation in the presence of hydrogen or mild reducing agents such as silanes.[20] Most of the methods rely on one or more of the following factors: a) harsh reaction conditions, b) stoichiometric reagents, c) hazardous/toxic reagents, d) expensive, scarce 2nd/3rd row transition metals, and e) expensive main group metal catalysts. An ideal procedure can reduce both aromatic and aliphatic ketones in the presence of various functional groups, would feature mild and environmentally friendly reaction conditions, use a sustainable and 'green' hydrogen source, and would not necessitate complex purification or extraction steps.

1.3.1 Wolff-Kishner reduction

The Wolff-Kishner reduction was reported in the early 20th century. The discovery was made independently by Ludwig Wolff[22] and Nikolai Kishner.[21] In this process, a carbonyl substrate is treated with hydrazine to form an intermediate hydrazone. The hydrazone is further deprotonated to produce a diimide anion that readily releases N_2 to yield an alkylanion under basic conditions.

In the final stage, the alkylanion is protonated by the solvent to give a methylene unit (Scheme **1.2**).
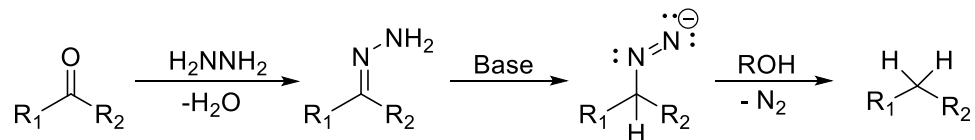
Scheme 1.2 Wolff-Kishner reduction of carbonyl compounds.

The initial procedure required one equivalent of hydrazine, high temperatures (200 °C) and long reaction times (50 – 100 h). The main drawbacks of the system were intolerance to base-sensitive functional groups and use of potentially explosive hydrazines. Initial variations of the reaction introduced glycols as high boiling solvents[29-30] but the first significant improvement was made by Huang-Minlon in 1946. Minlon heated the reagents to reflux in ethylene glycol and used distillation to remove excess water and unreacted hydrazine.[31] This, in turn, allowed for easily-sustained high temperatures without the cooling effect of water and thus reduced reaction times. While functional group tolerance was still a significant problem, the modified Wolff-Kishner-Minlon procedure soon became widely used as a standard carbonyl reduction method.

In 1955 Barton *et al.* discovered that deoxygenation of sterically hindered carbonyls can be achieved by substituting KOH with metallic sodium in Huang-Minlon conditions.[32] Another modification was introduced by Cram *et al.* in 1962: addition of preformed hydrazones to KO*t*Bu in anhydrous DMSO afforded hydrocarbons at room temperature.[33] The drawbacks of this process were the necessity to isolate the hydrazones and the requirement for slow addition to the base solution. In order to accelerate the hydrazone addition, Henbest *et al.* conducted the reaction in dry toluene under Cram's conditions.[34] While hydrazone isolation was still required, the incurred disadvantage was increased reaction temperature. Functional group tolerance was

6

partially solved by Caglioti in 1963. The necessity of using a strong base was removed by heating tosylhydrazones and a hydride donor in THF. Importantly, if NaBH$_3$CN is used as a hydride source, the system tolerates *ester*, *amide*, *cyano*, *nitro* and *chloro* substituents.[35] Forty years later, Myers discovered that treating carbonyls with 1,2-bis(*tert*-butyldimethylsilyl)-hydrazine in the presence of KO^{t}Bu and the catalytic amount of Sc(OTf)$_3$ afforded hydrocarbon products in high yields in DMSO at room temperature.[36] In addition, several large scale methods of modified Wolff-Kishner procedure have been recently developed.[37-39]

While significant advances to the original Wolff-Kishner procedure have been made, the system still suffers from substantial disadvantages. For example, reactions that proceed at lower temperatures require an additional step of hydrazone isolation, yet still necessitate explosive hydrazines as starting reagents. While Myers modification proceeds at the mildest conditions, the reaction costs are significantly increased due to the presence of Sc(OTf)$_3$ catalyst.

1.3.2 Clemmensen reduction

Acidic Clemmensen reduction was originally reported in 1913 by Eric Christian Clemmensen and can be considered to be complementary to the basic Wolff-Kishner procedure.[23-24] In the original method, carbonyl compounds were treated with excess amounts of amalgamated zinc and concentrated hydrochloric acid for 4 – 10 h under reflux (Scheme **1.3**). While the process works well for both aliphatic and aromatic ketones, the substrate scope is severely limited due to the aqueous acidic conditions. In addition, presence of excess mercury renders large scale industrial application unviable.
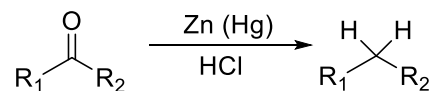
Scheme 1.3 Clemmensen reduction.

The exact reaction mechanism is still unclear due to its heterogeneous nature. Few mechanistic studies reported have found evidence for radical anion[40] and zinc carbenoid[41] mechanisms. Interestingly, alcohol substrates are usually not deoxygenated when subjected to Zn amalgam and HCl indicating that the reaction does not proceed through the alcohol intermediates.[42-43] Due to the ambiguity of the mechanism, few modifications have been reported. A significant improvement was, however, reported by Yamamura in 1967. The reaction was carried out using activated Zn and saturated aqueous HCl in the absence of toxic Hg (Et$_2$O, 0 °C) and afforded higher yields for aliphatic substrates.[44]. In 1996 Hiegel reported that aryl ketones can be successfully deoxygenated to form aryl alkenes upon reflux with Zn (Hg) in formic acid and ethanol for one hour.[45] The conversion was moderate and a mixture of different alkene products was obtained when the substrate contained an unbranched alkyl chain.

A basic version of the procedure was reported in 2007 by Zhang *et al.*[17] Hydroxy- and amino-9,10-anthracenediones have been deoxygenated using zinc powder in NaOH solution at reflux, albeit in moderate to high yields. The reaction is, however, sensitive to the presence and position of the *nitro* and *hydroxy* substituents and can yield alcohols instead. In addition, reaction times of 36 – 72 hours are required, thus rendering the procedure inconvenient for large scale application. The latest Clemmensen modification was reported in 2007 by Xu *et al.*[46] This reaction employs a Zn-TMSCl system in alcoholic solvents to deoxygenate complex ketone substrates within one hour at 0 °C. While reaction conditions are very mild, a volatile TMSCl additive is required.

1.3.3 Mozingo and Raney Nickel reductions

Raney nickel was patented by Murray Raney in 1926 as one of the first metal catalysts for hydrogenation of vegetable oils.[47] Due to the trademark protection, only alloys produced by Grace Davison and descendant companies are named Raney Ni, other skeletal alloys are usually referred to as Ni-Al, Cu-Al etc. Upon activation, Ni-Al alloys retain a high hydrogen content absorbed within the pores and therefore can be used as hydrogenation catalysts towards hydrogen acceptors.[48]

Mozingo reduction was first reported in 1943 as a method for thioketal conversion to the methylene unit.[26] Multiple thioketals were reduced using Raney Ni in moderate to good yields under relatively mild conditions (the substrates were heated to reflux in ethyl alcohol for 2 – 5 h). Inspired by this discovery, Wolfrom *et al.* adapted the method for carbonyl deoxygenation in a two-step procedure a year later (Scheme **1.4**).[25] Carbonyl compounds were heated to reflux in ethanol with 15 mass equivalents of Raney Ni for 5 hours. Compared to Clemmensen and Wolff-Kishner procedures, the modified Mozingo reaction had the advantage of milder conditions and tolerance of multiple functional groups. However, high "catalyst" loadings and an additional step to convert carbonyl units to thioketals were required. In addition, pyrophoric nature of Raney Ni presented safety risks and the alloy could not be recycled due to irreversible sulfur poisoning.
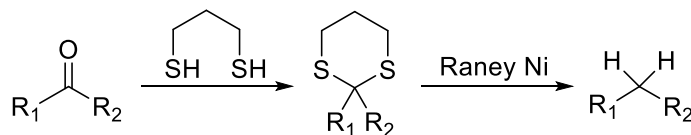
Scheme 1.4 Mozingo (thioketal) reduction

The first direct deoxygenation of aromatic ketones mediated by Ni-Al alloy was reported in 1942 by Papa *et al*.[49] The method necessitated highly basic conditions and suffered from the same lack of functional group tolerance as the Wolf-Kishner procedure, and thus went unnoticed by the scientific community. Deoxygenation under neutral conditions was first reported by Mitchell *et al.* in 1980.[16] The authors were investigating cleavage of carbon–thiomethyl bonds when they accidentally discovered deoxygenation of aromatic carbonyl compounds. Substrates with various functional groups were explored under optimized reaction conditions (heated to reflux in 50% aqueous ethanol solution, 3 – 6 h, twofold to fivefold excess of Raney Ni). While the system tolerated *methoxy*, *hydroxy*, *carboxy*, *carbomethoxy* and *dimethylamino* functional groups, *halo*, *cyano* and *nitro* groups were preferentially reduced. The effect of doping Raney nickel with chromium hydroxide and chromium chloride was investigated by Mason; however it led to the selective hydrogenation to alcohols and suppression of the C–O bond hydrogenolysis.[50-51]

In 2003, the Tashiro group reported the first Ni-Al mediated carbonyl deoxygenation in water.[52] While different aluminum alloys (Ni, Co, Fe, Cu) were investigated for acetophenone substrates, the results showed that only Ni-Al leads to quantitative hydrogenolysis of the C–O bond. A few years later, the authors reported deoxygenation of benzophenones in alkaline media (1% KOH solution).[53] The reaction was carried out at 90 °C instead of at reflux, however significant aromatic ring hydrogenation was observed and a mixture of products was obtained.

The latest development in Raney Ni deoxygenation was reported in 2011 and utilized 2-propanol as a sacrificial reagent/solvent in transfer hydrogenolysis.[54] Aromatic ketones were successfully deoxygenated in high yields within a few hours upon reflux. While a 5 : 1 mass ratio of Raney Ni to substrate is still required, the catalyst can be successfully recycled up to six times.

The general challenges in Raney Ni reductions remain storage and handling of pyrophoric alloys and high "catalyst" loadings. Even though recent research on catalyst recyclability lessens the higher costs associated with high loadings, the safety risks associated with the high pyrophoricity of activated alloys strongly limit large scale applications.

1.3.4 Borohydride reductants

Sodium borohydride was first synthesized in the 1940s by Herman Irving Schlesinger and Herbert C. Brown under military contract but the data were only published in 1953 upon research declassification.[55] Due to the ease of hydride transfer, $NaBH_4$ has been widely applied in a variety of reduction reactions, including the conversion of ketones and aldehydes to alcohols.[28] Nevertheless, large scale application of $NaBH_4$ is hindered by its high cost as a stoichiometric reagent.[56]

The first carbonyl deoxygenation mediated by $NaBH_4$ was reported by Gribble *et al.* in 1978.[18] The authors described the reduction of variety of benzophenone substrates at room temperature in trifluoracetic acid (Scheme **1.5**). Most substituents were tolerated, although highly electron withdrawing *nitro* groups hindered the reaction. When the substrate contained a mesityl ring on an α-carbon, no conversion was observed. The procedure was later adapted for the synthesis of alkylated indoles *via* deoxygenation of Friedel-Crafts acylation products.[57]
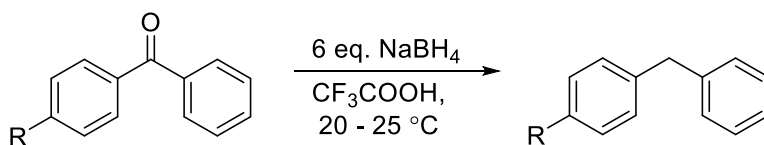
Scheme 1.5 Diaryl deoxygenation with sodium borohydride.

In 1987, NaBH$_4$ was reported to successfully deoxygenate acetophenone substrates and the corresponding alcohols within 2 hours in the presence of excess AlCl$_3$ (Scheme **1.6a**).[58] The reaction was theorized to proceed through the reduction of the carbonyl group to the corresponding alcohol, followed by a C–O bond cleavage to yield styrene. Finally, reduction of the olefin yields ethylbenzene. A more powerful AlCl$_3$-based system was reported a year later: *tert*-butylamine-borane could successfully reduce chloroacetophenones and dichloroaryl ketones to hydrocarbons within 1 – 20 hours (Scheme **1.6b**).[59] However, the yields were moderate and aliphatic ketones were only reduced as far as the corresponding alcohols. The main drawback of each method was the high amounts of expensive and hazardous reagents required.
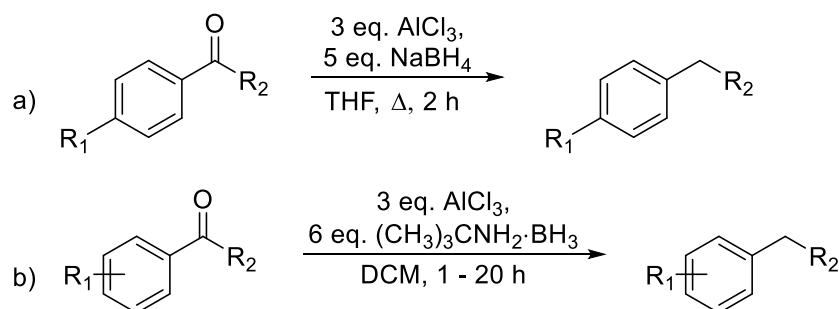
Scheme 1.6 Deoxygenation of aryl ketones in the presence of AlCl$_3$.

The same authors also explored ZnI$_2$/NaCNBH$_3$ for deoxygenation of aryl ketones and aldehydes (Scheme **1.7**).[60] Although aryl halides and substituents with *nitro* groups were not reduced, substrates with other electron withdrawing or neutral substituents only necessitated higher reaction temperatures than activated carbonyls. NaBH$_4$ was tested as a hydride source, however it did not give comparable results. In the absence of zinc iodide, the reaction yields alcohols after prolonged times.
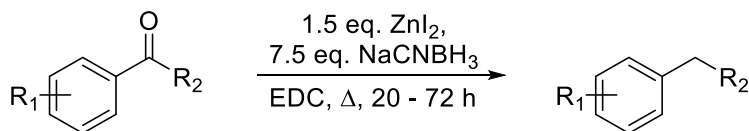
Scheme 1.7 Reduction by sodium cyanoborohydride.

While the early research exhibited promising results, the high costs of borohydrides combined with the required excess discouraged further research. The efforts focused on improving reaction conditions and selectivity using molecular hydrogen and exploring alternative hydrogen donors.

1.3.5 Direct deoxygenation with H₂

Molecular hydrogen represents a relatively 'green' and clean source of hydrogen atoms for reduction and cleavage of multiple bonds. However, this method has long been associated with high temperatures and pressures as well as expensive 2nd and 3rd row transition metal catalysts – partly due to the strength of the H–H bond[13] and partly due to the low dihydrogen ligand affinity towards the first row metals.[61] Since high-activity metals are required for H–H bond cleavage, unwanted hydrogenation of aromatic or conjugated systems in complex molecules is a frequently encountered problem. The phenomenon is common in carbonyl reductions due to the ease of C=C hydrogenation in comparison to C=O reduction or scission, thus making chemoselective hydrogenolysis of σ-C–O bonds in aromatic molecules rather challenging. Nevertheless, immense advancements in the area have been made in the last two decades ranging from catalysis by inexpensive first row metals to deoxygenation facilitated by frustrated Lewis pair (FLP) interactions.

1.3.5.1 Transition metal mediated hydrogenolysis

Heterogeneous Pt and Pd catalysts on alumina, silica, titania or carbide support were originally applied for reductive C=O bond cleavage and have been extensively investigated (Scheme 1.8).[62-63]
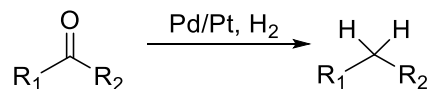
Scheme 1.8 Platinum or palladium catalyzed deoxygenation.

Both metals have a high propensity to hydrogenate phenyl rings preferentially under the reductive conditions and thus produce a mixture of products (Scheme **1.9**).[64] Effects of catalyst support,[27, 65-68] solvent,[69-71] doping,[72-76] and reaction mechanism[77] in heterogeneous Pd or Pt deoxygenation continue to be investigated but multiple reaction variables render optimization difficult.
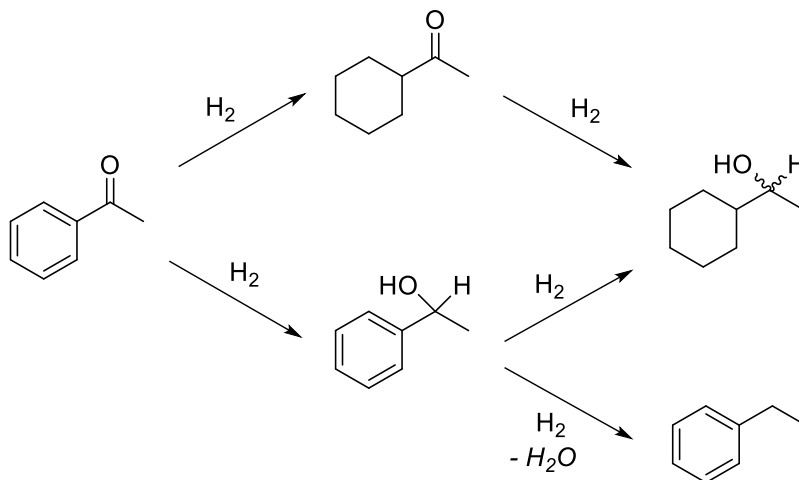
Scheme 1.9 Hydrogenation of aromatic ketones over late transition metal catalysts.

One of the latest publications in the field reports a selective deoxygenation of aryl ketones to give alkanes in high yields using a silica-supported chitosan Schiff-base Pd catalyst (Scheme **1.10**).[78] While the system shows high chemoselectivity for aromatic carbonyls at room temperature and atmospheric H_2 pressure, aliphatic ketones only undergo reduction to alcohols in poor yields. The main drawback of the system is complicated catalyst structure/synthesis and its cost.
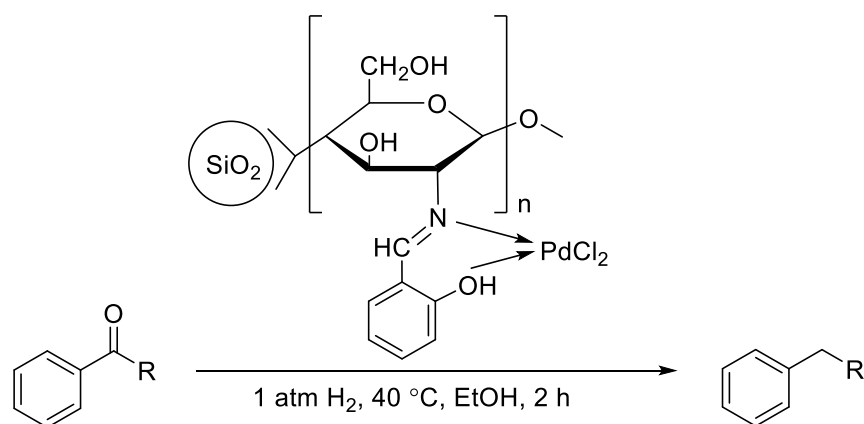
Scheme 1.10 Deoxygenation of aromatic ketones by SiO_2-chitosan-Schiff-base-Pd catalyst.

Heterogeneous polymetallic catalysts have also been investigated. Polyoxometalates supported on γ-alumina exhibit high activity towards deoxygenation of aliphatic and aromatic ketones, however, high hydrogen pressure (>23 atm) and temperature (>300 °C) are required.[79] Amorphous Ni(Co)–W–B and Co(La)–Ni–Mo–B catalysts were reported to exhibit high deoxygenation activity at 250 °C but competing hydrogenation of the aromatic rings occurs as well.[80-83]

Recent focus towards 'green' energy production and cost efficient catalysis has shifted research efforts to more economical and more environmentally friendly catalysts. One of the long-desired goals is replacement of precious and semi-precious metals with late 1st row transition metals (Fe,

15

Co, Ni and Cu) to allow for a significant reduction in operating costs. However, first-row metals tend to require harsh reaction conditions and higher catalyst loading to achieve equivalent results, and rarely ever do, particularly when applied to energy-intensive transformations like reductive C-O bond scission. Thus, efficient ketone deoxygenation by Fe, Co, Ni or Cu catalysts under mild conditions has not had much success.

The first C–O hydrogenolysis mediated by a first-row catalyst was reported in 2005 by Zaccheria *et al.*[84] Remarkably, aromatic ketones were quantitively deoxygenated to the corresponding methylene compounds by metallic copper supported on SiO_2 under nearly ambient conditions (toluene, 90 °C, 1 atm H_2). The heterogeneous catalyst was prepared by a conventional nitrate synthesis, calcinated in air at 430 °C and further activated at 270 °C and 1 atm H_2 prior catalytic tests. The conversion is usually completed within 10 hours (Scheme **1.11**). When the carbonyl group is β to the aromatic ring, only reduction to the hydroxyl group is observed. Condensation products were observed in the presence of electron-donating substituents on phenyl rings. The authors also investigated the necessity of acidic sites within the catalyst support (e.g. ZrO_2, Al_2O_3). Hydrogenolysis proceeded best in the absence of acidic additives, thus suggesting a presence of carbocation intermediates. The system exhibits high sensitivity to the reaction conditions (e.g. hydrogen pressure, catalyst loading, temperature) making the reproducibility rather problematic.[85]
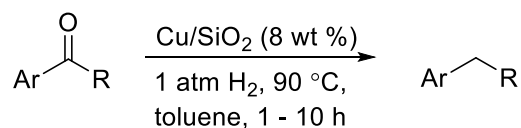
Scheme 1.11 Cu/SiO$_2$ mediated deoxygenation.

Another copper mediated hydrodeoxygenation of aryl ketones was reported in 2011 by Ma *et al* (Scheme **1.12**).[86] Copper was impregnated with chromium in order to increase the catalyst lifetime, and supported on γ-Al_2O_3. Introduction of Cr was reported to stabilize the catalyst and increase its activity by promoting dispersion of copper particles on the alumina. While Cu_{30}/γ-Al_2O_3 exhibited significantly lowered conversion rates within 30 hours, deoxygenation by $Cu_{30}Cr_{10}$/γ-Al_2O_3 remains stable over 200 h. Compared to the Cu/SiO_2 procedure developed by Zaccheria *et al.*, the system necessitated much harsher reaction conditions and higher catalyst costs.
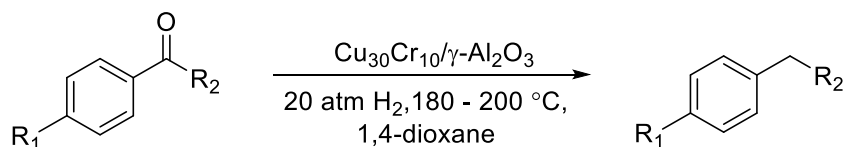
Scheme 1.12 Deoxygenation by Cu-Cr catalyst.

Heterogeneous Ni catalysts supported on silica and/or alumina have been known to hydrogenate aromatic ketones to produce benzylic alcohols; however, successive C–O bond scission has not been reported.[70] A Ni-catalyzed deoxygenation was reported in 2009 by Flores-Gaspar *et al* (Scheme **1.13**).[87] The [(dippe)Ni(μ-H)]$_2$ precatalyst **1** reduced various mono- and di-ketone substrates to the corresponding hydrocarbons in moderate yields, with high temperatures and extended reaction times required. The authors propose homogeneity of the catalyst based on conducted mercury tests but the exact mercury amounts were not measured preventing definitive conclusions. Further, the mercury test may not be very accurate as it only demonstrates amalgamation of a metal rather than giving a definitive proof of heterogeneity.
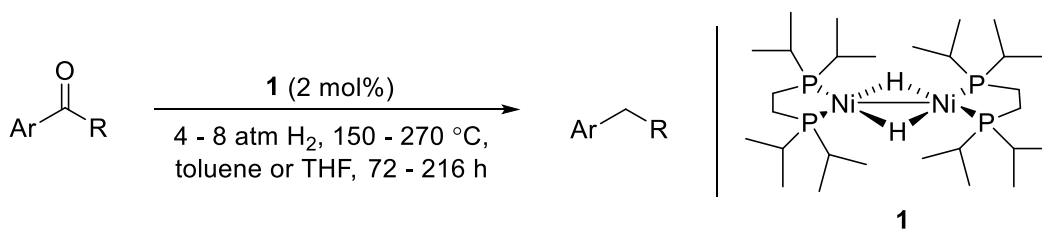
Scheme 1.13 Deoxygenation catalyzed by homogeneous Ni complex.

In 2015, a homogeneous cationic ruthenium hydride complex was reported by Kalutharage *et al.* for highly chemoselective deoxygenation of aliphatic and aromatic ketones (Scheme **1.14**).[88] Upon addition of the phenol (X-C$_6$H$_5$-OH), precatalyst **2** was found to deoxygenate ketones and aldehydes in the presence of C=C bonds. Isopropanol or molecular hydrogen can be used as reductants; higher hydrogen pressures and longer reaction times are required in case of aliphatic substrates. In the absence of the phenol, the reaction yields etherification products of 2-propanol. Interestingly, the nature of X-C$_6$H$_5$-OH ligand was found to determine the reaction mechanism.
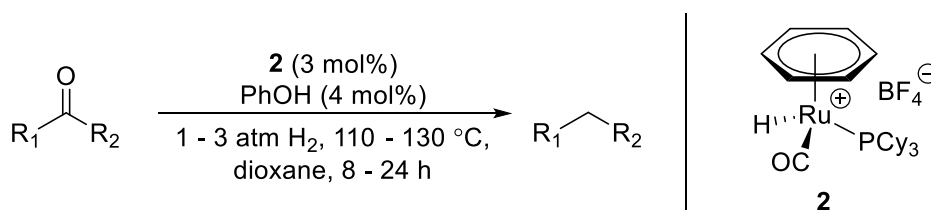
Scheme 1.14 Deoxygenation by ionic ruthenium hydride complex.

Electron releasing *p*-OMe-C$_6$H$_5$-OH contributes electron density to the ruthenium center increasing its nucleophilicity and affinity for H$_2$ activation. Hydrogen readily binds to the metal center in a concerted step and competes with a substrate for open coordination sites. Consequently, high H$_2$ pressures can inhibit the reaction. In contrast, electron withdrawing *p*-CF$_3$-C$_6$H$_5$-OH ligand renders Ru more electrophilic, and in turn, lowers its affinity for H$_2$ binding eventually leading to stepwise hydrogen addition and activation.

18

The homogeneous system demonstrates a great potential and allows important mechanistic investigations. Even though the price of ruthenium has been steadily decreasing over the last decade and currently is at a fraction of prices of other noble metals, the scarcity of Ru does pose a significant disadvantage.

Overall, significant progress has been observed in catalytic deoxygenation mediated by transition metals. A shift to readily available and cost efficient first-row metals presents a viable alternative to traditional precious metal catalysis. Even though comparatively low yields and harsh reaction conditions are yet to be improved, the significance of the ability of 1st row metals to cleave high strength bonds such as C–O is momentous.

1.3.5.2 Hydrogenolysis mediated by Frustrated Lewis Pairs

The emergence of FLPs has been one of the most remarkable advances in chemistry within the last few decades. Frustrated Lewis pairs are Lewis acid-base pairs that are prevented from reacting with each other by steric encumbrance and exhibit high reactivity towards bond cleavage of neutral small molecules such as hydrogen.[89] Representative FLPs consist of bulky phosphines or amines in combination with a strong boron Lewis acid, $RB(C_6F_5)_2$, or more usually, $B(C_6F_5)_3$ (Scheme **1.15**). Even though the catalytic activity of FLPs and H_2 has been widely explored,[90-91] their reactivity towards C–O hydrogenolysis in ketones has only been reported recently.

$$R_3P \ + \ B(C_6F_5)_3 \ \xrightarrow{\quad H_2 \quad} \ R_3PH^{\oplus} \ + \ ^{\ominus}HB(C_6F_5)_3$$
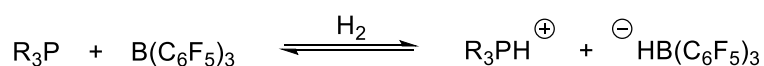
Scheme 1.15 General FLP-facilitated activation of hydrogen.

Ketone reactions commonly rely on the electrophilic nature of the carbonyl carbon and the use of strong nucleophile reagents. Oxygen in the carbonyl functionality possesses two lone pairs, is a weak nucleophile due to high electronegativity, and thus is a weak Lewis base, which reacts with Lewis acids accordingly. Generally, reactions between ketones and Lewis acidic organoboranes are irreversible and lead to Lewis adducts due to the high oxophilicity of electronegative boron.

FLPs have exhibited remarkable reactivity towards the reduction of multiple functional groups,[89-91] however, up until recently, ketone behavior as a Lewis base in FLPs has not been observed. The first example of hydrogen activation by ketone-B(C$_6$F$_5$)$_3$ was reported by Timo Repo in 2012 (Scheme **1.16**).[92] At room temperature boronic esters were formed, whereas full hydrogenolysis of C–O bonds in aromatic carbonyl compounds was observed at slightly elevated temperatures. A stoichiometric amount of B(C$_6$F$_5$)$_3$ was required and only moderate yields were achieved. Nevertheless, the pioneering work paved the way for further studies of ketones as part of FLP system.
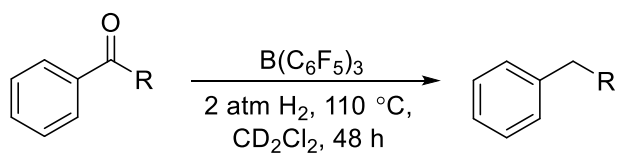
Scheme 1.16 Deoxygenation in stoichiometric ketone-B(C$_6$F$_5$)$_3$ system.

The first FLP-mediated procedure that employs catalytic amount of B(C$_6$F$_5$)$_3$ was reported in 2015 by Stephan (Scheme **1.17**).[93] Introduction of α-cyclodextrin or 4 Å molecular sieves to act as a Lewis base in hydrogen activation and cleavage allowed for a significant decrease in B(C$_6$F$_5$)$_3$ loading. Aliphatic ketones were reduced to alcohols in excellent yields while aryl and diaryl carbonyls underwent C–O bond hydrogenolysis in moderate to good yields under identical

conditions. In the latter case, molecular sieves also served as water absorbent. Although cyclodextrin could be successfully recycled for five successive runs, replacement of $B(C_6F_5)_3$ is required.
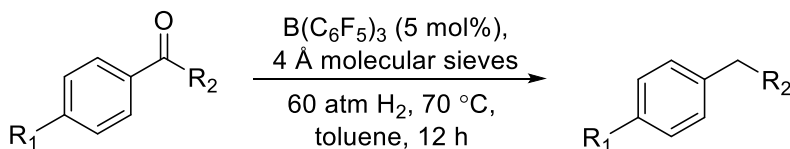
Scheme 1.17 Catalytic FLP-mediated deoxygenation of ketones.

FLP chemistry is still in its inception compared to more traditional fields such as transition metal catalysis. Nonetheless, this concept shows great potential in reductive catalysis, especially in ketone deoxygenation. The main issue associated with the reported procedures is the high cost of $B(C_6F_5)_3$. Even though the latest findings illustrate that catalytic amounts of the Lewis acid can be used, increased energy costs and safety risks associated with high pressures incur as a result.

1.3.6 Ketone deoxygenation under hydrosilylation conditions

The silicon-hydrogen bond is strongly polarized and, therefore, more reactive than the H–H bond.[13] Activation of the Si–H bond in hydrosilanes requires milder reaction conditions in comparison. Hydrosilylation of carbonyl compounds has been widely explored and can be readily achieved by various catalysts due to the silicon affinity for oxygen.[94] While hydrosilylation is an excellent procedure for the synthesis of silyl ethers, functional group reduction under such conditions is not 'atom-efficient': excess amounts of silanes are required to break one or two bonds and the process generates a considerable amount of waste that can be difficult to separate from the reaction mixture. In contrast, hydrosilanes are known not to reduce aromatic systems, therefore silane-based reductants offer high chemoselectivity for aromatic

ketones. In addition, inert atmosphere is usually not needed. The nature of catalyst, silane and the solvent have been shown to affect the outcome of the reaction, therefore optimization of the reaction conditions can be challenging and time consuming.

The field was pioneered in 1973 by West *et al* (Scheme **1.18**).[95] The reported system is nearly analogous to the borohydride reduction reported by Gribble *et al.*[18] Most reactions take place within 15 minutes but deoxygenation of deactivated *p*-chloroacetophenone necessitates 200 h for completion (100% yield). Compared to the NaBH$_4$ system, this procedure offers a wider substrate range, faster reaction times and milder hydride source.
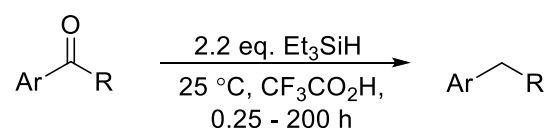
Scheme 1.18 First deoxygenation under hydrosilylation conditions.

It was later discovered that an acid solvent can be replaced by a Lewis acidic catalyst. In 1978, Fry *et al.,* reported an Et$_3$SiH-BF$_3$ system for carbonyl reduction and deoxygenation.[96] Aliphatic and aromatic ketones with electron donating substituents were deoxygenated, whereas aromatic carbonyls with deactivating substituents, such as cyano or nitro, were reduced to alcohols in 10 – 60 mins. The procedure was later adapted for the reduction to *m*-nitroethylbenzene.[97]

Jaxa-Chamiec *et al.* reported that deoxygenation can also be achieved *in situ* following Friedel-Crafts acylation (Scheme **1.19**).[98] The authors also state that polymethylhydrosiloxane (PMHS) can be substituted for Et$_3$SiH, however, this variant was only reported for one substrate. In general, poor to moderate yields were obtained.
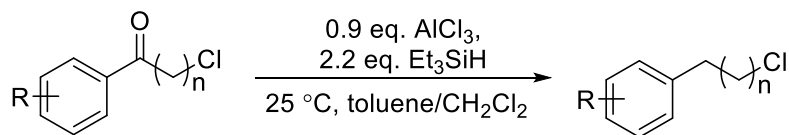
Scheme 1.19 Deoxygenation catalyzed by AlCl$_3$ under hydrosilylation conditions.

The costly alkylsilanes, relatively harsh reaction conditions, and moderate yields were presumably responsible for little to no further research into such reactions. The field was revived by the Baba group in 1999, reporting the deoxygenation of aryl and diaryl ketones catalyzed by InCl$_3$ (Scheme **1.20**).[99] Although the procedure affords only moderate to good yields, most reactions were completed within one hour and many functional groups such as halo or nitro were well-tolerated.
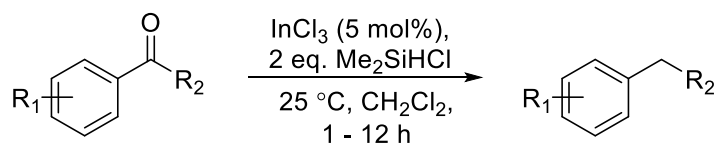
Scheme 1.20 Deoxygenation by InCl$_3$ under hydrosilylation conditions.

In order to compare catalytic activity within the same group, Choi *et al.*, explored the catalytic activity of GaCl$_3$ under similar reaction conditions (Scheme **1.21**).[19] The system exhibited comparable efficiency at lower catalyst loading (1 mol% instead of 5 mol%) and shorter reaction times but functional group tolerance was diminished. In the case of nitroaryl substrate, a low yield of methylene product was obtained and a significant amount of ether adduct was detected. The proposed mechanism involves a carbocation intermediate formed by desiloxylation of an intermediate silyl ether which can further react with another substrate to produce an ether or be protonated by the hydride from excess Me$_2$SiClH.

23
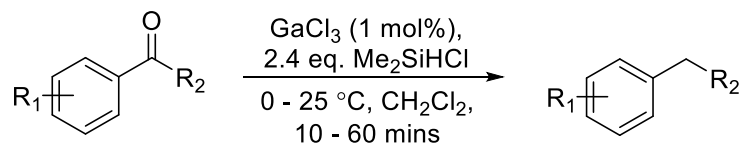
Scheme 1.21 Deoxygenation by GaCl$_3$ under hydrosilylation conditions.

The latest indium-catalyzed deoxygenation of aromatic ketones was reported in 2011 by Sakai *et al* (Scheme **1.22**).[100] Upon optimizing reaction conditions it was discovered that the combination of InBr$_3$ and Et$_3$SiH in CHCl$_3$ yielded the best results within an hour, although aliphatic ketones were only reduced to alcohols. When electron-withdrawing or ortho-substituents were present on the phenyl ring, silyl ethers were obtained instead of the desired hydrocarbon products. Interestingly, when InBr$_3$ was premixed with the silane for an hour prior to the addition of the substrate, symmetrical ethers were obtained as sole products.
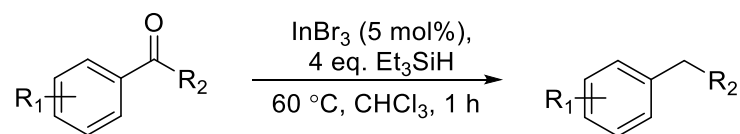
Scheme 1.22 Deoxygenation by InBr$_3$ catalyst under hydrosilylation conditions.

Ketone deoxygenation by post-transition metal halides was thus facile at ambient or relatively low temperatures and low catalyst loading. However, poor performance in the presence of electron withdrawing functional groups and relatively high costs of alkylsilanes could be considered a significant drawback. Polymethylhydrosiloxane represents a nearly ideal hydrosilylation reagent: it is mild, inexpensive, and readily available as a byproduct of the silicone industry. The first example of the use of PMHS in ketone deoxygenation under hydrosilylation conditions was published in 2002 by Chandrasekhar *et al* (Scheme **1.23**).[101] The authors used B(C$_6$F$_5$)$_3$, which was fairly unexplored as a Lewis acid prior to the rise of FLPs, to

activate PMHS. Both alkyl and aryl ketones were deoxygenated in 80 – 90 % yield within 20 mins.

$$R_1 \overset{O}{\underset{}{\parallel}} R_2 \quad \xrightarrow[\substack{25\,°C,\ CH_2Cl_2, \\ 5\text{ - }20\ \text{mins}}]{\substack{B(C_6F_5)_3\ (5\ \text{mol\%}), \\ 3\ \text{eq. PMHS}}} \quad R_1 \diagdown R_2$$
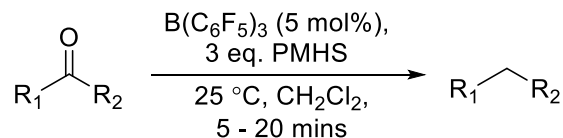
Scheme 1.23 Ketone deoxygenation under hydrosilylation conditions catalyzed by $B(C_6F_5)_3$.

The Lewis acidic character of $FeCl_3$ was successfully exploited in ketone deoxygenation by Dal Zotto *et al* (Scheme **1.24**).[102] $FeCl_3$ represents an inexpensive and abundant alternative to noble metal catalysts so it has been widely investigated for various catalytic procedures. The Zotto group discovered that $FeCl_3$ can efficiently assist in the cleavage of C–O bond in carbonyl compounds when exposed to microwave radiation. Good to excellent yields were obtained for aromatic ketones, even in the presence of *methoxy* substituents. Remarkably, aliphatic ketones were successfully deoxygenated as well, although in moderate yields. While the procedure is relatively mild and inexpensive, high temperature and external energy stimulus are required, thus introducing unnecessary complexity.
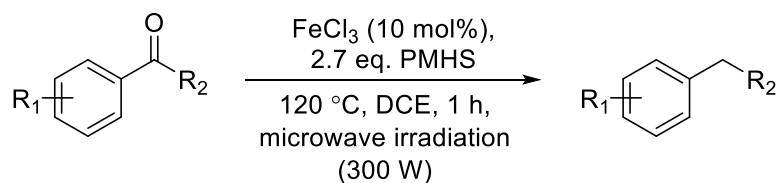
Scheme 1.24 Deoxygenation by $FeCl_3$ under hydrosilylation conditions.

Interestingly, the subsequent generation of catalysts to take advantage of PMHS reactivity were based on palladium. In 2011 Maleczka Jr. *et al.* reported that Pd-PMHS nanoparticles could successfully deoxygenate aromatic ketones in the presence of chlorobenzene (Scheme **1.25**).[20]

The authors proposed that hydrosilylation occurs in the first step to yield an alcohol. HCl, slowly generated from the reduction of PhCl, then assists Pd nanoclusters in the cleavage of the C–O bond. Investigation of various halide additives exhibited that chloride was necessary for deoxygenation, other halides led only to hydrogenation products. The reaction shows comparable results when trimethylsilyl chloride (TMSCl) is used instead of PhCl, however, the latter is a less expensive and a more inert option; chloroanisole was found to result in better yields for some substrates. Although the exact mechanism is still unclear, alcohols are produced exclusively in the absence of a chloroarene.
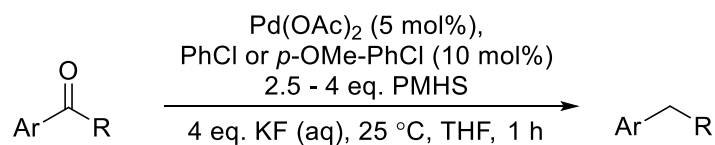
Scheme 1.25 Ketone deoxygenation by Pd-PMHS in the presence of chloroarenes.

A relatively similar system was reported by Wang *et al.* in 2013 (Scheme **1.26**).[103] The authors postulate that PMHS is halogenated upon reducing $PdCl_2$ to Pd^0. The halogenated byproduct is then assumed to react with the protic solvent to yield small amounts of HCl that assists Pd in the C–O bond cleavage. Compared to the procedure by Maleczka *et al.*, a less complex additive-free system offers significant advantages, although longer reaction times are required.
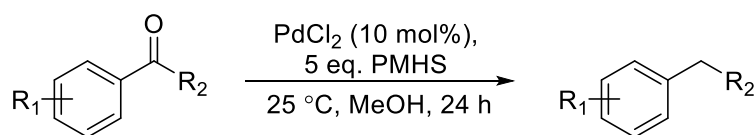
Scheme 1.26 Additive-free ketone deoxygenation by Pd-PMHS.

The first heterogeneous catalytic deoxygenation of aromatic ketones with PMHS was based on the same idea (Scheme **1.27**).[104] Initially, additive-free reactions were carried out, however, C–O

bond scission was determined to be the turnover limiting step. Compared to other acidic additives, PhCl provided the highest conversion and chemoselectivity under mild conditions. Deoxygenation of electron-rich ketones was facile but substrates with electron-withdrawing substituents or steric hindrance around the carbonyl group necessitated longer reaction times and/or higher temperatures to proceed. In case of the nitro substituent, reduction to the amine takes place prior to the carbonyl conversion.
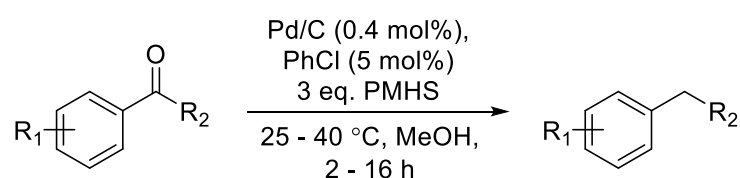
Scheme 1.27 Heterogeneous ketone deoxygenation by Pd/C-PMHS.

Overall, Pd-PMHS catalytic systems exhibit remarkable activity in the presence of acidic additives capable of controlled release of HCl. Nonetheless, the use of scarce and expensive palladium presents a significant drawback despite short reaction times and mild conditions.

High valence oxo-rhenium complexes have demonstrated high activity and chemoselectivity in the hydrosilylation of ketones and aldehydes.[105] Recently, the Fernandes group reported Re and Mo catalysts for deoxygenation of aromatic ketones with silane reductants (Fig. **1.3**).[106-109] Initial investigation into different oxo-Re catalysts revealed that Re^V exhibits higher reactivity towards deoxygenation than Re^{VII}, and the use of Cl ligand was superior to other halides. The highest conversion to deoxygenated products was observed when PhSiH$_3$ was used as a reducing agent.
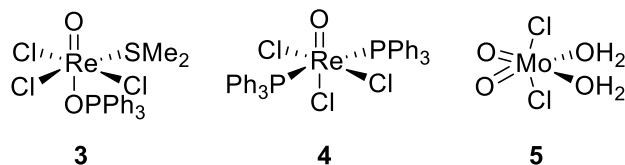
Figure 1.3 High valence Re and Mo catalysts.

Although the overall conversion was good, a mixture of alkanes and alkenes was obtained with both rhenium catalysts under hydrosilylation conditions (Scheme **1.28a**).[108] The problem was partially solved by using 2-propanol as a reducing agent; under these conditions, the procedure yielded alkenes exclusively (Scheme **1.28b**).[106] However, the reactions had to be performed at high temperatures, well above the boiling point of 2-propanol.
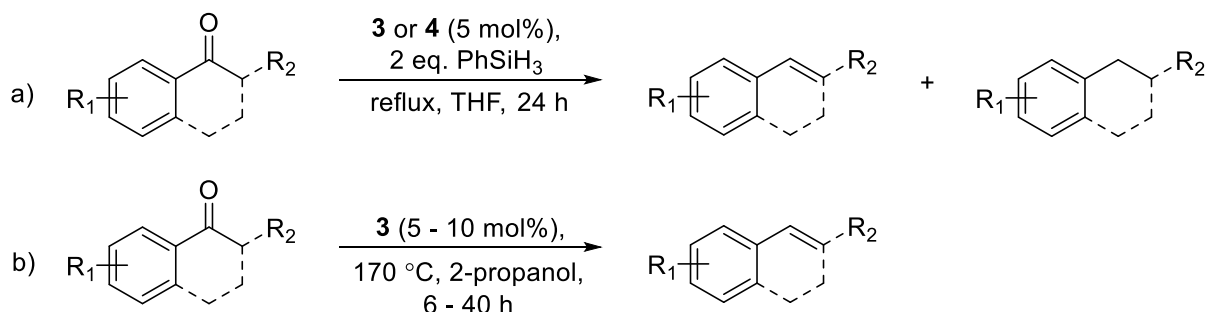
Scheme 1.28 Deoxygenation of aromatic ketones by Re catalysts.

Screening of molybdenum catalysts and silanes revealed that The Mo^{IV} complex **5** exhibits the highest catalytic activity in combination with PhSiH$_3$. Reaction conditions can be adjusted to selectively synthesize alkenes (Scheme **1.29a**)[107] or alkanes (Scheme **1.29b**).[109]
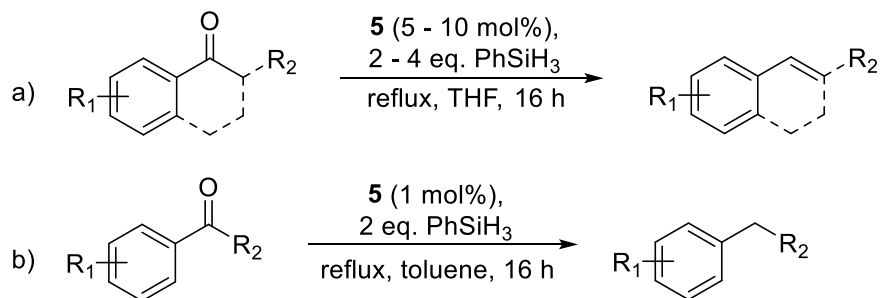
Scheme 1.29 Deoxygenation of aromatic ketones by Mo catalyst.

The efficiency of the deoxygenation was also affected by the nature of the substrate. Substrates with electron-withdrawing substituents resulted in lower yields and in some cases necessitated longer reaction times. Electron-donating substituents led to good to excellent conversions. Overall, while high valent oxomolybdenum and oxorhenium complexes show tunable activity for ketone deoxygenation, relatively harsh conditions are required. In addition, PhSiH$_3$ is relatively expensive compared to other silanes such as PMHS and is known to show some activity for carbonyl deoxygenation in a catalyst-free environment.[110] Therefore, it may not be the most suitable reagent for such catalysis.

The Stephan group has investigated highly electrophilic phosphonium cations as Lewis acid catalysts for ketone deoxygenation.[111] Given the success of catalytic B(C$_6$F$_5$)$_3$ in direct C–O hydrogenolysis using molecular hydrogen and PMHS, the reactivity in the phosphonium series was investigated using Et$_3$SiH. Interestingly, while >99 % conversion was observed, silyl ethers were synthesized selectively, thus highlighting the influence of the silane in such reactions. Cationic P^V Lewis acids with high electrophilicity were screened and exhibited high activity towards deoxygenation. Cationic precatalysts **6** and **7** were chosen for optimization of reaction conditions and substrate scope analysis (Fig. **1.4**). Deoxygenation of aromatic ketones was found

to be facile under mild conditions, giving excellent yields (Scheme **1.30a**). Halogen substituents on the aromatic rings were well-tolerated.
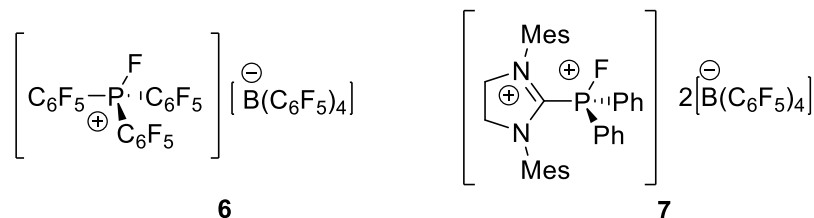
Figure 1.4 Cationic P^V Lewis acid catalysts.

Applying similar reaction conditions to aliphatic ketones led to mixtures of silyl ethers and alkanes or alkenes (Scheme **1.30b**). In most cases, deoxygenation products were obtained in <20% yields. This suggests that, as expected, ketones are first reduced to alcohols/silyl ethers and then subsequently deoxygenated to the corresponding methylene units, albeit slowly.
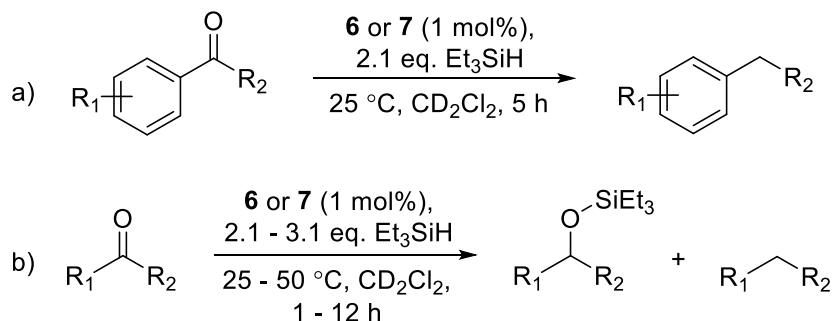
Scheme 1.30 Deoxygenation of ketones by cationic P^V Lewis acids.

Another excellent example of recent advances in transition metal-free deoxygenation of unsymmetrical diketones uses the NaI-TMSCl system (Scheme **1.31**).[112] Stoichiometric deoxygenation of di-ketones can be achieved by traditional methods such as Wolff-Kishner or Clemmensen reductions. Although more recent alternatives have been published,[113] the field has not received such broad attention as the defunctionalization of mono-ketones. In the work by

Yuan *et al.*, NaI was found to catalyze the regioselective deoxygenation of the C=O bond adjacent to the aryl group bearing electron-donating substituents. Interestingly, the reaction mechanism was proposed to proceed via a free radical pathway rather than the conventional reduction to alcohol followed by subsequent C–O bond hydrogenolysis.
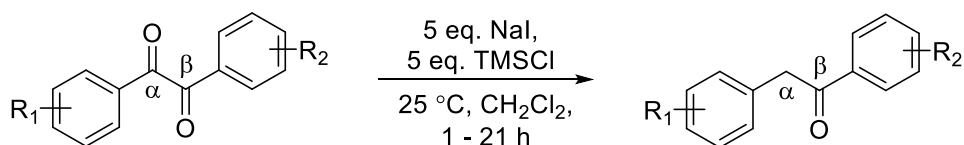
Scheme 1.31 Deoxygenation of diketones by NaI-TMSCl.

An investigation of additives revealed that the reaction only works in the presence of NaI; other sodium halides do not yield the desired conversion. HI has been reported to catalyze ketone deoxygenation (I_2 in H_3PO_4 media),[114] however, it was found not to be an active catalyst in the system described herein.

1.4 Conclusion

While catalytic deoxygenation of aliphatic ketones using hydrogen remains elusive, multiple procedures have been developed in the last two decades that deoxygenate aromatic ketones. Traditional methods such as Wolff-Kishner, Clemmensen and Raney Ni reductions and their recent modifications are still widely explored and applied. However, two main procedural pathways have emerged as strong alternatives.

Direct reductive deoxygenation with molecular hydrogen has been conventionally catalyzed by heterogeneous Pd or Pt systems. However, the toxicity, propensity for over-hydrogenation, and high costs associated with such catalysts has fueled research for more sustainable catalysts. The

most notable advancements include metal-mediated (Cu/SiO$_2$, Ni-phosphine and cationic Ru) C–O bond cleavage as well as hydrogenolysis catalyzed by frustrated Lewis pairs. Cu/SiO$_2$ represents a very mild, inexpensive and efficient procedure, yet reproducibility issues have been noticed both in literature[85] and in our own group. Nickel-catalyzed deoxygenation necessitates high temperatures and multi-day reaction times. Despite the high activity of the cationic ruthenium catalyst, the necessity for phenol ligands with varied electronic properties, the high costs of the catalyst, and the homogeneity of the system poses issues (such as recyclability) for large-scale applications. Although heterolytic activation of H$_2$ by FLPs represents a significant breakthrough in chemistry and is of high importance in fundamental research, the application of B(C$_6$F$_5$)$_3$-mediated catalysis on a large scale is hindered by the high costs and poor availability of boron-based Lewis acids.

Ketone deoxygenation under hydrosilylation conditions does provide high efficiency under very mild conditions and short reaction times, as compared to hydrodeoxygenation. However, the high loadings of silanes and Lewis acidic additives pose purification and recyclability issues. PMHS-Pd systems offer the highest conversions and selectivity while simultaneously employing the most convenient silane source; the procedures require *in situ* synthesis of a Lewis acid co-catalyst and are hampered by the cost of palladium. FeCl$_3$ offers a significantly less expensive alternative but necessitates harsh conditions and an external energy stimulus. Main group catalysts with high Lewis acidity offer good selectivity, short reaction times at ambient temperature and do not necessitate additives. Although PMHS works very well in the presence of expensive B(C$_6$F$_5$)$_3$, not only a more expensive Et$_3$SiH is used for phosphonium catalysts but the counterions ([B(C$_6$F$_5$)$_4^-$]) present an economical issue as well. Finally, even though NaI-TMSCl

procedure has high potential, it has not yet been explored for the reactivity towards monoketones.

Therefore, inexpensive and efficient ketone deoxygenation is still an issue for a large-scale synthesis of fine chemicals. Since high purity is one of the main requirements in pharmaceutical industry, direct hydrogenolysis with molecular hydrogen has a significant advantage over deoxygenation under hydrosilylation conditions. Based on previous research, the most economical and potentially effective approach is the use of first row transition metal catalysts. The current challenge can be solved by high-activity homogeneous hydrodeoxygenation (HDO) catalysis or the development of less-sensitive heterogeneous catalysts that yield reproducible results.

While nickel, copper and iron have been applied to catalytic deoxygenation, reactivity of cobalt in carbonyl HDO has not been reported until now. The work in this thesis is focused on the catalytic hydrodeoxygenation of aromatic ketones mediated by cobalt clusters. The challenges in precatalyst synthesis, optimization of reaction conditions, and substrate scope will be discussed in the following chapters.

Chapter 2. Design, synthesis and characterization of cobalt clusters bridged by triphenylphosphoranimide and triisopropylphosphoranimide ligands

2.1 Rationale

Despite high costs, scarcity and toxicity, the industrial synthesis of complex molecules is still dominated by highly reactive noble metal catalysts.[115-116] This is especially pronounced for reductive reactions that involve activation of molecular hydrogen[117] and hydrogenolysis of high energy bonds.[115, 118] Late first row transition metals are abundant, relatively inexpensive, and less toxic, presenting a more attractive alternative. However, the weaker M–H bond energy (when M = Fe, Co, Ni, Cu) compared to that of noble metals (Table **2.1**),[61] coupled with the strength of the H–H bond, leads to difficulties in hydrogen activation and formation of hydride intermediates in many hydrogenolysis reactions. Although homogeneous copper, nickel, cobalt and iron complexes have been explored for a variety of catalytic transformations, including carbonyl reduction to the alcohol,[119] applications to ketone deoxygenation have been scarce. Only recently, Ni and Cu complexes have been applied to hydrodeoxygenation of aromatic ketones,[84, 87] while ferric chloride ($FeCl_3$) has shown comparable reduction activity under hydrosilylation conditions.[102] However, reports on chemoselective *cobalt*-catalyzed hydrogenation and hydrosilylation in such a context are absent from the literature. Therefore, the work described in this thesis is focused on the design and catalytic reactivity of coordinatively unsaturated cobalt clusters for applications to reductive catalysis.

Table 2.1 Select M–H bond energies.[61]

M–H	Fe–H	Co–H	Ni–H	Cu–H	Ir$^+$–H	Pt–H	Au–H
Bond energy, [kcal/mol]	35	43	56	60	72	79	69

Industrial synthesis relies on both homogeneous and heterogeneous catalysts. In homogeneous systems, the catalyst is in the same reaction medium as the substrate(s), reagents, and product(s), whereas heterogeneous catalysts are in a different phase than the reactants.[120] Although both processes share many shortcomings such as catalyst poisoning, each method differs through distinct advantages and disadvantages (Table **2.2**). Defined homogenous catalysts can provide high chemo-, stereo- and regio-selectivity in hydrogenation reactions but they are disadvantaged by a limited application range. Defined soluble catalytic centres allow for determination of reaction mechanisms and facile structural adjustments to improve catalytic performance. In addition, equivalent dispersion of the catalyst molecules and identical activity from all the metal centres enables consistent reaction conditions and low catalyst loadings. However, difficulties in catalyst separation from the reaction media cause recyclability issues, increased catalyst loss, and product purification issues.[118, 120]

In contrast, heterogeneous catalysts are readily separated from the reaction mixtures and recycled, resulting in minimal catalyst losses and lower costs. Harsh reaction conditions are better tolerated due to the thermal stability of most supported metal catalysts, and the ligand-free transition metal environment generally allows for a broad range of applications. Nevertheless, the incompletely defined, multi-site catalyst structures often lead to low selectivity and complications in determining and understanding the reaction pathways. High catalyst loadings

can be required to attain a sufficient number of coordinatively unsaturated surface sites active for catalytic transformations.[120-121]

Table 2.2 Comparison of homogeneous and heterogeneous catalysts.[120]

Feature	Homogeneous catalysts	Heterogeneous catalysts
Selectivity	High	Low
Reaction conditions	Mild	Harsh
Active centres	All metal atoms	Surface sites
Structure and stoichiometry	Defined	Undefined
Thermal stability	Low	High
Application range	Limited	Broad
Recycling	Challenging	Easy
Catalyst – product separation	Difficult	Easy

At this stage, homogeneous catalysis is better suited to chemoselective deoxygenation of ketones in fine chemicals synthesis. Nevertheless, most industrial hydrodeoxygenation catalysts are heterogeneous due to scale requirements, ease of recyclability and extended lifetimes. Although the cost efficiency of such procedures presents a significant advantage, heterogeneity inhibits the development of more efficient alternatives, a consequence of uncontrolled synthesis and poorly determined reaction mechanisms. To date, only two viable homogeneous ketone deoxygenation procedures have been reported. Reactions catalyzed by bisphosphine nickel complex **1** require harsh conditions, are too slow for industrial application and may actually be heterogeneous.[87] Cationic ruthenium catalyst **2** is expensive and necessitates additives to cleave the C–O bond, resulting in high costs and high catalyst losses (Fig. **2.1**).[88]
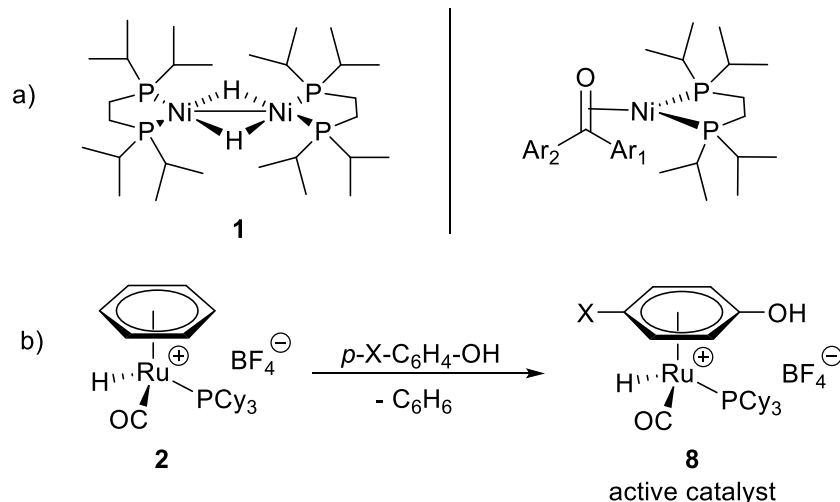
Figure 2.1 Examples of literature catalysts for hydrodeoxygenation of ketones.

An inexpensive and efficient homogeneous catalyst for ketone deoxygenation/hydrogenolysis is highly desired. For the initial phase of our research, homogeneous catalysts are targeted to allow for facile modification of the catalyst centre and initial mechanistic determination. Subsequently, the optimized catalyst can in principle be grafted onto silica or alumina, retaining high chemoselectivity while allowing for facile product separation and catalyst recycling.[122]

2.2 Catalyst design principles

Catalysis is reliant on vacant coordination sites at the metal centre(s) that facilitate substrate binding.[117-118, 123] A common strategy employs the dissociation of dative ligands to yield the active catalyst. Not only does this approach necessitate the use of ligands that do not play a direct role in the catalytic cycle but dissociation may be irreversible and can lead to catalyst decomposition in its resting state. The dissociation is also strongly affected by the properties of other supporting ligands as evidenced by the development of well-known Grubbs catalysts.[124-130] In this case, the trans-influence and trans-effect play significant roles in the formation of the

active catalyst. Likewise, the coordinated ligands strongly affect the reaction mechanism: for example, hydrogenolysis of the C–O bond by complex **2** is only possible when *in situ* replacement of a η^6-benzene ligand by a phenol additive takes place (Fig. **2.1b**).[88]

A second approach employs 'bulky' ligands to create sterically-enforced coordinative unsaturation around the metal centres.[131] Although the need for supporting ligands and dissociation is eliminated, the sterically crowded environment can inhibit substrates from accessing the metal centre. A careful choice of ligands is thus necessary to prevent the steric inhibition of the catalytic reaction. Importantly, careful steric control of the metal catalysts allows us to design polymetallic clusters that resemble the coordinatively unsaturated surface sites in heterogeneous catalysts.[117, 121, 132-133] Metal cooperation within the polymetallic clusters alleviates the burden of carrying out a full catalytic cycle for a single metal centre. Specifically, for late 1st row transition metals, the requirement for high oxidation states [e.g., Ni(IV)] in reactions that proceed through oxidative addition is then removed.[134] For example, sterically large bisphosphine ligands stabilize the dimeric Ni precatalyst **1** and allow for the formation of the catalytically active monomeric species (Fig **2.1a**). This strategy was thus used to design new cobalt clusters for the catalytic hydrogenolysis of the C=O bonds.

Dative bonding, ease of stabilizing precatalysts and reasonable control of the ligand sphere led to the prevalence of phosphine ligands in homogeneous catalysis. Modification of the phosphorus substituents allows for precise steric and electronic adjustments according to ligand cone angle characterization and electronic measurements.[131, 135-136] Consequently, a vast array of phosphine ligands is accessible for use in catalyst design. However, the 'steric bulk' of the phosphines

manifests directly at the phosphorus centre, close to the coordination centres, while phosphines are also unlikely to act as bridging ligands and form polymetallic clusters. [123, 136-137]

2.2.1 Anionic phosphoranimide supporting ligands: versatile bonding and steric influence

The phosphoranimide ligand $[NPR_3]^-$, also known as phosphoraneiminato or phosphinimide, was originally reported by Staudinger and Meyer in 1919.[138] Research into phosphoranimide properties and complexes with transition metals followed soon after.[139-141] The interest in the ligand was propelled by its versatile bonding modes, high thermal stability, and electronic properties that can be readily tuned by changing the nature of phosphorus substituents.

The monoanionic $[NPR_3]^-$ unit is usually isolated as an alkali metal salt and is isoelectronic to a variety of ligands such as $[Cp]^-$, $[OSiR_3]^-$, $[OCR_3]^-$, $[OPR_3]^-$, and $[NSiR_3]^-$. The $[NPR_3]^-$ ion lies structurally between the resonance forms depicted in Figure **2.2**. In resonance structure A, the ligand acts as a 4-electron donor and can form two bonds to a coordinated metal centre. In structure B, the zwitterion contains higher electron density on nitrogen and can accommodate up to three M–N bonds *via* 6-electron donation.
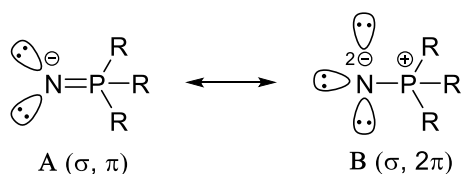
Figure 2.2 Lewis resonance structures of phosphoranimide ligands.

While the discrete anion is not known, the alkali metal salts have been obtained as tetrameric[142] or hexameric[143] structures depending on the substituent size.[144-145] When coordinating to transition metals, phosphoranimide bonding modes are primarily governed by the oxidation state

of the metal centre (Fig. **2.3**). Metals in high oxidation states with empty d orbitals can participate in bonding mode **A** with a terminal phosphoranimide ligand acting as a 6-electron donor (σ, 2π). Examples include $[ReO_3(NPPh_3)]$[146] **9**, $[WCl_5(NPCl_3)]$[147] **10** and $[MoNCl_3(NPPh_3)]_2^-\cdot C_7H_8$ **11**.[148] In mode **B**, the $[NPR_3]^-$ moiety donates four electrons to the metal centre (σ, π) and retains a lone pair on the nitrogen atom. Therefore, a M–N–P bond angle of ~160° is observed for complexes such as $[WCl_4(NPCl_3)_2]$ **12**.[147] Low or medium oxidation state metals lead to ligand bridging and mixtures of different bonding modes (e.g. **A/B** or **A/D**), as evidenced by $[Mo(NPPh_3)_4]^{2+}$ **13** (bonding modes **A** and **B**). Unsymmetrical or symmetrical bonding takes place when $[NPR_3]^-$ donates six electrons and acts as a μ^2-bridging ligand to coordinate to two metal centres. When the phosphoranimide ligand acts as an unsymmetrical μ^2-bridging ligand (mode **C**), different bond lengths to the metal are observed (e.g. 1.84 and 2.01 Å in $[TiCl_3(NPMe_3)]_2$ **14**).[149] In complexes with symmetrical bridging such as $[FeCl_2(NPEt_3)]_2$ **15** (mode **D**), equal bond lengths to the metal centre are detected (1.91 Å).[150] Lastly, metals in low oxidation states with occupied d orbitals form only single bonds (σ) with the phosphoranimide (mode **E**). In this case, the phosphoranimide moiety generally acts as μ^3-bridging ligand, as evidenced by heterocubane clusters $[NiCl(NPMe_3)]_4$ **16**[151] and $[CoI(NPMe_3)]_4$ **17**.[152]
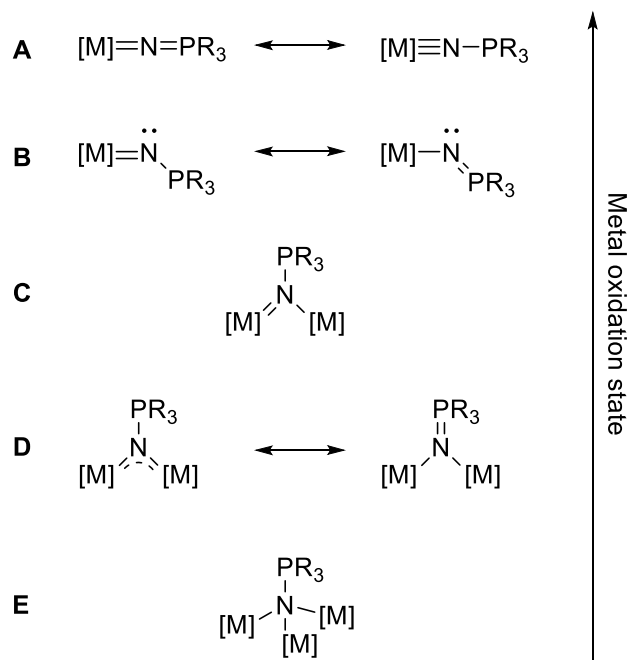
Figure 2.3 Binding modes of phosphoranimide ligands.

The structures of metal phosphoranimide clusters of the same oxidation state are also affected by the steric size of the phosphorus substituents and the ligand environment around the metal centre (Fig. **2.4**). Heterocubane structures with μ^3-bridging [NPR$_3$]$^-$ ligands are obtained when substituents are small (R=Me, Et), e. g., [CoCl(NPMe$_3$)]$_4$ **18**.[152] In contrast, large substituents such as R = *tert*-butyl form binuclear clusters with only μ_2-bridging [NP^{t}Bu]$^-$ ligands (e.g. [CoCl(NP^{t}Bu$_3$)]$_2$ **19** and [Mg$_2$(μ_2-NP^{t}Bu$_3$)$_2$(NP^{t}Bu$_3$)$_2$] **20**).[153] Lastly, substituents of intermediate steric bulk (^{i}Pr or Ph) drive the formation of trimeric structures such as reported for [Mg$_3$(μ_2-NP^{i}Pr$_3$)$_4$(NP^{i}Pr$_3$)$_2$] **21**.[154]
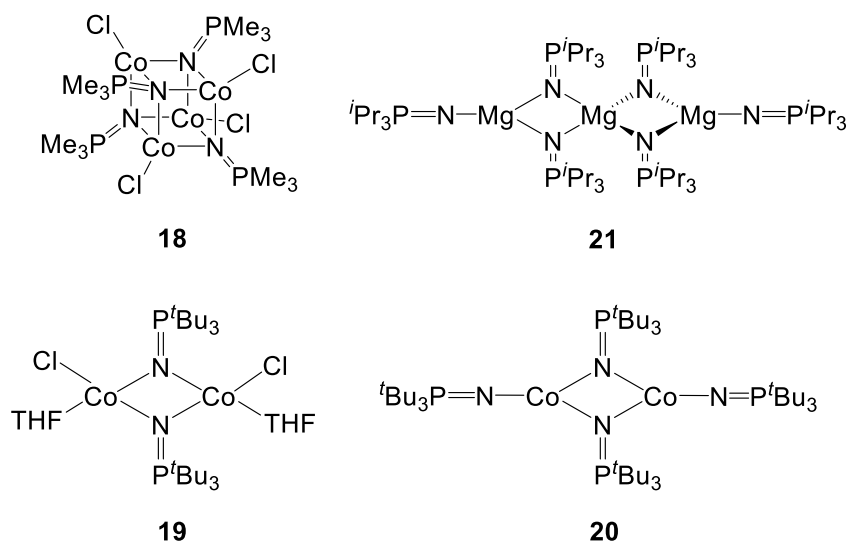
Figure 2.4 Structures illustrating the effect of the size of phosphorus-bound substituents.

The concept of tunable 'displaced steric bulk' is one of the most attractive characteristics of the phosphoranimide moiety. Tolman cone angle comparison between isolobal cyclopentadienyl and *tert*-butylphosphoranimide ligands reveals similar volume being occupied by both ligands (Fig. **2.5**).[131] Yet, the 'extra' nitrogen atom in the phosphoranimide ligand leads to the distancing of the metal and the 'steric bulk' of the ligand. This 'remote steric effect' is paramount in our catalyst design because it allows substrate binding and reactions on a metal that is relatively unhindered by the supporting ligands. In the case of the phosphoranimide ligand, the steric factor can be readily adjusted by the choice of substituents.
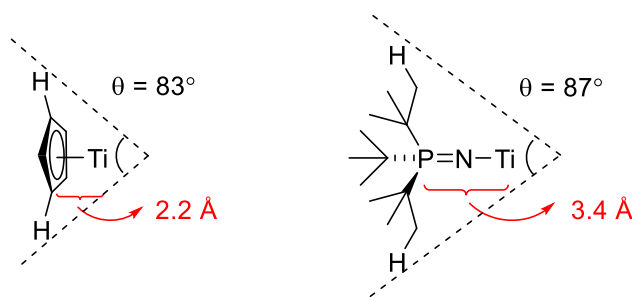
Figure 2.5 Tolman cone angles of Ti-Cp and Ti-NP^{t}Bu fragments.[155]

42

Phosphorus substituents also play a significant role in the electronic environment around the coordination centre. Whereas electron rich alkyl groups (e.g. *tert*-butyl, *iso*propyl, ethyl) indirectly donate electron density to the metal centre, making it more nucleophilic, electron-withdrawing aryl substituents (e.g. phenyl) increase the electrophilic character of the metal centre. This affects the bonding of other ligands as well as the reactivity of the clusters: while nucleophilicity of the metal centres increases the affinity for H–H bonds and favours catalytic steps such as oxidative addition, electrophilic character promotes the reductive elimination required to release the reaction products (Fig. **2.6**). As both oxidative addition and reductive elimination are prevalent in a variety of catalytic reactions, subtle changes in the phosphorus substituents affect the reaction mechanism and control the catalytic turnover and the reaction outcome.
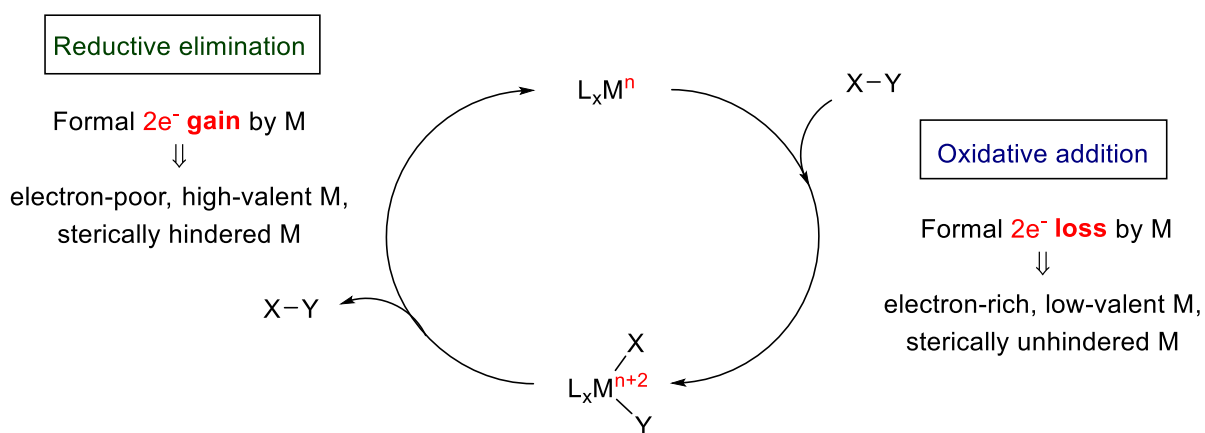
Figure 2.6 Representation of oxidative addition and reductive elimination steps in a catalytic cycle.

2.2.3 Previous work in Stryker Group

The coordination chemistry of phosphoranimide complexes has garnered substantial attention over the years.[140-141] The most significant advances in the field were made by the Dehnicke[141, 143,]

[156-158] and Stephan groups.[154, 159-160] Unfortunately, the lack of standardized procedures for ligand and complex preparation leaves the reactivity of such complexes largely unexplored. Initially, Dehnicke *et al.*, developed a molten trimethylsilyl-trialkylphosphoranimide/metal salt metathesis procedure for cluster synthesis (Scheme **2.1**). However, the necessity of hazardous azides, low and variable yields, and purification issues render the procedure inefficient.[141] In addition, this method only works for small and low-melting silylphosphoranimides such as $[NPMe_3]^-$ and $[NPEt_3]^-$.

$$MX_2 \xrightarrow[\text{160 - 210°, 2 - 5 h}]{\substack{\text{3 - 7 eq. } Me_3SiNPR_3, \\ \text{4 - 10 eq. KF}}} 0.25$$

M = Fe, Co, Ni Zn
X = Cl, Br, I
R = Me, Et
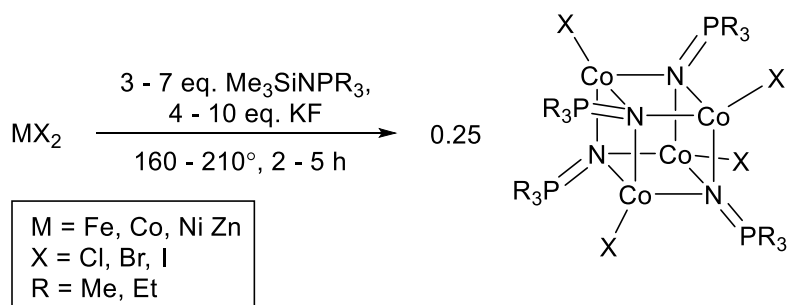
Scheme 2.1 Dehnicke procedure for phosphoranimide cluster synthesis.

Dr. Robin Hamilton in the Stryker group took a different approach.[161] The synthesis of secondary amines *via* triphenylphosphinimines was first reported in 1970[162] and proved to be readily adaptable to the synthesis of common phosphoranimide ligands, except $^tBu_3P$. Although the exact pathway is dependent on the phosphorus substituents, the new procedure avoids the use of hazardous azides and allows for an amenable scalability (Scheme **2.2**). In the first step, a variety of less polar solvents (e.g. CH_2Cl_2, toluene, Et_2O etc) can be used to convert the phosphine to the dibromophosphorane *i*. The solvent choice is dictated by the phosphorus substituents and the solubility of the resulting phosphines and phosphoranes. The subsequent reaction step is also governed by the phosphorus substituents. Sterically smaller phosphoranimide salts are synthesized in a one-pot reaction: the phosphoranium salt *ii* is produced *in situ* from a reaction

with potassium amide, itself generated from liquid ammonia and KH. The salt is further deprotonated *in situ* to form the potassium phosphoranimide (Scheme **2.2a**). An easier, albeit longer two-step synthesis can be carried out for more sterically demanding phosphoranimide ligands (Scheme **2.2b**). In the first step, the phosphoranium salt *ii* is produced and isolated from a reaction with one equivalent of lithium amide. The isolated product is then deprotonated using excess NaH and $NaNH_2$ to yield the sodium phosphoranimide. The latter method requires isolation of the intermediates but the ammonia-free procedure is operationally simpler.

$$PR_3 \ + \ Br_2 \xrightarrow{\text{solvent, rt, overnight}} R_3PBr_2 \quad \textit{i}$$

a) $R_3PBr_2 \xrightarrow[\text{NH}_3 \text{ (l), rt, overnight}]{\text{4 eq. KH}} KNPR_3$ ⎯ $R = Me, Et, {}^nBu$

b) 1. $R_3PBr_2 \xrightarrow[\substack{\text{Et}_2\text{O or THF, rt,} \\ \text{overnight}}]{\text{LiNH}_2} [R_3PNH_2]Br \quad \textit{ii}$ ⎯ $R = Ph, Cy, {}^iPr$

2. $[R_3PNH_2]Br \xrightarrow[\text{THF, rt, overnight}]{\substack{\text{1. 6 eq. NaH} \\ \text{2. 3 eq. NaNH}_2}} NaNPR_3$
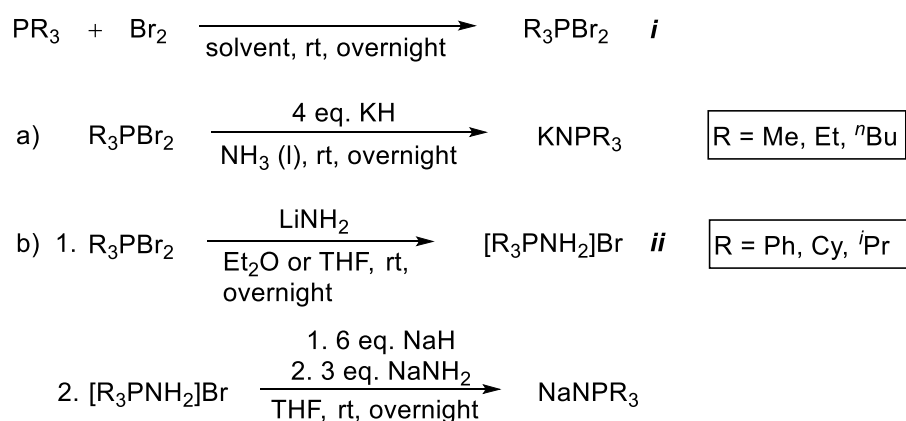
Scheme 2.2 Phosphoranimide synthesis developed in the Stryker group.

The new ligand preparation route allows for the efficient syntheses of most phosphoranimide ligands in high yields (80-90%). Consequently, the group successfully synthesized known and new late first-row transition metal phosphoranimide clusters by salt metathesis between solubilized metal halides and alkali metal phosphoranimide salts.[153, 161, 163-166] As expected, the nuclearity of the cluster was dependent on the metal oxidation state, stoichiometry, and steric properties of the phosphoranimide ligands, as illustrated (Fig. **2.7**).
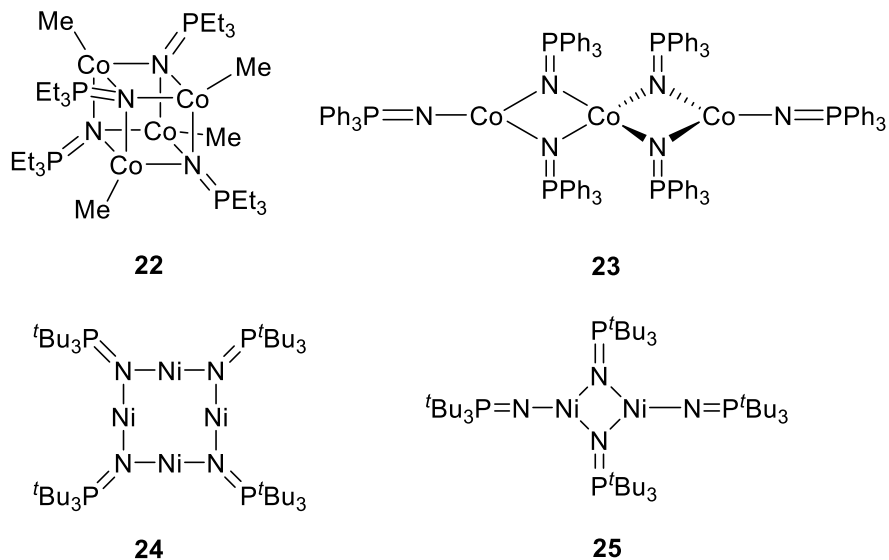
Figure 2.7 Selected phosphoranimide clusters synthesized in the Stryker group.

Clusters such as **22**, **24** and **25** were investigated as precatalysts in hydrogenation reactions and hydrogenolysis of carbon–heteroatom bonds. Promising reactivity was observed.[153, 163, 165]

2.2.4 Phosphoranimide ligands with intermediate sized substituents

Although complexes of varied steric bulk have been synthesized by the group, catalytic investigations centred on the use of triethyl- and tri-*tert*-butylphosphoranimide clusters of nickel, cobalt, and iron. The reactivity of trimetallic compounds such as $[Co_3(\mu_2\text{-}NPPh_3)_4(NPPh_3)_2]$ **23** was not explored in detail. Research into the use of phosphoranimide ligands with intermediate sized substituents would 'fill in the gap' and allow us to determine the influence of intermediate steric factors, diminished electron-richness, and unique *collinear* structure in catalytic reactivity.

Triphenylphosphine and triisopropylphosphine have similar Tolman cone angles (Fig. **2.8**)[135] and their respective phosphoranimide counterparts form trimetallic clusters (e.g. **21**, **23**).

Consequently, it can be assumed that both phosphoranimide ligands occupy a similar volume in space.
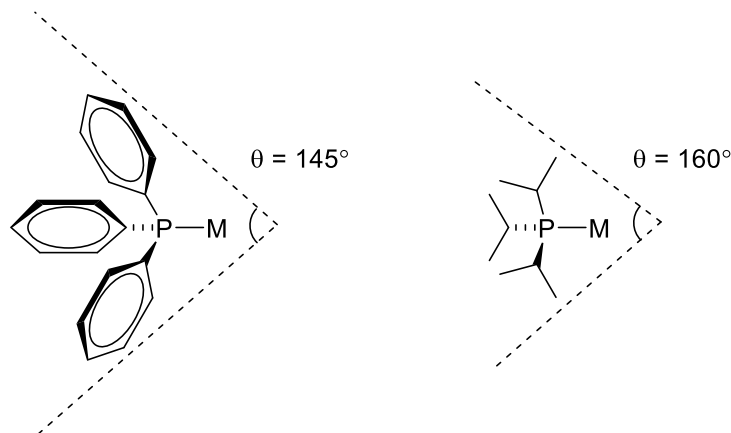
Figure 2.8 Tolman cone angle comparison between triphenylphosphine and triisopropylphosphine ligands.

Nevertheless, the ligands have significantly different electronic properties.[131] Manipulation of the phosphorus substituents within a similar size range would permit direct investigation of the influence of electronic factors in ketone deoxygenation and may also allow for the determination of the turnover limiting step. The work in this thesis, however, is not a direct mechanistic study. Instead, we focus on optimization of precatalyst for hydrogen activation, reaction scope, and catalytic conditions.

Both phosphoranimide ligands are readily synthesized according to the ammonia-free procedure (Scheme **2.2b**). Triphenylphosphoranimide ligand is advantageous: triphenylphosphine is an inexpensive, solid and air-stable phosphine.[167] In contrast, triisopropylphosphine is expensive, pyrophoric, and volatile; hence, conversion to the phosphoranimide is more hazardous, more time-consuming, and requires more safety precautions.[168]

The homoleptic triphenylphosphoranimide cobalt cluster **23** was first synthesized and characterized by Dr. Robin Hamilton (Fig. **2.9**).[164] As expected for cobalt(II), the phosphoranimide ligands in the trimer adopt a mix of coordination modes. Symmetrical μ^2-bridging is observed for four ligands that link the three cobalt (II) centres (Fig. **2.3**, mode **D**), while two display terminal coordination to the outer cobalt atoms, each with a Co–N–P angle of 163.4° (Fig. **2.3**, mode **B**). Although the cluster is easily synthesized in a one-step procedure (Scheme **2.3**), it suffers from low solubility. Therefore, extraction and use are confined to tetrahydrofuran (THF) and aromatic solvents.

a)

23

b)
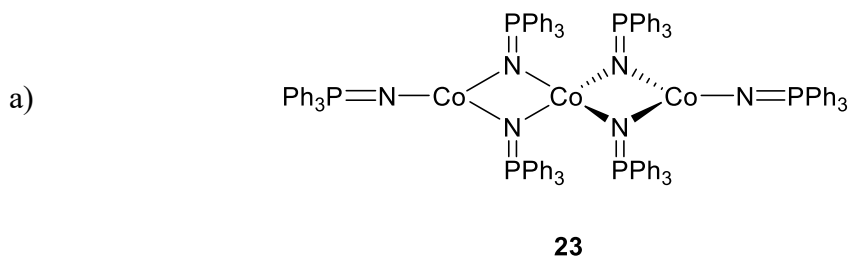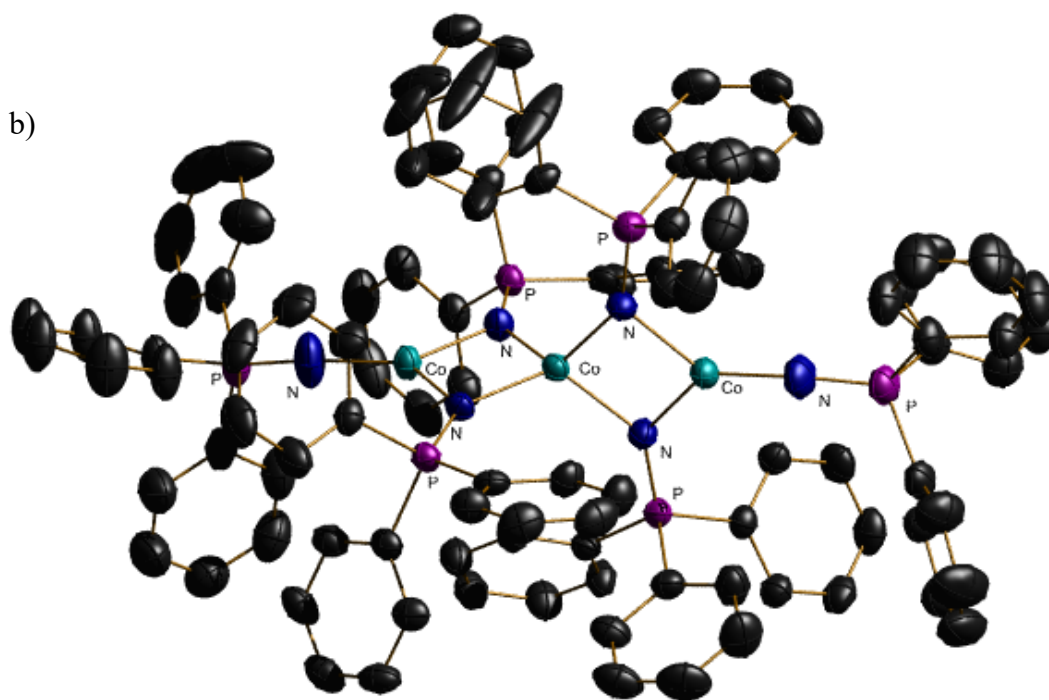
Figure 2.9 a) Structure of $[Co_3(\mu_2\text{-}NPPh_3)_4(NPPh_3)_2]$ **23**, b) ORTEP diagram of **23** with non-hydrogen atoms represented by Gaussian ellipsoids at 20% probability. Hydrogen atoms have been omitted for clarity.

$$CoBr_2 \xrightarrow[\text{THF, overnight}]{Ph_3PNNa} [Co_3(\mu_2\text{-}NPPh_3)_4(NPPh_3)_2]$$
23
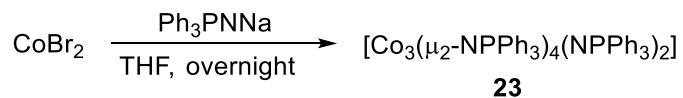
Scheme 2.3 Synthesis of $[Co_3(\mu_2\text{-}NPPh_3)_4(NPPh_3)_2]$ **23**.

2.3 Results and discussion

2.3.1 Co(I) clusters bridged by triphenylphosphoranimide ligands

Initially, our aim was to synthesize a monovalent, homoleptic tetrametallic cobalt cluster $[Co(NPPh_3)]_4$ **26** analogous to the two-coordinate copper analogue, $[Cu(NPPh_3)]_4$ **27**.[169] A procedure developed by Dr. Camacho-Bunquin for the synthesis of $[Ni(NP^tBu_3)]_4$ **24**[153, 166] was

adapted for this purpose (Scheme **2.4**). Unfortunately, competitive under- and overreduction with Na/Hg amalgam leads to irreproducible results. Similarly, the synthesis of rigorously pure [Co(NP$'$Bu$_3$)]$_4$ **28** also has not been be achieved within our group.[163, 170] In addition to the amalgam reduction, the use of organic reducing agents (e.g. 1,4-dihydro-1,4-bis(trimethylsilyl)-pyrazine) was also explored, with no success.

$$\text{CoX}_2 \xrightarrow[\text{-78 C} \rightarrow \text{0 °C, overnight}]{\text{Ph}_3\text{PN·Na·THF, dropwise}} \text{[Co(}\mu_2\text{-NPPh}_3\text{)X]}_2 \qquad \text{X = Cl, Br}$$

$$\text{[Co(}\mu^2\text{-NPPh}_3\text{)X]}_2 \xrightarrow[\text{rt, overnight}]{\text{1.1 eq 1\% Na/Hg}} \text{[Co(}\mu_2\text{-NPPh}_3\text{)]}_4$$

26
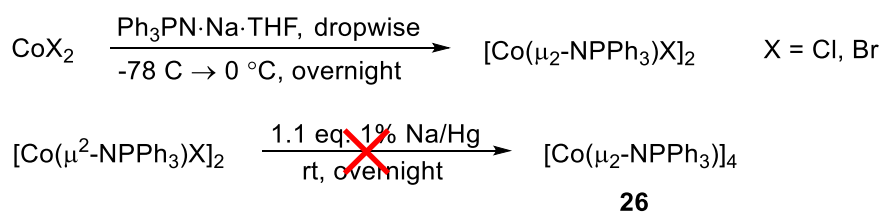
Scheme 2.4 Attempted synthesis of [Co(NPPh$_3$)]$_4$ **26**.

The main challenge in the first step of the synthesis is to avoid competitive formation of the bis(phosphoranimide) trimer **23**. Therefore, a slow addition of the triphenylphosphoranimide to a cold solution of CoCl$_2$ was used. The proposed intermediate [Co(μ^2-NPPh$_3$)Cl(THF)]$_2$ **29** has almost no solubility in common solvents (and very low solubility in THF), which causes difficulties in extraction and purification. Unfortunately, the paramagnetic nature of Co (II) makes it difficult to obtain and interpret meaningful NMR data; no information about the structure of the intermediate could be acquired.[171] Substituting the THF-soluble CoBr$_2$ slightly increases the solubility of the targeted bimetallic cluster [Co(μ_2-NPPh$_3$)Br(THF)]$_2$ **30** and allows for the synthesis at room temperature. The reaction produces the same results regardless of temperature and regardless if the ligand is added dropwise as a solution or all at once as a solid (Scheme **2.5**). The low solubility of the proposed intermediate **30** prevents successful isolation of pure material; further preparations were carried out *in situ* presuming a full conversion to **30**.
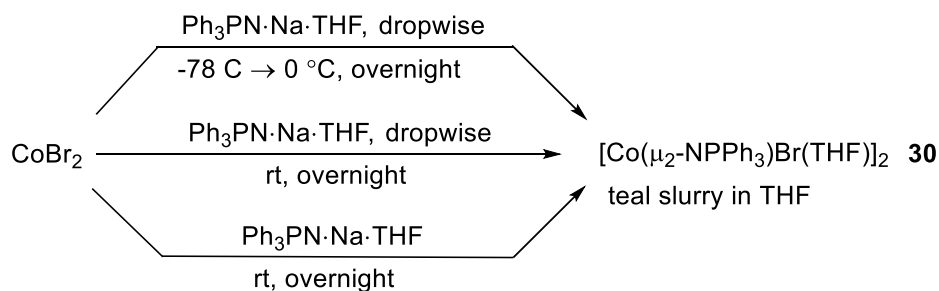
Scheme 2.5 Synthetic pathways to proposed intermediate **30**.

Characterization of complex **30** was challenging; the appearance of the slurry and the results of *in situ* reduction and further salt metathesis were used to determine the success of the synthesis. Work by Roesky group[172] and unpublished work reported by Jeremy Gauthier in the Stryker group[173] (Fig. **2.10**) leads us to believe that intermediate **30** is bimetallic, similar in structure to [Co(μ_2-NPPh$_3$)(HNPPh$_3$)Br]$_2$ **31**, with terminal halide and triphenylphosphoraniminium ligands. Four-coordinate cobalt and iron clusters with bridging triphenylphosphoranimide ligands tend to adopt dimeric structure. We presume that dative coordination of tetrahydrofuran stabilizes the dimeric unit in our complexes.

The reaction between CoBr$_2$ and sodium triphenylphosphoranimide in toluene yields a highly insoluble product that does not undergo further reduction with the Na/Hg amalgam. We suspect that the lack of dative solvent coordination leads to the formation of halide-bridged oligomers or structural rearrangements instead. Nevertheless, the lack of available characterization prevents us from making definitive conclusions.
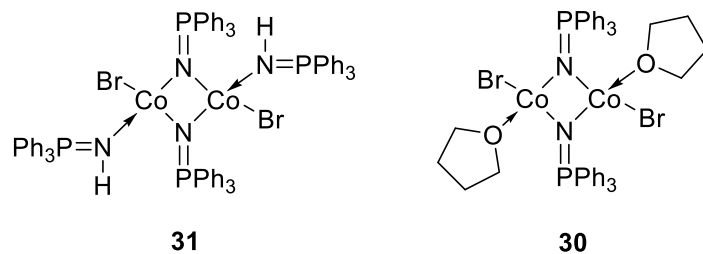
Figure 2.10 Structures of $[Co(\mu_2\text{-NPPh}_3)(\text{HNPPh}_3)\text{Br}]_2$ **31** and proposed $[Co(\mu^{2\text{-}}\text{NPPh}_3)(\text{THF})\text{Br}]_2$ **30**.

2.3.2 Synthesis of mixed-ligand Co(II) clusters

2.3.2.1 Rationale

Given that the reduction of cobalt(II) monophosphoranimide dimers was irreproducible, we shifted our efforts to expanding the array of 'hydrogenolysis ready' Co(II) clusters. Previous research in the group established conclusively that homoleptic bis(phosphoranimide) M(II) clusters (M = Fe, Co, Ni) undergo hydrogenolysis to form catalytically active metal – hydride clusters.[165, 174] Hydrogenolysis proceeds by a concerted cleavage of the terminal metal–phosphoranimide bonds and yields metal-hydride and neutral phosphoranimine (Scheme **2.6**). However, the strong (4e) metal–nitrogen bonds require harsh reaction conditions for cleavage,[13, 141] and, the basic phosphoranimine is strongly coordinating, inhibiting catalyst performance.
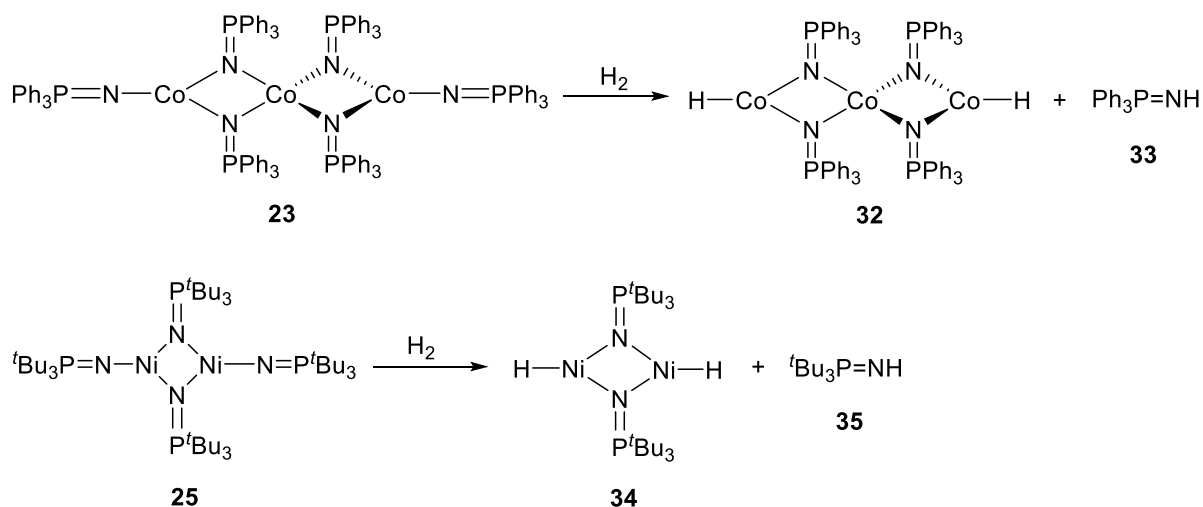
Scheme 2.6 Proposed hydrogenolysis of the bis(phosphoranimide) Co(II) and Ni(II) clusters.

Dr. S. Mitton group encountered catalyst poisoning by free phosphoranimine while investigating the hydrogenolysis of trimeric [Co(NPPh$_3$)$_2$]$_3$ **23**. Dr. Mitton initially observed little to no reactivity under the hydrogen pressure. The addition of an electrophilic activator, such as 9-BBN, cleaves and intercepts the phosphoranimide preventing the phosphoranimine coordination (Scheme **2.7**).[170, 175] Under these conditions, hydrogenation catalysis proceeds readily. However, the use of external additives to promote catalyst initiation is generally undesirable.
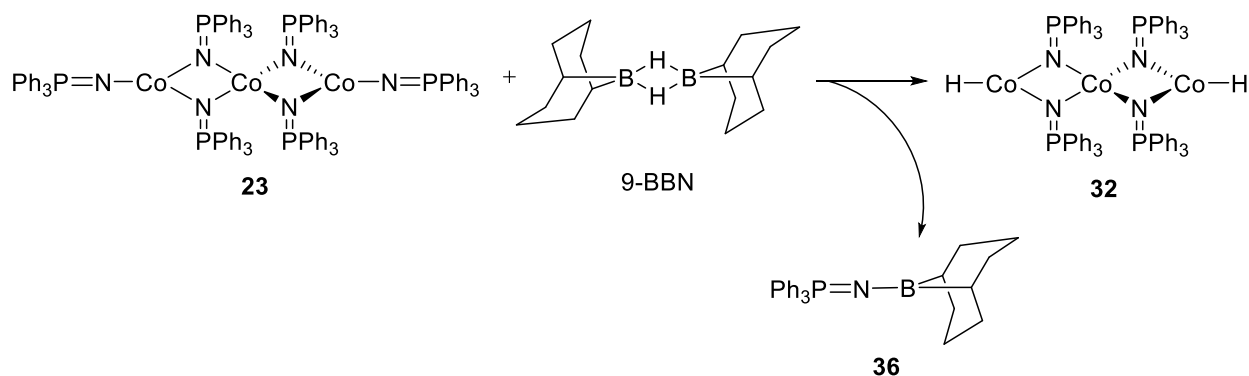
Scheme 2.7 The proposed reaction between cluster **23** and 9-BBN.

2.3.2.2 Anionic alkoxide and siloxide terminal ligands in M(II) clusters

Installing more labile, 'hydrogenolysis ready' terminal ligands to M(II) clusters would simplify the precatalyst activation, while careful ligand choice can prevent the catalyst inhibition by liberated neutral ligand. Anionic σ-donor ligands (*X*-type) participate in minimal π-bonding and should allow for a facile metal–X bond hydrogenolysis. The most common *X*-type ligands are halides, alkyls, and alkoxides[176] except not all of them are suited for our purposes. Hydrogenolysis of the strong metal – halide bonds is thermodynamically unfavourable and produces strongly acidic by-products.[13] In contrast, terminal alkyl ligands yield coordinatively inert alkanes upon the catalyst activation and have been investigated extensively by previous group members.[165] Unfortunately, for high-spin systems lacking a low-lying vacant d-orbital, the absence of a lone electron pair on the adjacent atom strongly inhibits heterolytic dihydrogen activation. Alkyl-capped clusters exhibit low activity under mild reaction conditions, requiring partial oxidation to form a mixed-valence cluster, which undergoes facile σ-bond metathesis under hydrogen.[165, 174] The η^3-allyl ligand, however, occupies two coordination sites; facile isomerization to the η^1-allyl opens coordination site for M–C bond hydrogenolysis.[177-178] However, allyl precatalyst synthesis is imperfect and suffers from reproducibility and scalability issues.[179]

The alkoxide ($[OCR_3]^-$) and siloxide ($[OSiR_3]^-$) ligands are isoelectronic to the phosphoranimide functionality, but much less electron-donating. Many late transition metal alkoxide and siloxide complexes readily react with molecular hydrogen to form metal hydrides and alcohols or silanols, which do not irreversibly poison metal catalysts.[180-183]

Tert-butoxide and trimethylsiloxide ligands are readily available and sterically large. Both [OCMe$_3$]$^-$ and [OSiMe$_3$]$^-$ are strongly electron-releasing but the differences between Si and C significantly affect the electronic ligand properties and bonding. Higher electropositivity of the silicon atom results in a stronger σ-donating character of the siloxide ligand compared to the alkoxide. Vacant, low energy Si–C σ*-orbitals are of π-symmetry and can accept backbonding from the oxygen *p*-orbitals. Consequentially, the electron density around the oxygen atom is decreased and not available for the M–O π-bonding.[182] Thus, metal–ligand π-bonding is stronger for the alkoxide ligands and strengthen further as the M–O–C bond angle approaches 180° maximizing orbital overlap.[184-185] Smaller bond angles indicate that little-to-no π-bonding takes place. In general, the [OCMe$_3$]$^-$ ligand is more labile than the siloxide counterpart. Therefore, installing [OCMe$_3$]$^-$ and [OSiMe$_3$]$^-$ as terminal ligands for Co(II) phosphoranimide clusters should facilitate catalyst activation step without significant catalyst poisoning.

2.3.2.3 Synthetic strategy

Having selected the terminal ligands, we next established the targeted cluster nuclearity. Exchanging the terminal ligands for alkoxides in the trimetallic precatalyst [Co(NPPh$_3$)$_2$]$_3$ **23** would most likely retain the trimeric skeleton. However, the strong Co–N bonds[13] render the metathesis reactions relatively unfavourable; the reaction would likely require harsh reaction conditions and could lead to a mixture of the reaction products making protolytic metathesis unfavourable. Consequentially, we selected the proposed intermediate [Co(μ$_2$-NPPh$_3$)Br(THF)]$_2$ **30** as a good candidate for anionic ligand exchange. We hoped that replacing the halide ligands with siloxide or alkoxide would preserve the dimeric 'backbone' of the starting material and allow us to investigate the influence of nuclearity in the catalyst reactivity.

2.3.2.4 Synthesis and characterization of [Co(NPPh₃)(OSiMe₃)(THF)]₂ 37

The reaction between CoBr₂ and triphenylphosphoranimide at room temperature generates a turbid, teal solution of intermediate **30** (Scheme **2.8**). The addition of KOSiMe₃ affords an immediate colour change to deep blue and significantly increased solubility. Isolation of the product provided the desired siloxide cluster **37** in 50–85 % yield.

$$CoBr_2 \xrightarrow[\text{THF, rt, overnight}]{Ph_3PN \cdot Na \cdot THF} \underset{\mathbf{30}}{[Co(\mu_2\text{-}NPPh_3)Br(THF)]_2} \xrightarrow[\text{THF, rt, overnight}]{2 \text{ eq. KOSiMe}_3} \underset{\substack{\text{deep blue, 50 - 85 \%}\\\mathbf{37}}}{[Co(NPPh_3)(OSiMe_3)(THF)]_2}$$
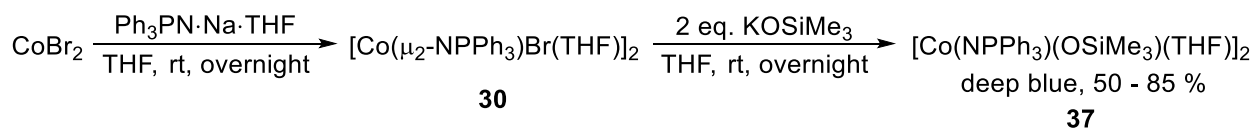
Scheme 2.8 Synthesis of proposed [Co(NPPh₃)(OSiMe₃)(THF)]₂ **37**.

Dative coordination of solvent in an unknown ratio impacts the interpretation of combustion analyses. To simplify the task, THF was used to extract crude [Co(NPPh₃)(OSiMe₃)(THF)]₂ **37** despite the convenient solubility in aromatic solvents. Unfortunately, both NaBr and KBr are slightly soluble in polar ethereal solvents, so the extraction was conducted twice using a minimal amount of THF. Although the purification steps decrease the isolated yield, complex **37** was isolated as a deep blue solid and characterized by elemental analysis and FT-IR, and the Signer MW method.[186] The synthesis has been repeated multiple times at different scales and yields consistent results.

Determination of the carbon content by elemental analysis proved to be rather challenging. Organometallic compounds, especially those incorporating phosphorus, can exhibit low carbon values.[187] Furthermore, combustion analysis of triphenylphosphoranimide clusters often produces data that deviates from the expected carbon content.[188-193] Nitrogen and hydrogen

values are more consistent with anticipated elemental composition and have been used to interpret our data. Although the exact cluster size cannot be inferred from these results, the EA is consistent with an empirical formula of [Co(NPPh$_3$)(OSiMe$_3$)(THF)], inclusive of the THF. The THF is fully retained even after drying *in vacuo* for two days at 10^{-6} Torr. Similar to [Co(μ_2-NPPh$_3$)(HNPPh$_3$)Br]$_2$ **31** (Fig. **2.11**), we propose a dimeric structure for **37.** The reaction yield was 50–85 %, depending on scale and precise purification procedure.
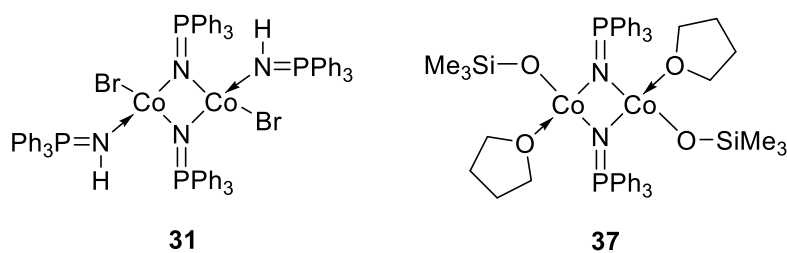
Figure 2.11 Comparison between the structure of **31** and the proposed structure of **37**.

Multiple attempts to obtain single crystals XRD analysis were unsuccessful – the exact structure of **37** remains elusive. The Signer method for solution phase molecular weight determination[186] suggests that the complex undergoes equilibrium dissociation in THF to give monomeric [Co(NPPh$_3$)(OSiMe$_3$)(THF)$_x$] **38** as the major fraction (Fig. **2.12** and Appendix A1.1). The monomer, however, may be unstable and decompose shortly. Multiple Co(II) species likely equilibrate in solution obstructing the crystallization of a single cluster.

Me3Si—O
PPh3
||
N
Co   Co
O—SiMe3
||
PPh3
O
O

37

993.06 g/mol

[Co(NPPh₃)(OSiMe₃)(THF)]

38

496.13 g/mol

Signer method
(found)

397.75 g/mol
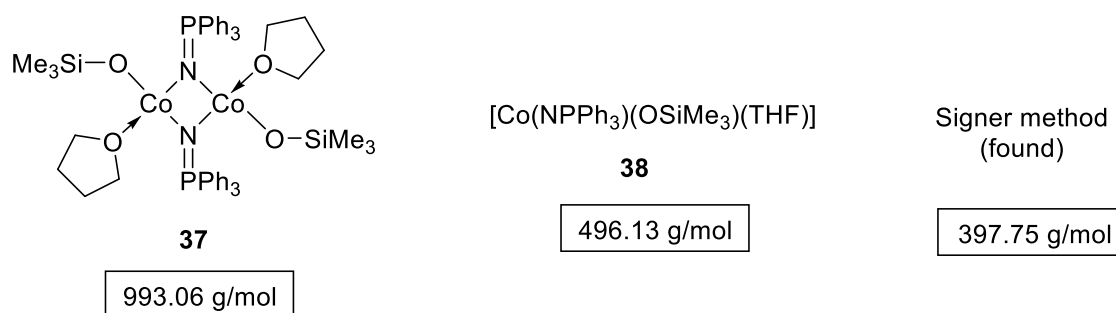
Figure 2.12 Molecular weight comparison possible structures of **37** and results from Signer method.

Cast film FT-IR analysis from THF is consistent with the combustion analysis, indicating the presence of both triphenylphosphoranimide and trimethylsiloxide ligands (Fig. **2.13**). Characteristic aromatic peaks are observed for the triphenylphosphoranimide (aromatic C=C at 1483, 1589 cm⁻¹, aromatic C-H at 3054 cm⁻¹ and aromatic overtones at 1700-2000 cm⁻¹), while *sp³* C–H peaks (3012, 2946, 2891 cm⁻¹) arise from the THF and trimethylsiloxide ligands. The presence of [OSiMe₃]⁻ is further confirmed by strong Co–O–Si peaks at 700-1000 cm⁻¹.[194] Since the characteristic metal-phosphoranimide M–N–P peaks (~1100 cm⁻¹)[140] and C–O peaks from tetrahydrofuran (~1050-1200 cm⁻¹)[195-196] occur in the same region, further IR studies are required to identify the individual vibrations. A strong stretch at 1436 cm⁻¹ is indicative of an acyclic P=N bond.[197] The weak absorption at 3349 cm⁻¹ is not assigned, but may arise from decomposition of the catalyst due to exposure to atmospheric moisture and oxygen.
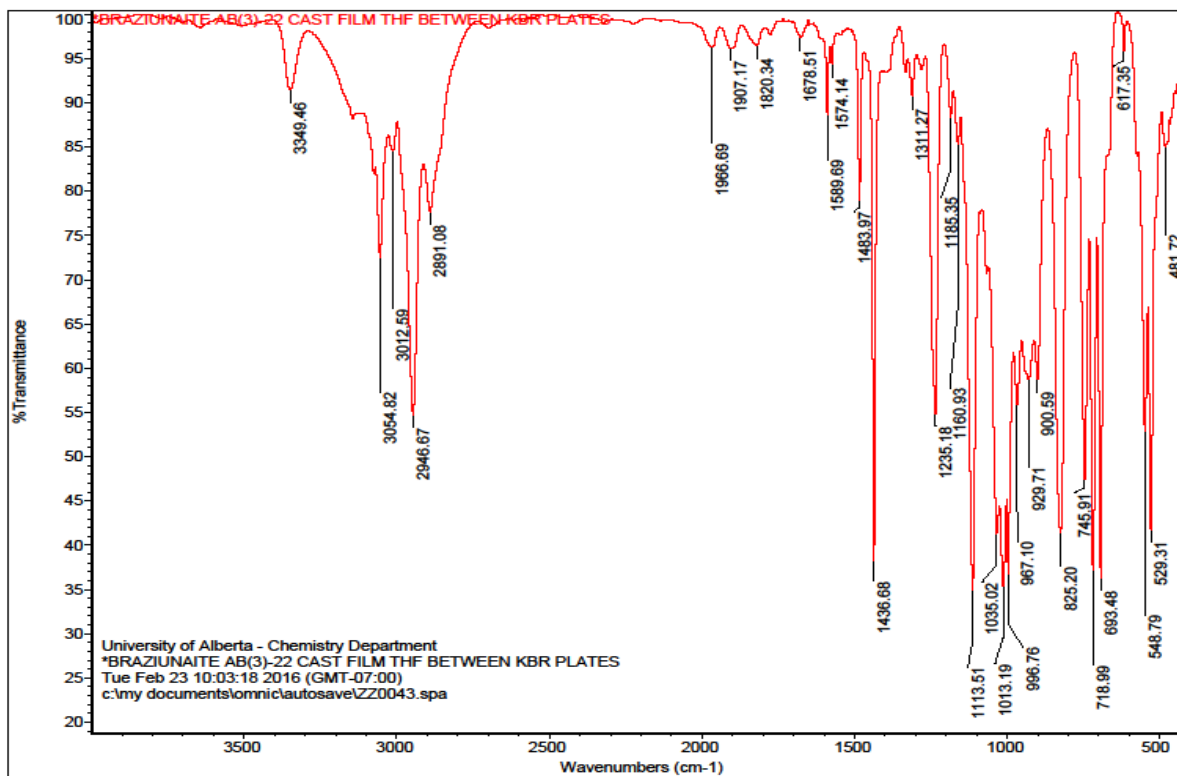
Figure 2.13 FT-IR spectrum of [Co(NPPh₃)(OSiMe₃)(THF)]₂ **37**.

Electrospray Ionization (ESI-MS) and Nanowire-Assisted Laser Desorption/Ionization (NALDI) techniques confirmed the presence of triphenylphosphoranimide. The extent of air and moisture sensitivity of **37** is unknown; it is possible that cluster decomposition occurs upon unintended contact with the atmosphere during the sample insertion. More rigorous air- and water-free analysis and crystallographic data is needed to confirm the proposed structure and nuclearity of [Co(NPPh₃)(OSiMe₃)(THF)]₂ **37**.

2.3.2.5 Synthesis and characterization of [Co(NPPh₃)(OᵗBu)(THF)]₂ 39

Synthesis of [Co(NPPh₃)(OᵗBu)(THF)]₂ **39** was carried out according to the same procedure described above (Scheme **2.9**). The crude product was extracted twice using a minimal amount

of THF, isolated as a green solid, and analyzed by EA and FT-IR. The yields vary between 40–75%.

$$CoBr_2 \xrightarrow[\text{THF, rt, overnight}]{\text{Ph}_3\text{PN·Na·THF}} [Co(\mu_2\text{-NPPh}_3)Br]_2 \xrightarrow[\text{THF, rt, overnight}]{\text{2 eq. KO}^t\text{Bu}} [Co(NPPh_3)(O^tBu)(THF)]_2$$

$$\textbf{30} \qquad\qquad \text{green, 40 - 75 \%}$$
$$\textbf{39}$$
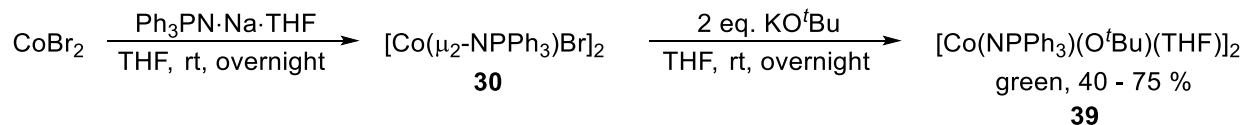
Scheme 2.9 Synthesis of the proposed $[Co(NPPh_3)(O^tBu)(THF)]_2$ **39**.

As expected, EA values support an empirical formula of $[Co(NPPh_3)(O^tBu)(THF)]$ with retained solvent coordination even after *high vacuo*. Although a solution MW determination was not conducted, cluster **39** is likely equilibrating between dimer and monomer in solution. The synthesis of **39** exhibits immense sensitivity to reaction conditions (e.g., concentrations, temperature, time). This suggests that clusters of different nuclearity may form irreversibly under varying conditions, with THF capping the unsaturated terminal sites. Agostic interactions between the cobalt centres and methyl hydrogens from the *tert*-butoxide ligand have been observed in [Co–O^{t}Bu] complexes[198] and could promote THF dissociation and cluster rearrangement in our complex.

FT-IR spectroscopy from a THF cast confirms the presence of both triphenylphosphoranimide and *tert*-butoxide ligands (Fig. **2.14**). As discussed for $[Co(NPPh_3)(OSiMe_3)(THF)]_2$ **37**, aromatic absorptions and multiple sp^3-C–H stretches are characteristic, but identification of discrete ether and phosphoranimide absorptions is problematic due to overlap. The overlay spectrum of complexes **37** and **39** demonstrates a high similarity in structure and confirms that the strong, sharp absorptions at 700–1000 cm^{-1} in the spectrum of **37** arise from the Co–O–Si bonds (Appendix A1.2).
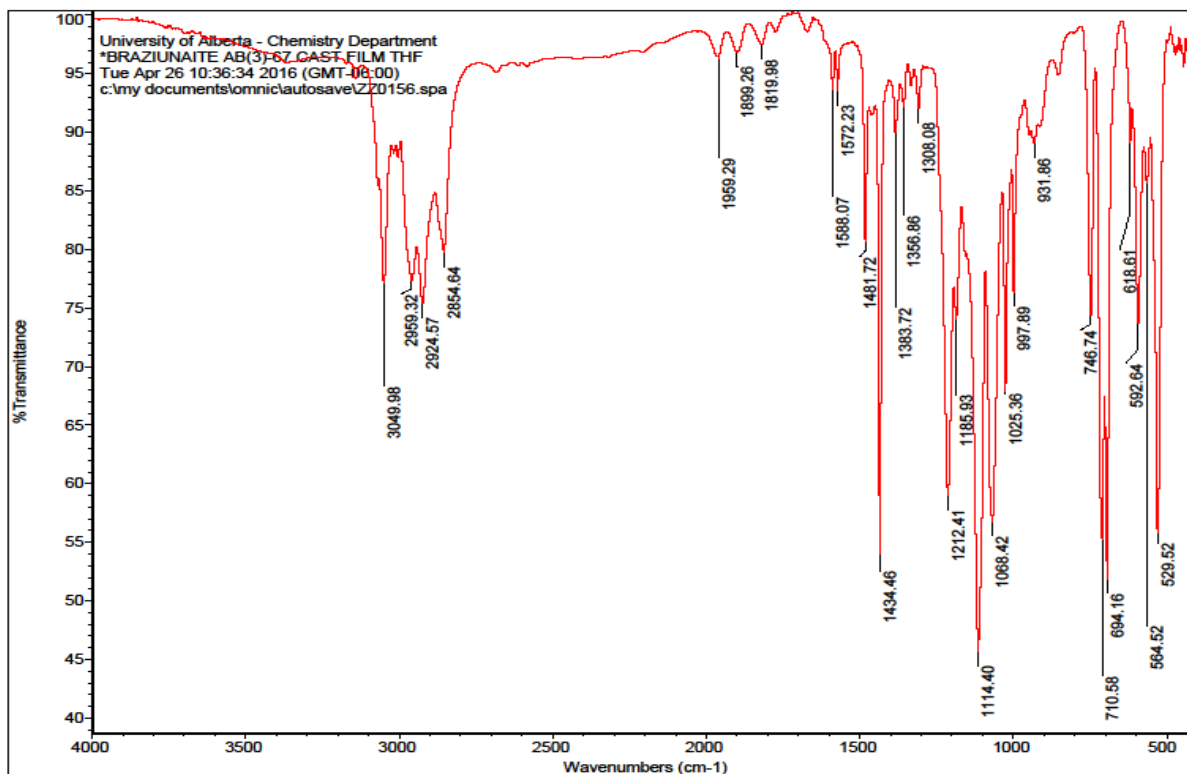
Figure 2.14 FT-IR spectrum of [Co(NPPh$_3$)(O^{t}Bu)(THF)]$_2$ **39**.

2.3.2.6 Synthesis and characterization of [Co(NP^{i}Pr$_3$)$_2$]$_3$ 40

The bis(triisopropylphosphoranimide)cobalt cluster [Co(NP^{i}Pr$_3$)$_2$]$_3$ **40** was prepared by the reaction of two equivalents of the triisopropylphosphoranimide ligand with CoBr$_2$. The complex was isolated by trituration into hexanes to afford a dark green, oily solid in 83–87% yield (Scheme **2.9**). Although the crystal structure has not been obtained, the cluster is expected to be trimetallic, analogous to [Mg$_3$(μ$_2$-NP^{i}Pr$_3$)$_4$(NP^{i}Pr$_3$)$_2$] **21** and [Co$_3$(μ$_2$-NPPh$_3$)$_4$(NPPh$_3$)$_2$] **23**.
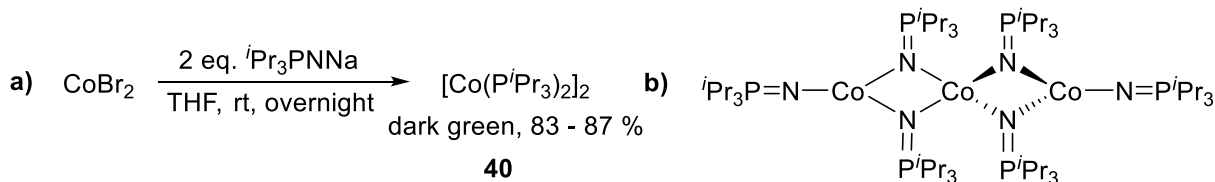
Scheme 2.10 a) Synthesis and b) the proposed structure of $[Co(NP^iPr_3)_2]_3$ **40**.

The triisopropylphosphoranimide ligand offers significantly improved cluster solubility over triphenylphosphoranimide. Reaction products are easily extracted using nonpolar solvents (e.g. pentane, hexanes), eliminating contamination by NaBr salts. Elemental analysis indicates an empirical formula of $[Co(NP^iPr_3)_2] \cdot S$; however, it is unclear whether the solvent (S) is residual THF or hexane. Based on the previously characterized trimeric cobalt and magnesium clusters, solvent coordination to the metal is unlikely, although the solvent may be interstitial within the crystal lattice. Despite earlier difficulties, combustion analysis was definitive and reproducible. The FT-IR spectrum supports the presence of alkyl rather than aromatic substituents, but it does not convey additional information (Appendix A1.3). This synthesis was only repeated twice due to the limited availability of the ligand, but the consistent EA data are indicative of a facile and reproducible procedure.

Synthesis of a cluster analogous to $[Co(NPPh_3)(OSiMe_3)(THF)]_2$ **37** did not yield the desired results. The same procedure instead produces a hexane-soluble blue solid, similar in appearance to **37**, along with a brown precipitate that is insoluble in alkanes (Scheme **2.11**). We expected that $[Co(NP^iPr_3)(OSiMe_3)]_2$ **41** would be soluble in alkanes, but the product from hexane extraction was inconsistent with the proposed structure. The obtained elemental composition did not correlate with any of the anticipated reaction products. The strongly electron-donating nature of the *iso*propyl substituents substantially increases the electron density around the metal(s),

possibly precluding the THF coordination required to stabilize dimetallic clusters. No definitive
data have been obtained to support or refute such hypothesis.

$$CoBr_2 \xrightarrow[\text{THF}]{\begin{array}{l} \text{1. } ^iPr_3PNNa\text{, rt, overnight,} \\ \text{2. } KOSiMe_3\text{, rt, overnight} \end{array}} [Co(NP^iPr_3)(OSiMe_3)(THF)]_x$$
$$\textbf{41}$$
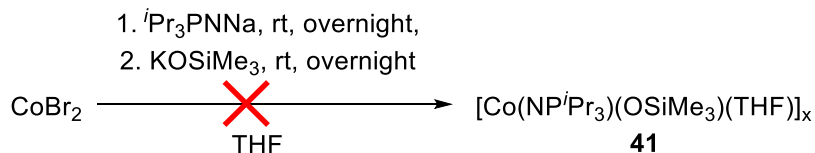
Scheme 2.11 Unsuccessful synthesis of proposed cluster $[Co(NP^iPr_3)(OSiMe_3)]_2$ **41**.

2.4 Conclusions

Multiple cobalt clusters supported by phosphoranimide ligands with the intermediate size
substituents have been synthesized. Although elemental analysis and FT-IR data confirm the
formation of the desired complexes, further characterization is needed to obtain full structural
information.

A consistent synthesis of $[Co(NPPh_3)(OSiMe_3)(THF)]_2$ **37** has been established allowing for the
exploration of its catalytic reactivity toward hydrogenation and hydrogenolysis. The cluster is
presumed to be dimeric in the solid state, with μ^2-bridging triphenylphosphoranimide and
terminal trimethylsiloxide and tetrahydrofuran ligands. In contrast, only an irreproducible
synthesis of the analogous *tert*-butoxide cluster $[Co(NPPh_3)(O^tBu)(THF)]_2$ **39** could be
demonstrated. The homoleptic $[Co(NP^iPr_3)_2]_3$ **40** was successfully prepared in a reproducible
procedure and likely consists of a trimeric skeleton with four bridging and two terminal
phosphoranimide ligands. The catalytic reactivity of the reported clusters towards the
deoxygenation of aromatic ketones is discussed in the following chapter.

Chapter 3. Deoxygenation of aromatic ketones by cobalt clusters

3.1 Previous work in the Stryker group and project rationale

Dr. S. Mitton first investigated the catalytic activity of $[Co(NPPh_3)_2]_3$ **23** in our group. He discovered that the cluster can successfully reduce aromatic ketones to the corresponding alcohols in the presence of catalytic amounts of 9-BBN and potassium *tert*-butoxide (Scheme **3.1**). The reaction leads to mixtures of hydrocarbon and benzylic alcohol using aromatic aldehyde substrates.[170] Importantly, no reductive activity is observed in the absence of any one component: KO*t*Bu, 9-BBN, or the cobalt catalyst.
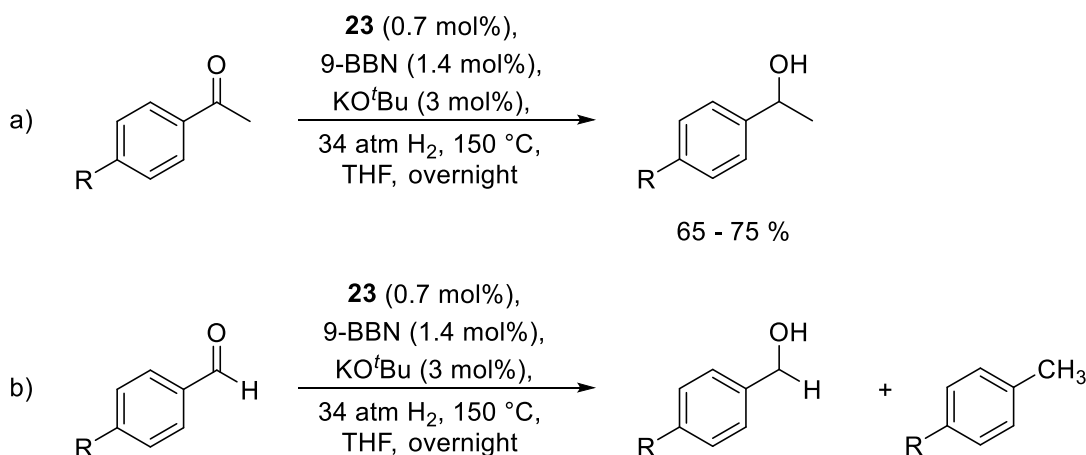
Scheme 3.1 Deoxygenation of aromatic a) ketones and b) aldehydes by the precatalyst **23**.

As previously discussed, hydrogenolysis of the metal-phosphoranimide bonds in trimer **23** is challenging and results in the formation of the neutral phosphoranimine that poisons the active catalyst by irreversible coordination. This issue prompted the search for an effective activator to generate the catalytically-active hydride and irreversibly sequester the terminal phosphoranimide ligand. The Stephan group first reported the synthesis of phosphinimino boranes in 2014 by the

reaction of silylated phosphinimines with 9-Cl-9-BBN (Scheme **3.2a**).[175] Dr. Mitton adapted the procedure for our purposes. Substitution of 9-Cl-9-BBN by 9-BBN (9-borabicyclo[3.3.l]nonane) delivers a hydride to afford the catalytically active cobalt hydride, with concomitant formation of triphenylphosphinimine borane **36** (Scheme **3.2b**). Isolation and analysis of [Co$_3$(μ_2-NPPh$_3$)$_4$(H)$_2$] **32** proved to be challenging; recrystallization did not produce single crystals suitable for X-ray crystallography. However, Ph$_3$PN-9-BBN, the expected by-product, was detected by ^{1}H NMR and ^{31}P spectroscopy, suggesting that the reaction occurs.
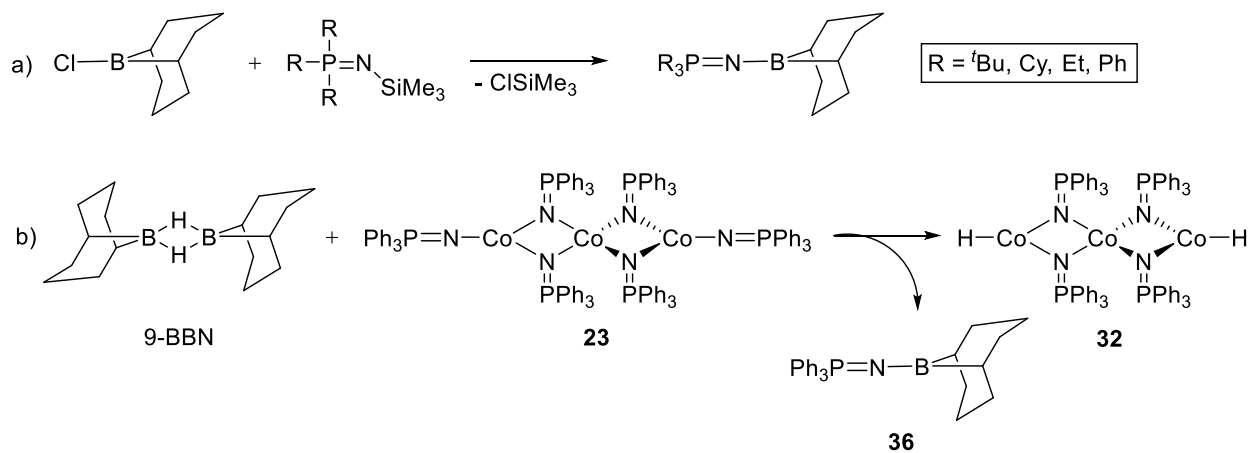
Scheme 3.2 a) Synthesis of the phosphinimine-substituted boranes by Stephan group[175] and b) the proposed reaction between 9-BBN and cluster **23**.[170]

Strongly basic KO^{t}Bu is likely acting as co-catalyst to the hydridocobalt phosphoranimide catalyst. Potassium *tert*-butoxide catalyzed hydrogenation of ketones to the corresponding alcohols was first reported in 1964 by Walling, *et al.*[199] However, the reaction requires high base loadings and harsh reaction conditions (~20 mol% KO^{t}Bu, >200 °C, >100 atm H$_2$). Berkessel, *et al.* recently proposed that the hydrogenation proceeds through a ternary transition state – a concerted, single step heterolytic hydrogen activation, as illustrated (Scheme **3.3a**).[200] We presume that our reactions proceed through a similar six-membered transition state in which

cobalt hydride replaces the hydrogen (Scheme **3.3b**). The cobalt hydride transfers to the electrophilic carbon with a concomitant formation of a cobalt alkoxide which readily hydrogenolizes to regenerate the hydridocobalt catalyst.[181] Six-membered transition states are common in catalytic transfer hydrogenations of polar bonds, especially in reactions with active transition metal hydride intermediates.[201-203]
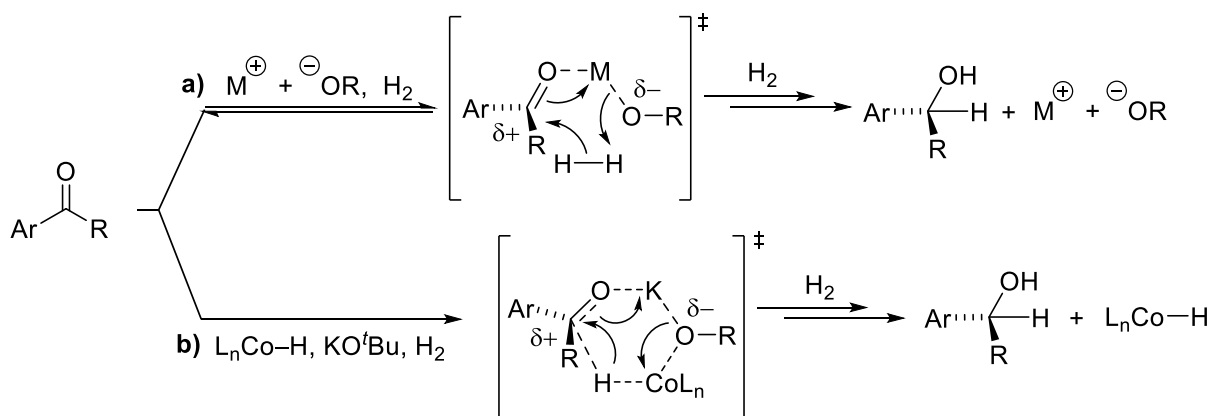
Scheme 3.3 a) A proposed mechanism for KO^{t}Bu catalyzed hydrogenation of aromatic ketones[200] and b) the proposed transition state in the hydrogenation of ketones in our reactions.

Investigating the hydrogenation of aldehydes revealed that the addition of two equivalents of KO^{t}Bu promotes an unprecedented C–O σ-bond hydrogenolysis (Scheme **3.4**). Deoxygenation produces water, which can cause catalyst decomposition due to the moisture sensitivity of the metal phosphoranimide clusters. In our reactions, the complete deoxygenation obtained indicates
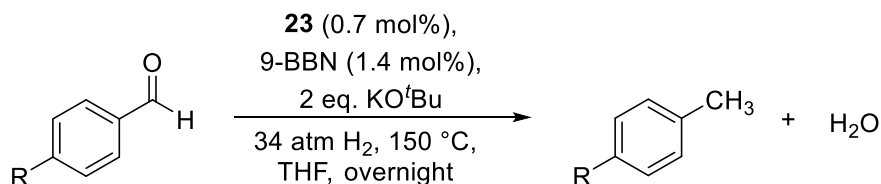
Scheme 3.4 Hydrodeoxygenation of aromatic aldehydes by precatalyst [Co(NPPh$_3$)$_2$]$_3$ **23** and excess KO^{t}Bu.

that KO^{t}Bu is an effective water scavenger under high base concentrations. Consequently, we were most curious to see if this reaction could be extended to the deoxygenation of aromatic ketones and other unsaturated compound classes.

3.2 Results and discussion

3.2.1 Hydrodeoxygenation of aromatic ketones in the presence of excess KO^{t}Bu

The precatalyst [Co(NPPh$_3$)$_2$]$_3$ **23** is only moderately active towards the hydrogenation of aromatic ketones. Therefore, we screened [Co(NPPh$_3$)(OSiMe$_3$)(THF)]$_2$ **37**, [Co(NPPh$_3$)(O^{t}Bu)(THF)]$_2$ **39**, and [Co(NP^{i}Pr$_3$)$_2$]$_3$ **40** for catalytic hydrodeoxygenation of ketones. In this study, the activity of clusters [Co(NPPh$_3$)(OSiMe$_3$)(THF)]$_2$ **37** and [Co(NPPh$_3$)(O^{t}Bu)(THF)]$_2$ **39** was explored in detail. The catalytic activity of more electron-rich [Co(NP^{i}Pr$_3$)$_2$]$_3$ **40** was also briefly examined under the optimized reaction conditions. Catalyst loading was calculated presuming dimeric structures of clusters **37** and **39** and a trimeric structure for **40**, as discussed in Chapter 2. The use of 9-BBN in select reactions allowed us to compare the efficiency of the 'hydrogenolysis ready' terminal ligands to specific activation using the borane.

3.2.1.1 Hydrodeoxygenation of aromatic ketones catalyzed by [Co(NPPh$_3$)(OSiMe$_3$)(THF)]$_2$ 37 and [Co(NPPh$_3$)(O^{t}Bu)(THF)]$_2$ 39

The reduction of 4-acetylbiphenyl **42** in the presence of catalytic 9-BBN and two equivalents KO^{t}Bu yields a mixture of 1-(4-biphenylyl)-1-ethanol **43** and 4-ethylbiphenyl **44** after heating overnight at 150 °C under 34 atm hydrogen (Eqn. **3.1**). Only a trace of the starting material **42** was detected by ^{1}H NMR spectroscopy, however, the combined yield of the isolated products did

not amount to the total conversion observed. Analysis by GC-MS indicated the presence of dimeric products, reasonably attributed to aldol condensation by-products, favoured at high temperature in the presence of a strong base.[204] GC-MS analysis also indicates that a significant amount of biphenyl **45** (15%) is also formed in particular reactions, although it is unclear whether this results from contamination or catalytic C–C bond cleavage. Importantly, no reduction products are observed in the absence of the cobalt precatalyst, demonstrating that our reaction conditions are too mild to proceed by KO^{t}Bu-catalyzed carbonyl hydrogenation.

Cat.:		**43**	**44**
	37	48%	15%
	39	69%	12%
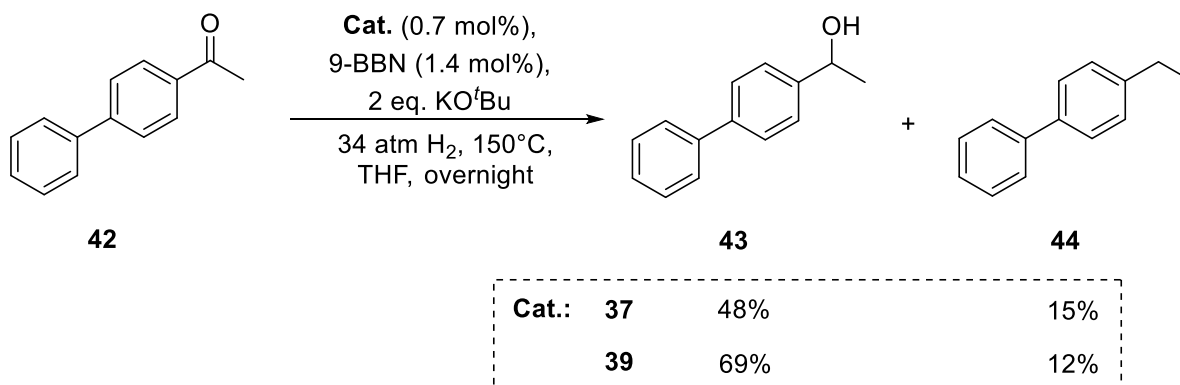
Equation 3.1 Reductive deoxygenation of 4-acetylbiphenyl **42** by precatalysts [Co(NPPh₃)(OSiMe₃)(THF)]₂ **37** and [Co(NPPh₃)(O^{t}Bu)(THF)]₂ **39**.

Comparably low yields of 4-ethylbiphenyl **44** are obtained using each precatalyst. Curiously, the amount of isolated 1-(4-biphenylyl)-1-ethanol **43** differs considerably. Analogous results obtained from reactions with and without 9-BBN indicate that both *tert*-butoxide and siloxide ligands undergo facile Co–O bond hydrogenolysis (Table **3.1**, entries 1 – 4). Only in the absence of 9-BBN is biphenyl **45** observed, suggesting that a structurally altered catalyst is obtained in the absence of the activator (Table **3.1**, entries 2 and 4). Varying the catalyst loading from 0.35 mol% to 2 mol % in cobalt leads to comparable yields demonstrating that only a small

amount of active cobalt phosphoranimide species is needed for full conversion (Table **3.1**, entry 3 vs. entries 5 – 6).

Table 3.1 Deoxygenation of 4-acetylbiphenyl **42** by precatalysts **37** and **39**.

Entry	Catalyst	9-BBN, [mol%]	Temperature, [°C]	Conversion, [%]	Yield, [%] 43	Yield, [%] 44
1	39	1.4	150	95	69	12
2	39	-	150	96[a]	39	21
3	37	1.4	150	97	48	15
4	37	-	150	89[b]	44	11
5 [c]	37	0.7	150	94	48	25
6 [d]	37	4.0	150	91	64	20
7[e]	37	1.4	150	97	83	3
8	39	1.4	110	97	85	0
9	39	-	110	15	13	0
10	37	1.4	200	100[f]	0	39

Quantified by ^{1}H NMR using hexamethyldisiloxane as an internal standard. [a] A 17 % yield of biphenyl **45** was detected by GC-MS. [b] A 15 % yield of biphenyl **45** was detected by GC-MS. [c] The reaction was carried out with 0.35 mol% catalyst loading. [d] The reaction was carried out with 2 mol% catalyst loading. [e] Toluene was used as a solvent instead of THF. [f] 10 % of biphenyl **45** was detected by GC-MS.

Solvent has a profound effect on the catalysis, both conversion and yield.[205] The low solubility of our clusters limits the reaction medium to THF and aromatic solvents. Using toluene instead of THF leads to an 83% yield of 1-(4-biphenylyl)-1-ethanol **43** but only trace amounts of deoxygenation (Table **3.1**, entry 7). Most likely, the reduction initially yields a potassium alkoxide intermediate **46** which has little to no solubility in toluene, inhibiting any subsequent hydrogenolysis (Scheme **3.5**). Work-up thus results in nearly exclusive formation of 1-(4-biphenylyl)-1-ethanol **43**.
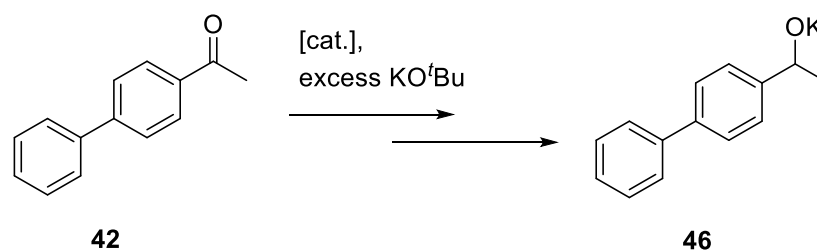
Scheme 3.5 Presumed intermediate in the reduction of 4-acetylbiphenyl **42** in the presence of excess KO^{t}Bu.

Catalyst activity and yields are also strongly affected by temperature. Exclusive hydrogenation to 1-(4-biphenylyl)-1-ethanol **43** occurs at 110 – 140 °C (Table **3.1**, entries 8 – 9). At low temperature, activation by 9-BBN is required to achieve high conversion; only 13% of 1-(4-biphenylyl)-1-ethanol **43** is obtained from hydrogenolysis alone. Moderate temperatures (≥150 °C) lead to mixtures of benzylic alcohol and hydrocarbon, independently of the addition of 9-BBN (Table **3.1**, entries 1 – 7). At 200 °C, 100% conversion and a 39% yield of 4-ethylbiphenyl **44** are obtained (Table **3.1**, entry 10). No starting material or 1-(4-biphenylyl)-1-ethanol **43** or any other reaction by-products were detected despite the low yield.

Clusters [Co(NPPh$_3$)(OSiMe$_3$)(THF)]$_2$ **37** and [Co(NPPh$_3$)(O^{t}Bu)(THF)]$_2$ **39** thus show substantial and analogous reactivity towards aromatic ketones under hydrogen. The irreproducibility of the synthesis of **39** prompted us to concentrate our efforts on investigating the catalytic activity of the precatalyst **37**. We examined progression of the reaction at 200 °C in order to investigate the mass balance problem.

3.2.1.2 Catalytic hydrodeoxygenation of 4-acetylbiphenyl at 200 °C

Both ketone hydrogenation and deoxygenation are fast and facile at 200 °C. An 80% conversion of 4-acetylbiphenyl is observed within 30 minutes, yielding 75% of 1-(4-biphenylyl)-1-ethanol **43** and 3 % of 4-ethylbiphenyl **44** (Fig. **3.1**). The concentration of 4-ethylbiphenyl **44** continues to increase over the next 30 mins, but both 4-acetylbiphenyl **42** and 1-(4-biphenylyl)-1-ethanol **43** are consumed at roughly equivalent rates, indicating that the C–O bond hydrogenolysis is competitive with carbonyl reduction. The concentration of 4-ethylbiphenyl **44** sharply increases within the 1–2 h time frame suggesting that C–O bond cleavage is preferential to carbonyl hydrogenation at high concentration of benzylic alcohol **43**. After 2 h, the reaction produces similar amounts of 1-(4-biphenylyl)-1-ethanol **43** and 4-ethylbiphenyl **44.** Further consumption of both ketone and alcohol occur slowly, but the concentration of 4-ethylbiphenyl **44** remains constant at 27%.
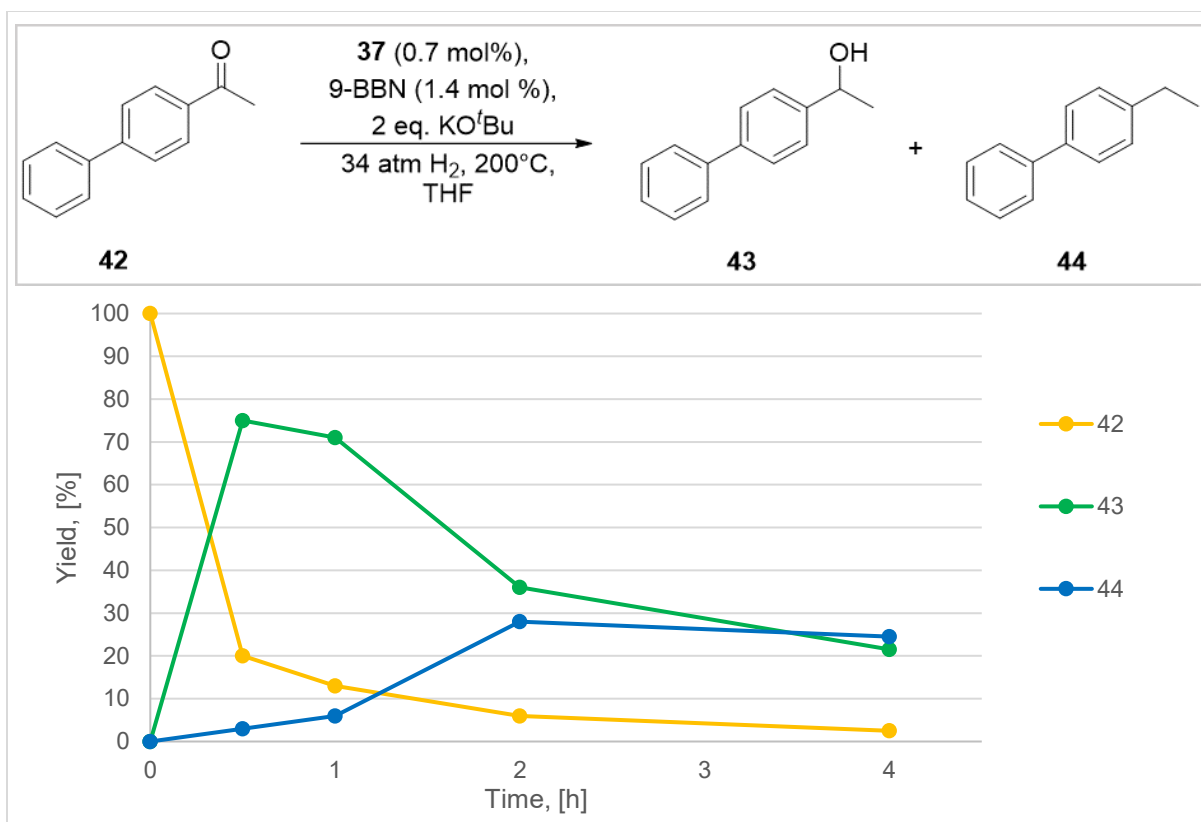
Quantified by ^{1}H NMR using hexamethyldisiloxane as an internal standard.

Figure 3.1 Time studies in the deoxygenation of 4-acetylbiphenyl **42** by **37** at 200 °C.

GC-MS analysis suggests that dimerization and C–C bond activation take place, albeit to a small extent. The GC-MS results indicate that a significant fraction of the dimeric by-products arise from aldol condensation and subsequent hydrogenation(s) of the resulting enone. Although both the dimers and biphenyl **45** are detected within 4 h, only biphenyl **45** and 4-ethylbiphenyl **44** are recovered from the overnight reaction (Table **3.1**, entry 10). Importantly, the 4-vinylbiphenyl **47** intermediate is also present early in the reaction in trace amounts, although its origin was initially unknown.

To confirm the origin and nature of the side reactions, we investigated the deoxygenation of 1-(4-biphenylyl)-1-ethanol **43** (Scheme **3.6**). Only 32% yield of 4-ethylbiphenyl **44** was observed

72

after 2 h despite proceeding to 85% conversion, representing a 53% product loss (Scheme **3.6a**). In comparison, only 30% loss of mass balance is observed after 2 h when 4-acetylbiphenyl **42** is used as a substrate (Scheme **3.6b**). Deoxygenating 1-(4-biphenylyl)-1-ethanol **43** also produces dimers, that do not arise from aldol condensation, along with traces of 4-vinylbiphenyl **47** in 2 h, but no dimerization product is seen after the overnight reaction (Scheme **3.6a** vs Scheme **3.6c**). Nearly identical and only slightly increased yields of 4-ethylbiphenyl **44** are obtained overnight
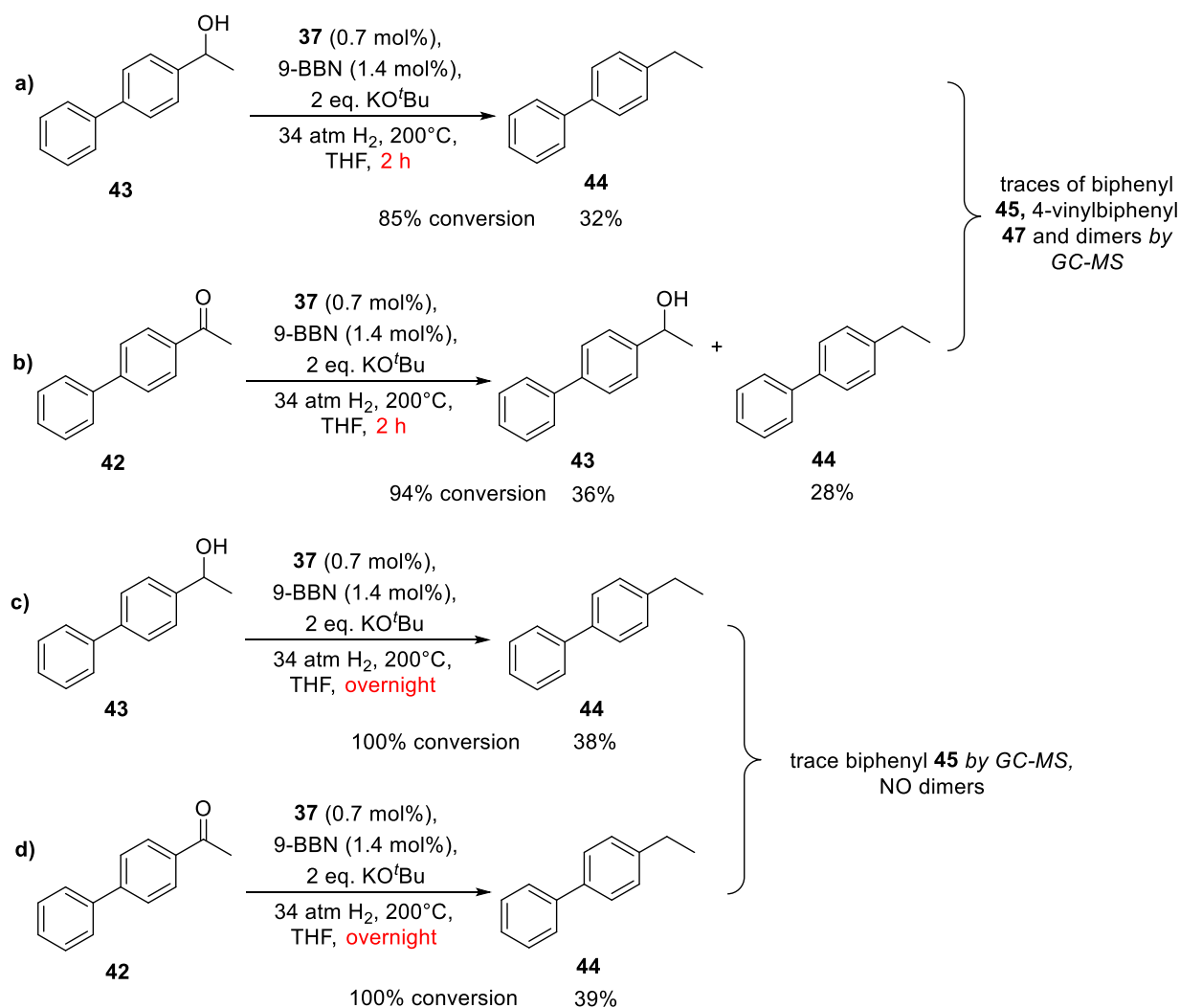
Scheme 3.6 Comparison between deoxygenation of 4-acetylbiphenyl **42** and 1-(4-biphenylyl)-1-ethanol **43** by **37**.

73

using either a ketone or an alcohol substrate (Scheme **3.6c-d**). Thus, the loss of mass balance is largely attributable to further conversion(s) of the dimers.

Control reactions were carried out to assess the effect of the catalyst and the base. Only 0.5% of 1-(4-biphenylyl)-1-ethanol **43** and 2% of 4-ethylbiphenyl **44** were obtained after 4 h in the absence of the cobalt catalyst (Scheme **3.7a**); however, some compound loss was observed. When the base is absent, the presumed hydridocobalt cluster only performs stoichiometric deoxygenation (Scheme **3.7b**) with minimal loss of mass balance.
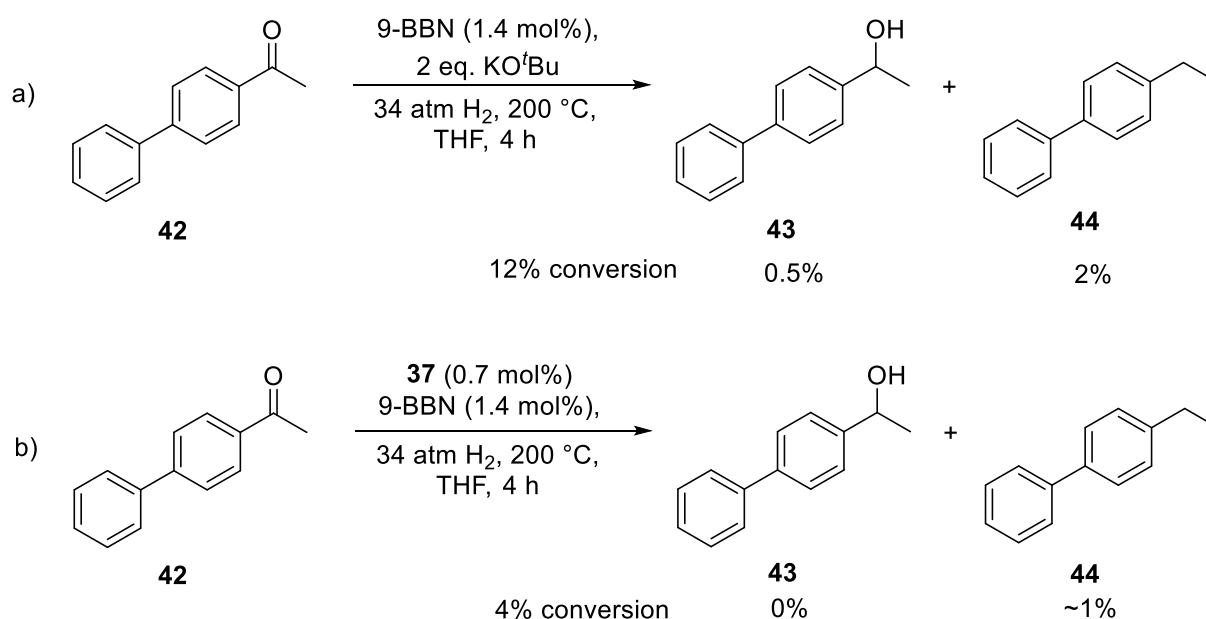
Scheme 3.7 Control reactions in the absence of a) the cobalt catalyst and b) KO^{t}Bu.

These results indicate two major side reaction pathways giving a mixture of products. Metal-mediated scission of the C–O σ-bond may proceed *via* bond homolysis to yield alkyl-substituted benzylic radicals. KO^{t}Bu can also generate radicals or accelerate their formation by a single electron transfer under harsh reaction conditions.[206] The long-lived alkyl substituted benzylic radicals can then dimerize, disproportionate to 4-ethybiphenyl **44** and 4-vinylbiphenyl **47**,[207] or

react with the dimers or oligomers present in the reaction mixture.[208] The 4-vinylbiphenyl **47** intermediate would be highly reactive under our reaction conditions, possibly polymerizing to poly(4-vinylbiphenyl), and thus is only detected in trace amounts.[209] Hydrodeoxygenation of the alcohol only yields dimers formed from benzylic radicals, while dimeric aldol adducts are also present when the substrate is a ketone. Overall, uncontrolled radical additions yield a mixture of different large molecular weight by-products each time; the oligomers, especially those incorporating aromatic rings, suffer from low solubility and are nonvolatile precluding extraction and detection by GC-MS.[210] The by-products could also be thermally labile and decompose under the harsh reaction conditions overnight.

Given the complexity of possible side reactions, identification and characterization of the reaction by-products was probed no further. We focused our efforts towards finding the optimal conditions for the selective deoxygenation of ketone substrates. Product loss is significantly less pronounced at lower reaction temperatures; we sought to obtain comparable deoxygenation rates under milder reaction conditions.

3.2.1.3 Catalytic hydrodeoxygenation of aromatic ketones by [Co(NP^{i}Pr$_3$)$_2$]$_3$ 40

In light of the inexplicable results obtained with the precatalyst [Co(NPPh$_3$)(OSiMe$_3$)(THF)]$_2$ **37**, we wanted to assess the electronic effect of the supporting phosphoranimide ligands. We hoped that a strongly electron-donating triisopropylphosphoranimide would sufficiently increase the electron density around the cobalt centres to facilitate the C–O bond hydrogenolysis at milder temperatures, consequentially suppressing the undesired reactions.

Cluster [Co(NP^{i}Pr$_3$)$_2$]$_3$ **40** exhibits somewhat different reactivity from the precatalysts [Co(NPPh$_3$)(O^{t}Bu)(THF)]$_2$ **39** and [Co(NPPh$_3$)(OSiMe$_3$)(THF)]$_2$ **37**. Deoxygenation at 150 °C under otherwise optimal conditions results in exclusive hydrogenation to 1-(4-biphenylyl)-1-ethanol **43** (Table **3.2**, entry 1). This contrasts strongly with the product ratios obtained with clusters **37** and **39**. At 4 h and 200 °C under hydrogen (34 atm), a 90 % conversion was observed with a 34 % yield of 4-ethylbiphenyl **44** (Table **3.2**, entry 2). However, strikingly similar results are obtained using precatalyst **37**.

Table 3.2 Deoxygenation of 4-acetybiphenyl **42** by the precatalyst **40**.

Entry	Temperature, [°C]	Solvent	Time[a]	Conversion, [%]	Yield, [%]	
					43	**44**
1	150	THF	O/N	96	91	3
2	200	THF	4 h	90	24	34

Quantified by ^{1}H NMR using hexamethyldisiloxane as an internal standard. [a] O/N = 17 h.

These results demonstrate that the electron-releasing triisopropylphosphoranimide ligand does not improve the reaction yields or rates. The precatalyst **40** is most likely a trimer but we do not know how many cobalt centres participate in the catalytic transformation. The catalyst loading can be adjusted presuming only one or two active cobalt sites per cluster (0.35 mol% and 0.7 mol%, respectively). However, the heteroleptic triphenylphosphoranimide clusters afford

significantly greater deoxygenation at 150 °C at 0.35 mol% catalyst, suggesting that the triisopropylphosphoranimide cluster is not as reactive (Table **3.1**, entry 5). Further, comparable results are obtained from the reactions at 200 °C and 34 atm H_2 with either the precatalyst **37** or **40** (Table **3.2**, entry 2 vs. Fig. **3.1**), indicating that the *electronic nature of the supporting ligands does not play a significant role in catalyst activity under harsh reaction conditions*. This unexpected outcome suggests that under the reaction conditions, decomposition of the phosphoranimide precatalysts produces similar, if not identical, cobalt nanoparticles.

3.2.1.4 Heterogeneity tests

Mercury poisoning tests are generally conducted as a preliminary assessment of the catalyst homogeneity; suppression of catalytic activity in the presence of Hg indicates an amalgamation of heterogeneous metal(0) particles.[211] In our experiments, the relatively low cost of the triphenylphosphoranimide ligand and the established large-scale synthesis makes the precatalyst $[Co(NPPh_3)(OSiMe_3)(THF)]_2$ **37** most suitable for such tests. We previously showed that similar conversion and yields are obtained at pressures between 20–34 atm H_2. Consequentially, we began by assessing the mildest reaction conditions.

Addition of excess metallic mercury to the reaction medium significantly affects the reaction rates (Fig. **3.2**). The addition of 300 equivalents (per precatalyst cluster) of mercury has almost no effect on the reaction yields after 4 h at 200 °C, but increasing the amount of Hg tenfold decreases the conversion to 22%. About 4% of 1-(4-biphenylyl)-1-ethanol **43** and 7% of 4-ethylbiphenyl **44** were produced, indicating that the ketone hydrogenation step is impacted more than the successive deoxygenation. At lower temperatures, the presence of 300 Hg equivalents almost fully suppresses catalysis, affording only 11 % conversion.
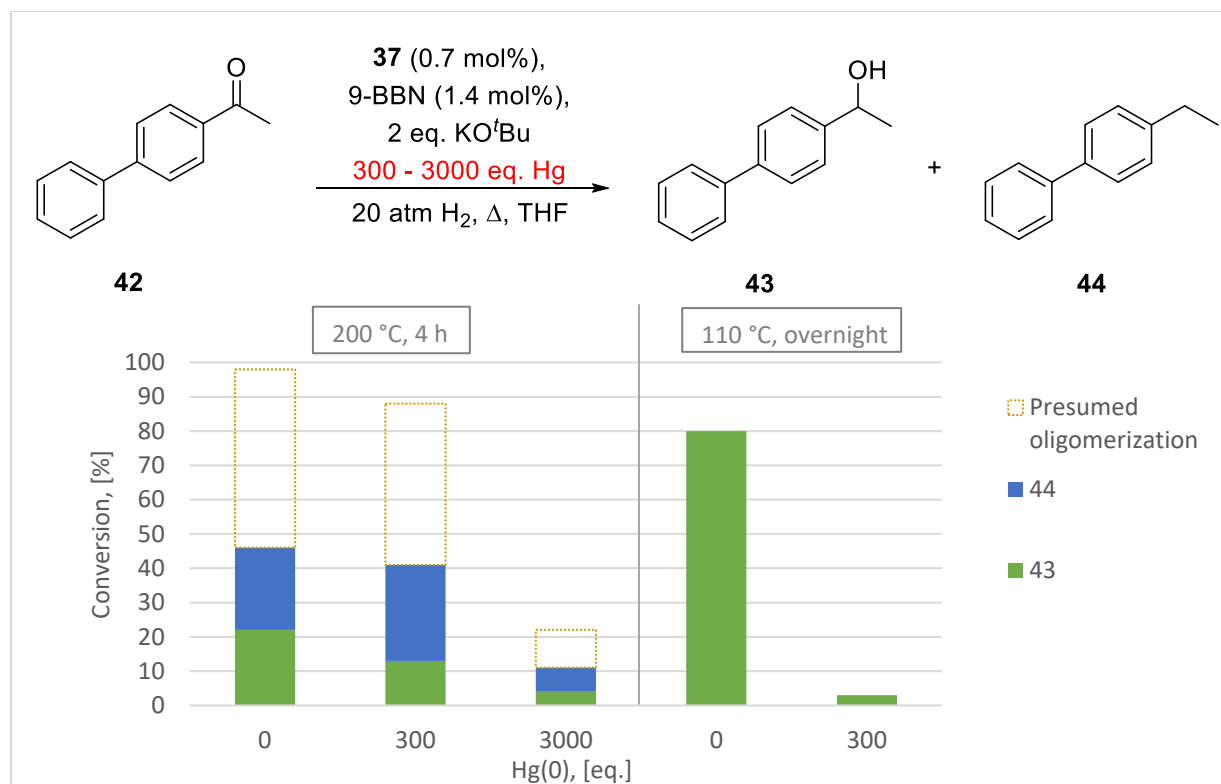
Quantified by ^{1}H NMR using hexamethyldisiloxane as an internal standard.

Figure 3.2 Mercury poisoning tests at 110 °C and 200 °C.

Mercury suppression clearly highlights the heterogeneity of the active catalyst(s); however, the extent of decomposition is unknown. Although the reaction rates are diminished in the presence of Hg, catalyst activity is not fully suppressed. It is possible that mixtures of both heterogeneous and homogeneous catalysts are present throughout the reaction, significantly impacting the reaction rates and potential mechanistic determinations.

Structural differences among precatalysts [Co(NPPh$_3$)(O^{t}Bu)(THF)]$_2$ **37**, [Co(NPPh$_3$)(OSiMe$_3$)-(THF)]$_2$ **39**, and [Co(NP^{i}Pr$_3$)$_2$]$_3$ **40** lead to considerable variations in thermal stability. Consequentially, each cluster decomposes to a different extent under otherwise identical reaction conditions. For instance, homoleptic, thermally robust phosphoranimide complexes such as

[Co(NPPh$_3$)$_2$]$_3$ **23** and [Co(NP^{i}Pr$_3$)$_2$]$_3$ **40** may require higher temperatures or longer reaction times to fully decompose. In contrast, clusters with more labile terminal ligands such as alkoxide or siloxide are expected to decompose more rapidly under milder conditions. Indeed, the minimal deoxygenation activity observed at 150 °C using precatalyst **40** may be due to very slow precatalyst decomposition (Table **3.2**, entry 1).

3.2.1.5 Pre-decomposition experiments

Deliberate thermal decomposition under hydrogen was investigated to eliminate the induction period and provide self-consistent experimental results. Many supported heterogenous catalysts are synthesized from solutions of commercially available M(II) or M(I) precursors, such as metal nitrates or carbonates. A calcination process induces thermal decomposition of the metal precursors and produces metal oxides which are subsequently reduced to M(0) by H$_2$, CO, or alcohol vapor.[84, 121, 133, 211] Catalyst pre-activation under a hydrogen flow shortens the induction periods in related catalytic reactions.[212]

In principle, thermal decomposition of clusters **37**, **39**, and **40** under hydrogen pressure should give the same or similar active catalyst under complete pre-decomposition conditions. Because [Co(NPPh$_3$)(OSiMe$_3$)(THF)]$_2$ **37** is readily prepared on large scale, this precatalyst was used for heterogeneous catalyst generation. Subjecting precatalyst **37** and two molar equivalents of 9-BBN to the 'harshest' hydrogenation conditions for 1 h (34 atm H$_2$, 200 °C) affords a black film coating on the stir bar and glass insert (Table **3.3**). The precipitate was difficult to transfer and insoluble in common organic solvents; therefore, small-scale decomposition procedures were carried out for each catalytic reaction. The ratio of the reagents was maintained to ensure the same cobalt loading in each reaction. After decomposition, the reaction vessels were vented and

transferred into the glovebox for substrate loading, followed by pressurization, and thermolysis outside of the glovebox.

Table 3.3 Catalyst pre-decomposition/-activation conditions.

		9-BBN, KO^{t}Bu		
[Co(NPPh$_3$)(OSiMe$_3$)]$_2$ **37**		$\xrightarrow{\text{34 atm H}_2,\ 200\ °C,\ \text{THF, 1 h}}$	**Cat_1A-D**	

Entry	Catalyst	KO^{t}Bu, [eq.][a]	9-BBN eq.[b]	Time, [h]
1	*Cat_1A*	300	2	2
2	*Cat_1B*	300	2	1
3	*Cat_1C*	-	2	1
4	*Cat_1D*	-	-	1

[a] 300 equiv of KOtBu relative to precatalyst **37** is equivalent to two equiv per substrate. [b] 2 eq. relative to precatalyst **37**.

The effects of KO^{t}Bu, 9-BBN, and pre-decomposition time were investigated (Table **3.3**). When both KO^{t}Bu and 9-BBN are present in the reaction mixture during decomposition (Table **3.3**, entries 1 – 2), catalytic reactions at 150 °C result in a minimal conversion of 4-acetylbiphenyl and no deoxygenation after 1 h (Table **3.4**, entries 1 – 2). Pre-decomposing only precatalyst **37** and 9-BBN (*Cat 1C*), prior to adding KO^{t}Bu and substrate, leads to a 78% yield of 1-(4-biphenylyl)-1-ethanol **43** within 1 h at 150 °C (Table **3.4**, entry 3). At 200 °C and 34 atm, the reaction affords 88 % conversion but only 19 % deoxygenation after 1 h (Table **3.4**, entry 4). Importantly, a 57% yield of aldol dimerization products is observed when only one equivalent of KO^{t}Bu per substrate is used (Table **3.4**, entry 5). Similar results were obtained without catalyst pre-activation: the use of one equivalent of base leads to significant diversion to undesired side

reaction(s) (97% conversion, 14% 1-(4-biphenylyl)-1-ethanol **43**, 9% 4-ethylbiphenyl **44**, and 35% aldol condensation).

Table 3.4 Deoxygenation of 4-acetylbiphenyl **42** with pre-activated catalysts *Cat_1A-D*.

Entry	Cat.	KO^{t}Bu, [eq.]	Pressure, [atm]	Temperature, [°C]	Conversion, [%]	Yield, [%] 43	Yield, [%] 44
1	*Cat_1A*	-	34	150	4	2	0
2	*Cat_1B*	-	34	150	7	6	s
3	*Cat_1C*	2	34	150	86	78	s
4	*Cat_1C*	2	34	200	88[a]	47	19
5	*Cat_1C*	1	34	200	98[b]	28	1
6	*Cat_1C*	2	1-2	200	19	10	8
7	*Cat_1D*	2	34	200	4	2	2

Quantified by ^{1}H NMR using hexamethyldisiloxane as an internal standard. s = stoichiometric. [a] 4% of biphenyl was detected by GC-MS. [b] GC-MS demonstrates the following results: 98% conversion, 38% of 1-(4-biphenylyl)-1-ethanol **43**, 1% of 4-ethylbiphenyl **44** and 57% dimerization.

Pre-decomposed catalyst *Cat_1C* under low pressure (1–2 atm) affords only 36% conversion, but C–O bond hydrogenolysis remains competitive (Table **3.4**, entry 6). In the absence of borane and KO^{t}Bu (*Cat_1D*), only 4% conversion was observed despite the high H$_2$ pressure (Table **3.4**, entry 7).

Our results thus establish that the active catalyst is heterogeneous. Deliberately decomposing the precatalyst **37** under H_2 results reduces the induction periods for the catalytic reaction. The C–O bond hydrogenolysis itself is relatively rapid once the active catalyst is formed, but it requires high temperatures and pressures (200 °C, 34 atm H_2). During the catalyst pre-decomposition, 9-BBN presumably functions to irreversibly sequester the phosphoranimide moiety. The stoichiometry of KO^{t}Bu, however, plays a crucial role in the product distribution. Lowering the base loading to one equivalent per substrate leads to very significant diversion to aldol condensation. Therefore, we sought alternatives to KO^{t}Bu as the water scavenger in hopes of suppressing any aldol condensation.

3.2.2 Deoxygenation of aromatic ketones in the presence of molecular sieves

Complete deoxygenation under reductive conditions yields H_2O, a catalyst deactivator, as the by-product. Stoichiometric KO^{t}Bu (2 equiv) serves both as a co-catalyst in the activation step and as a water scavenger. However, the high concentration of KO^{t}Bu induces destructive oligomerization. Molecular sieves (MS) are synthetic zeolites, insoluble porous aluminosilicates with a uniform pore size (typically 3-5 Å). They are used extensively for their drying capacity.[213-214] Precise control of the pore size is achieved by altering the mineral composition of the zeolite and presents an array of specialized absorbents for entrapment of molecules of different sizes. [215-216] Molecular sieves are commonly used in catalysis as dessicants, for example, in the catalytic deoxygenation of aromatic ketones by $B(C_6F_5)_3$, the Sharpless epoxidation, and oxyfunctionalization of alkanes.[93, 217-220]

We earlier explored the use of activated 3Å molecular sieves as an *in situ* drying agent in concert with the KO^{t}Bu catalytic activation. However, in this reaction, the addition of molecular sieves

did not increase the extent of deoxygenation (Scheme **3.8a**). In contrast, the introduction of activated molecular sieves to the reactions using *pre-decomposed* catalyst results in complete deoxygenation of 4-acetylbiphenyl **42** overnight at 200 °C, *even at low hydrogen pressure* (Scheme **3.8b**). Base-free heterogeneous reaction conditions, as expected, suppress the aldol condensation. Trace amounts of 4-vinylbiphenyl **47** and 13% yield of dimerization were detected by GC-MS supporting the notion that benzylic radicals are formed during the C–O bond cleavage. Encouraged by these remarkable results, we sought to optimize catalyst decomposition conditions to obtain the most active cobalt particles.
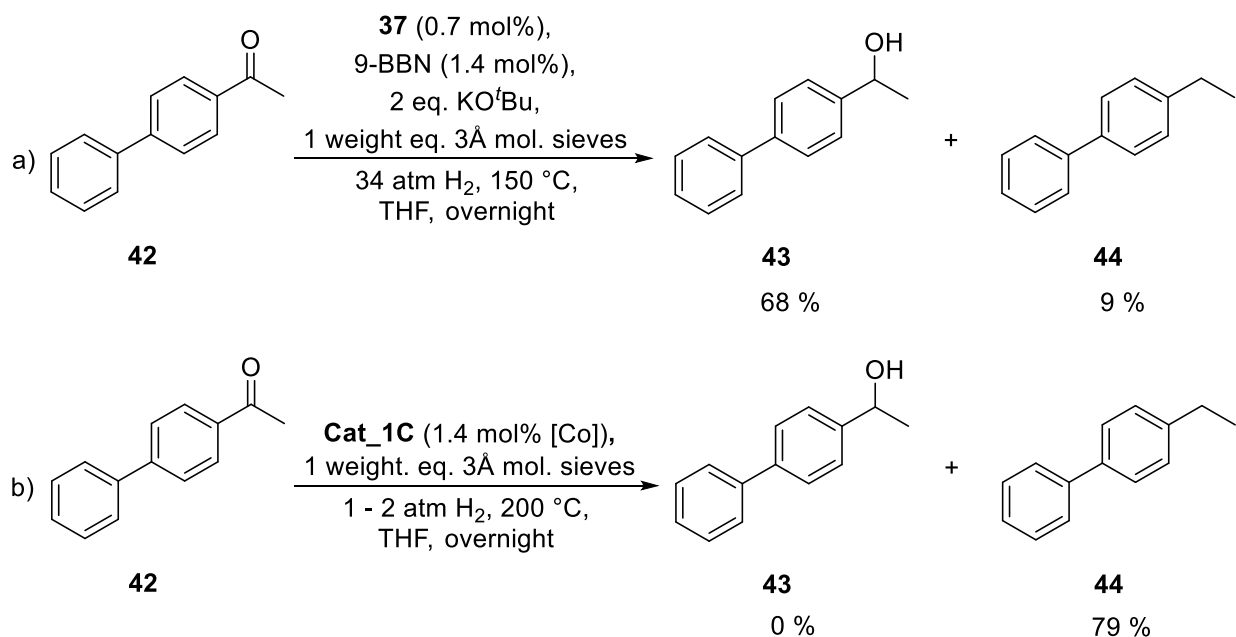
Scheme 3.8 Catalytic deoxygenation of 4-acetylbiphenyl **42** in the presence of 3 Å mol. sieves with and without KO*t*Bu as a co-catalyst. a) A reaction catalyzed by homogeneous cluster **37** and KO*t*Bu. b) A reaction catalyzed by pre-decomposed *Cat_1C*.

3.2.2.1 Catalyst optimization. Hydrodeoxygenation of aromatic ketones using pre-decomposed phosphoranimide clusters

Four catalysts were evaluated, changing variables considered important to the catalyst generation (Table **3.5**). In addition to previously examined heterogeneous catalysts *1C* (Table **3.5**, entry 1) and *1D* (Table **3.5**, entry 2), one supported catalyst was prepared. Immobilization of heterogeneous catalysts on molecular sieves and use as a dual catalyst support and water scavenger dates back at least to the early 1990's.[217, 220-221] Thus, activated molecular sieves were added for catalyst pre-decomposition (Table **3.5**, entry 3, *Cat_1E*). In addition, the influence of the cobalt precursor was investigated to probe the role of the supporting ligands, if any, in catalyst generation or HDO reaction (Table **3.5**, entry 4, *Cat_2A*).

Table 3.5 Catalyst pre-decomposition/-activation conditions.

$$[Co(NPPh_3)(OSiMe_3)]_2 \xrightarrow[\text{34 atm } H_2, \, 200\,°C, \\ \text{THF, 1 h}]{\substack{\text{9-BBN,}\\ \text{3 Å mol. sieves}}} \text{Cat\_1C-E}$$

37

$$[Co(NPPh_3)]_3 \xrightarrow[\text{34 atm } H_2, \, 200\,°C, \\ \text{THF, 1 h}]{\text{9-BBN}} \text{Cat\_2A}$$

23

Entry	Catalyst	9-BBN, [eq.]	3 Å mol. sieves, [wt. eq.]
1	*Cat_1C*	2	-
2	*Cat_1D*	-	-
3	*Cat_1E*	2	1
4	*Cat_2A*	2	-

The activity of the four catalysts was then assessed at low hydrogen pressure. As reported above, the deoxygenation catalyzed by *Cat_1C* gives 4-ethylbiphenyl **44** (79%), but the reaction is slow

Table 3.6 Deoxygenation of 4-acetylbiphenyl **42** by *Cat_1C-E* and *Cat_2A* in the presence of 3 Å molecular sieves.

Entry	Cat.	Temperature, [°C]	Time[c]	Conversion, [%]	Yield, [%]	
					43	44
1	*Cat_1C*	200	O/N	100	0	79
2	*Cat_1C*	200	2.5 h	4	2	0
3	*Cat_1C*	150	O/N	22	18	s
4	*Cat_1C*	110	O/N	8	3	0
5	*Cat_1D*	200	O/N	79	55	24
6[d]	*Cat_1E*	200	O/N	41	18	14
7	*Cat_2A*	200	O/N	100	0	100
8	*Cat_2A*	200	2.5 h	2	2	0
9	9-BBN[e]	200	O/N	0	0	0

Quantified by ^{1}H NMR using hexamethyldisiloxane as an internal standard. s = stoichiometric. [a] The [Co] loading is based on the nuclearity of each precatalyst: 1.4 mol% [Co] for precatalyst **37** and 2.1 mol% [Co] for precatalyst **23**. [b] One weight equivalent per substrate. [c] O/N = 17 h. [d] Mol. sieves were added in the catalyst pre-decomposition step and not with the substrate. [e] Prior to the catalytic reaction, 9-BBN was dissolved in THF and subjected to the pre-decomposition conditions (34 atm H$_2$, 200 °C, 1 h).

and requires very high temperature. The catalyst prepared in the absence of 9-BBN (*Cat_1D*) is less active than *Cat_1C*, giving a mixture of benzylic alcohols and hydrocarbons (Table **3.8**, entry 5). Similar results were observed for the catalyst supported on molecular sieves, albeit with much lower conversion (Table **3.6**, entry 6). Pre-decomposition of the homoleptic cluster [Co(NPPh₃)₂]₃ **23** in the presence of two equivalents of 9-BBN, however, produces an active catalyst (*Cat_2A*) that affords a quantitative yield of 4-ethylbiphenyl **44** overnight. (Table **3.6**, entry 7). The activity correlates well to that observed for *Cat_1C* (Table **3.6**, entry 2 vs. entry 8).

Thus, heterogeneous cobalt catalysts slowly deoxygenate ketones in the absence of KO^{t}Bu at low H₂ pressure. The 9-BBN activator is essential for the formation of active catalyst, but decomposing the precatalyst onto molecular sieves interferes with catalyst activation. The similar activity of *Cat_2A* and *Cat_1C* suggests that both precatalyst clusters **23** and **37** provide very similar heterogeneous catalysts. The reaction does not proceed in the absence of the cobalt precatalyst, confirming that 9-BBN and the molecular sieves are not themselves active towards carbonyl reduction (Table **3.6**, entry 9). Importantly, an induction period was observed for the 'pre-activated' catalyst indicating that catalyst generation may not be complete under the investigated activation conditions.

3.2.2.2 Investigation into the active catalyst: a preliminary assessment

Analysis of the heterogeneous particles and the resulting THF solution upon the catalyst pre-decomposition allows an examination of the components of the active catalyst (Scheme **3.9**). Decomposition of precatalyst **37** returns a clear, colorless solution and an insoluble black film. The THF solution was used to prepare a sample for FT-IR spectroscopy.

$[Co(NPPh_3)(OSiMe_3)]_2$ **37** $\xrightarrow[\text{THF, 1 h}]{\substack{\text{2 eq. 9-BBN} \\ \text{34 atm } H_2,\ 200\ ^\circ C,}}$ **Cat_1C**

precipitate → **Cat_1C**-*solid* *black solid*

THF solution → **Cat_1C**-*liquid* *clear, colorless solution*
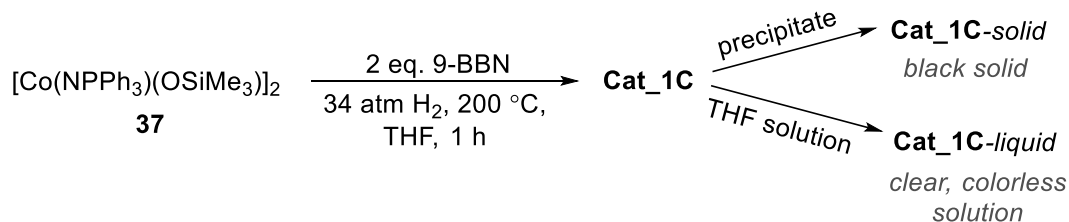
Scheme 3.9 Decomposition of the precatalyst **37** and its separation into liquid and solid phases.

The interpretation of the FT-IR spectrum is challenging (Fig**. 3.3**). Characteristic aromatic absorptions (aromatic C–H at 3058 cm^{-1}, aromatic C=C at 1486, 1590 cm^{-1}, and aromatic overtones at 1728, 1767 and 1817 cm^{-1}) indicate the presence of liberated triphenylphosphoranimide. A strong -OH absorption at 3286 cm^{-1}, indicative of trimethylsilanol **49**, unfortunately precludes the observation of any phosphoranimine N–H band between 3300–3600 cm^{-1}. It is unclear whether the silanol **49** is a primary product of hydrogenolysis or arises from the equilibrium of triphenylphosphoranimine **33** and silyl boronate **48** (Scheme **3.10**). The B–N bonds are observed between ~1200–1400 cm^{-1} and 600 – 900 cm^{-1}, depending on the substituents.[222-223] The overlap of B–N and Si–O bands in the fingerprint region prevents assignment of individual bands.[224] However, the increased number of absorptions from 1200–1400 cm^{-1}, compared to the FT-IR spectrum of precatalyst **37** (Fig. **2.12**), suggests that triphenylphosphinimine borane **36** is indeed formed.
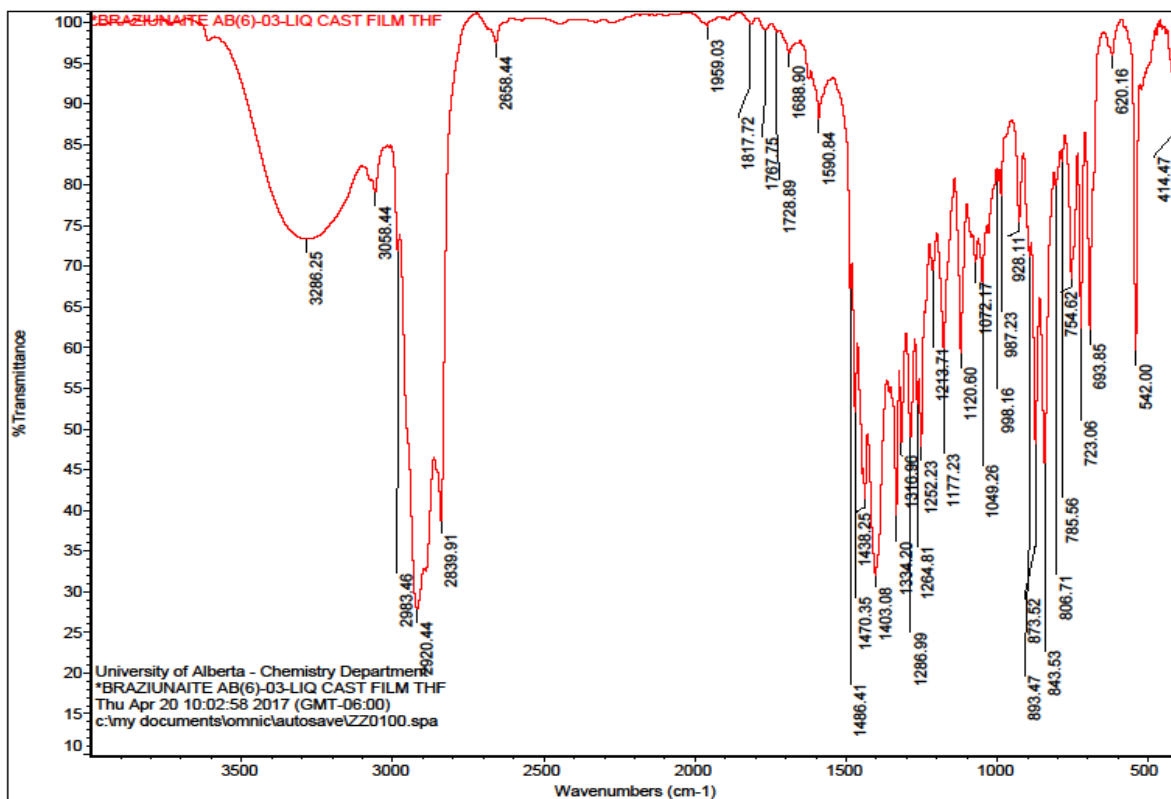
Figure 3.3 Cast film FT-IR spectrum of the *Cat_1C-liquid*.
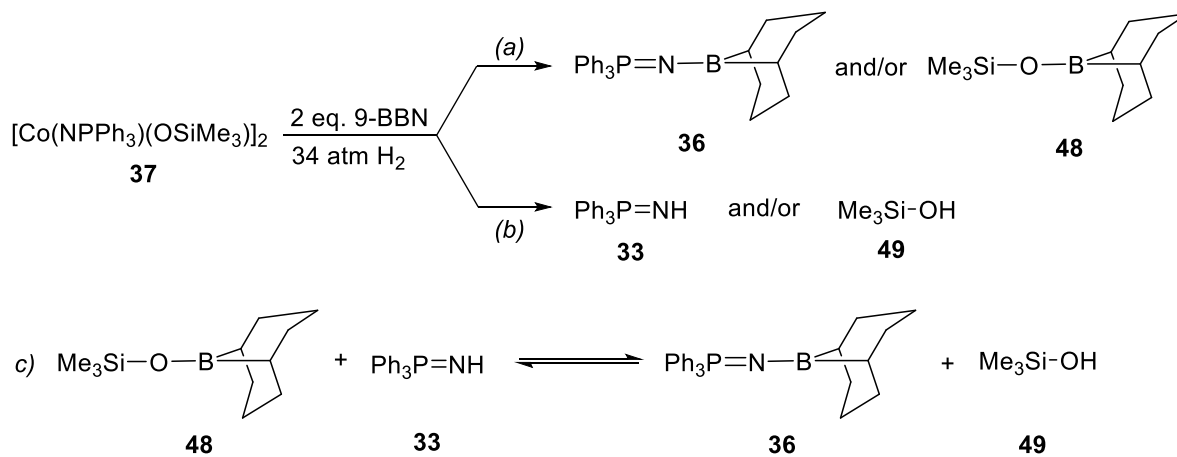
Scheme 3.10 Possible reactions under the catalyst pre-decomposition/-activation conditions.

Analysis of the ^{31}P NMR spectrum of the THF extract indicated the complete absence of neutral

Ph₃P=NH **33** (35.35 ppm in DMSO-d_6[225]) or Ph₃P=N–9-BBN **36** (6.5 ppm in toluene-d_8[175]),

suggesting that the ligand remains with the pre-activated heterogeneous catalyst. Similar tri-*tert*-butylphosphoranimide nickel retain coordinated phosphoranimide ligands that act as templating agents in nanoparticle formation.[226] The ^{1}H NMR spectrum of the THF extract shows significant paramagnetic broadening, indicating the presence of some paramagnetic species in the sample, which might have precluded the detection of phosphorus signals. Most revealing, however, is a weak absorption at 1959 cm^{-1} in the FT-IR spectrum, characterisric of a terminal Co–H bond;[227] thus, the solution may contain some [Co(NPPh$_3$)(H)(THF)]$_2$ **50**.

Both the heterogeneous film and the THF extract were investigated for catalytic activity. In the reduction, the washed cobalt film affords an 88% conversion and a 55% yield of 4-ethylbiphenyl **44** under standard conditions (Table **3.7**, entry 1). In contrast, no catalytic activity is observed upon adding 4-acetylbiphenyl **42** and activated sieves to the filtered THF solution (Table **3.7**, entry 2). This establishes that the active catalyst is the heterogeneous phase, which contains "decorated" cobalt particles. The diminished activity of the isolated particles suggests that the heterogeneous catalyst may act in concert with the THF-soluble species to achieve optimal catalytic turnover. We suspect that bound and templating phosphoranimide ligands may slowly undergo hydrogenolysis to yield the ligand-free catalyst and triphenylphosphoranimine **33** under the reaction conditions. The free phosphoranimine coordinates to the active cobalt sites to inhibit turnover.

Table 3.7 Deoxygenation of 4-acetylbiphenyl **42** by *Cat_1C-x* at 200 °C.

Entry	Cat.	Conversion, [%]	Yield, [%]	
			43	**44**
1	*Cat_1C-solid*	88	32	55
2	*Cat_1C-liquid*	0	0	0

Quantified by ^{1}H NMR using hexamethyldisiloxane as an internal standard. [a] One weight equivalent per substrate.

The identical decomposition procedure was used to activate precatalyst **23**, giving an insoluble black film and a clear brown solution (Scheme **3.11**). The extract retains the colour upon filtration, suggesting the presence of soluble cobalt complexes. The homoleptic phosphoranimide cluster **23** is thermally rather stable; it may not fully decompose during the short activation time.
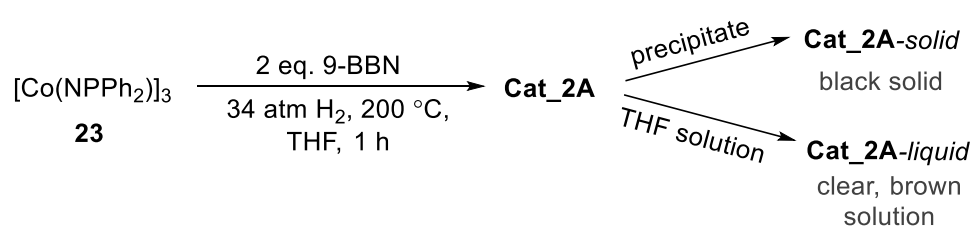
Scheme 3.11 Decomposition of precatalyst **23** and separation into liquid and solid phases.

The presence of soluble $[Co(NPPh_3)_2(H)(THF)]_2$ **51** is indicated by broad terminal Co–H stretch at 1958 cm^{-1} in the FT-IR spectrum (Fig. **3.4**).[227] Characteristic aromatic absorptions and an N–H
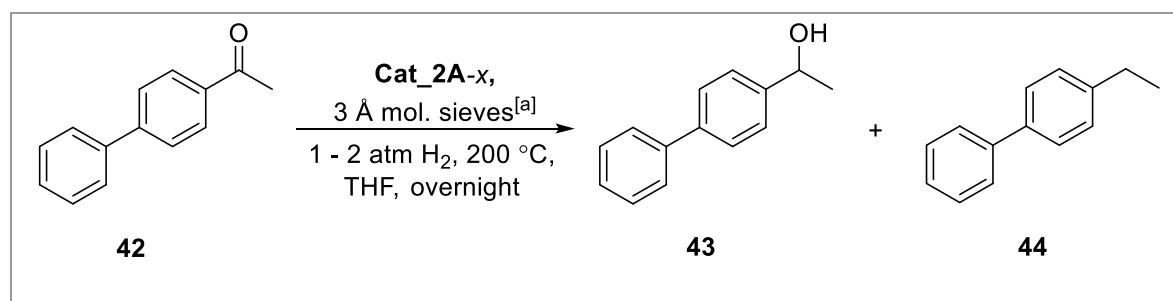
bond (3200 cm^{-1}), possibly broadened by hydrogen bonding, indicate that some phosphoranimine **33** is liberated. The formation of triphenylphosphinimine borane cannot be confirmed by FT-IR.
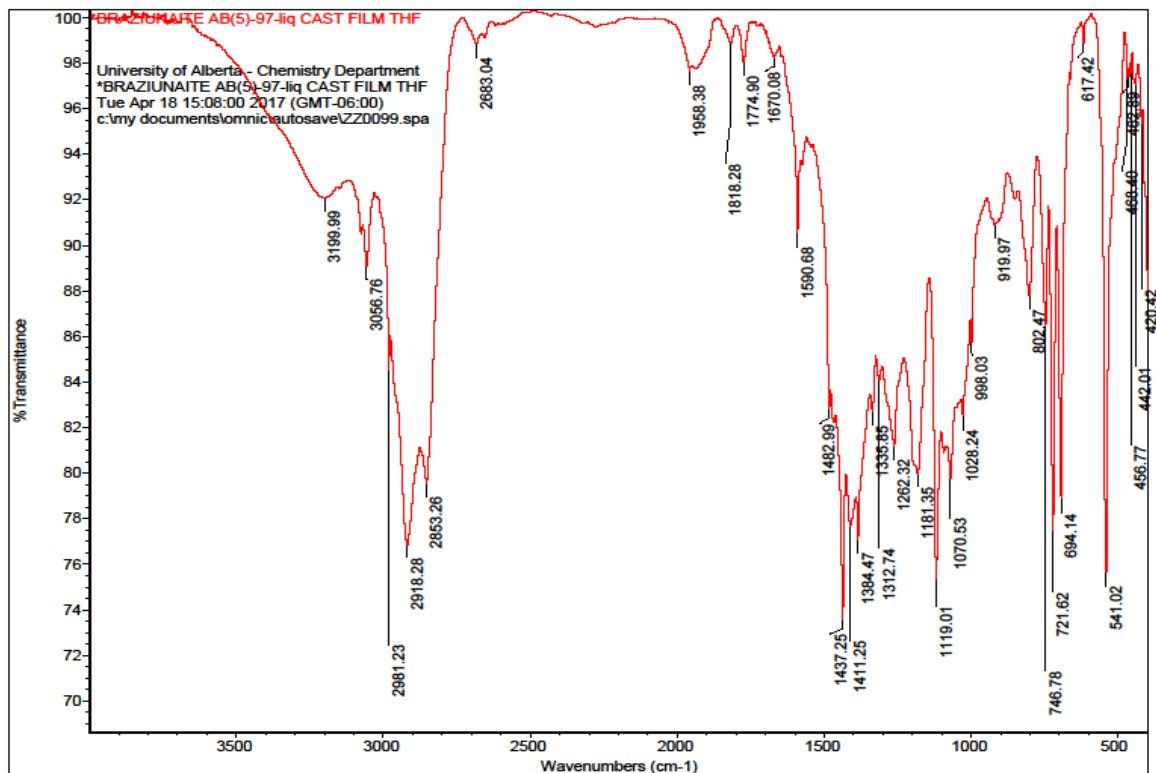
Figure 3.4 FT-IR spectrum of the *Cat_2A-liquid*.

Catalytic reductions using *Cat_2A-solid* and *Cat_2A-liquid* are consistent with the FT-IR data. Nearly identical conversions are observed in reactions of each catalyst, but with significantly different product distributions. *Cat_2A-solid* affords 27% 1-(4-biphenylyl)-1-ethanol **43** and 58% 4-ethylbiphenyl **44** (Table **3.8**, entry 1), whereas the product ratio is reversed using *Cat_2A-liquid* (Table **3.8**, entry 2). We conclude that homogeneous [Co(NPPh$_3$)$_2$(H)(THF)]$_2$ **51** cluster(s) slowly decompose further to produce more reactive, ligand-free heterogeneous cobalt particles.

Table 3.8 Deoxygenation of 4-acetylbiphenyl **42** by *Cat_2A-x* at 200 °C.

Entry	Cat.	Conversion, [%]	Yield, [%]	
			43	**44**
1	*Cat_2A-solid*	85	27	58
2	*Cat_2A-liquid*	86	52	32

Quantified by ^{1}H NMR using hexamethyldisiloxane as an internal standard. [a] One weight equivalent per substrate.

The supporting ligands thus play a significant role in the cluster decomposition. Decomposition of the thermally stable, homoleptic phosphoranimide cluster [Co(NPPh$_3$)$_2$]$_3$ **23** is incomplete and leads to a mixture of heterogeneous cobalt particles and homogeneous cobalt hydride species at the activation conditions. In contrast, more thermally labile [Co(NPPh$_3$)(OSiMe$_3$)(THF)]$_2$ **37** more readily decomposes to afford a heterogeneous cobalt film. The cobalt nanoparticles likely retain a number of coordinated triphenylphosphoranimide ligands that undergo hydrogenolysis to yield Ph$_3$PNH **33** under hydrodeoxygenation conditions. Nonetheless, the exact role of phosphoranimide ligands in forming the active catalyst is still largely unknown.

3.2.2.3 Deoxygenation of aromatic ketones using simple cobalt salts

The triphenylphosphoranimine **33** inhibits catalytic activity. The eventual liberation of the triphenylphosphoranimide ligands during catalyst activation suggests that active cobalt catalysts might be derived from simpler, phosphoranimide-free cobalt precursors.

Facile salt metathesis and high solubility make cobalt(II) bromide a common precursor for the synthesis of phosphoranimide clusters.[140-141, 153] Treatment of anhydrous $CoBr_2$ and two equivalents of 9-BBN under decomposition conditions returns a catalytically inactive light blue solution (Table **3.9**, entry 1). *In situ* preparation of $[Co(O^tBu)_2]_x \bullet nKBr$ by metathesis provided a strongly basic precatalyst, which was then decomposed thermally under hydrogen in the presence and absence of borane activator (Table **3.9**). The influence of the alkali metal alkoxide was also evaluated (Table **3.9**, entry 4).

Table 3.9 Decomposition of $CoBr_2$.

$$CoBr_2 \xrightarrow[\text{34 atm } H_2, \text{ 200 °C,}]{\text{9-BBN, MO}^t\text{Bu}} \text{Cat\_3A-D}$$
$$\text{THF, 1 h}$$

Entry	Catalyst	9-BBN, [eq.]	MO^{t}Bu	Base, [eq.][a]
1	*Cat_3A*	2	-	-
2	*Cat_3B*	2	KO^{t}Bu	2
3	*Cat_3C*	-	KO^{t}Bu	2
4	*Cat_3D*	-	NaO^{t}Bu	2
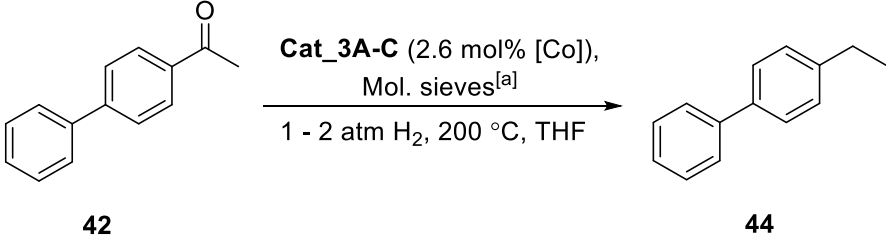
[a] Molar equivalent to $CoBr_2$.

In the absence of alkoxide (Table **3.9**, entry 1), no catalytic activity was observed towards aromatic ketones (Table **3.10**, entry 1). In stark contrast, the addition of KO^{t}Bu leads to the formation of a highly active catalyst that fully deoxygenates 4-acetylbiphenyl **42** at 200 °C and 1–2 atm H_2 (Table **3.10**, entry 2). The presence of 9-BBN, however, is no longer necessary (Table **3.10**, entry 3). Remarkably, deoxygenation proceeds to completion in 2.5 h (Table **3.10**, entry 4), strongly contrasting with the slow reaction rates observed for *Cat_1C* and *Cat_2A*

(Table **3.6**). Equally remarkably, GC-MS tentatively suggests that partial or complete hydrogenation of one aromatic ring also takes place producing a mixture of minor (12%) over-hydrogenation products. NMR spectroscopy was ambiguous, with minor resonances and overlap with the major product, precluding further structural elucidation. Although hydrogenation of aromatic compounds by cobalt catalysts is rare, Muetterties, *et al*., reported the catalytic hydrogenation of substituted arenes by $(\eta^3\text{-}C_3H_5)Co[P(OMe)_3]_3$ **52** under ambient conditions.[228-233]

Table 3.10 Deoxygenation of 4-acetylbiphenyl **42** by *Cat_3A-C*.

Entry	Cat.	Mol. sieves	Time[b]	Conversion, [%]	Yield, [%] 44
1	*Cat_3A*	3 Å	O/N	0	0
2	*Cat_3B*	3 Å	O/N	100	100
3	*Cat_3C*	3 Å	O/N	100	83[c]
4	*Cat_3C*	3 Å	2.5 h	100	96
5	*Cat_3D*	3 Å	2.5 h	100	99
6	*Cat_3D*	4 Å	2.5 h	100	88[d]

Quantified by ^1H NMR spectroscopy using hexamethyldisiloxane as an internal standard. [a] One weight equiv per substrate. [b] O/N = 17 h. [c] A 12% yield of deoxygenated, partly hydrogenated products were obtained by GC-MS. [d] A 7% yield of deoxygenated partly hydrogenated products were obtained by GC-MS.

Preparation of the catalyst starting from NaO^{t}Bu rather than the potassium salt (*Cat_3D*) does not change the catalytic activity (Table **3.10**, entry 5). Because 3Å molecular sieves contain potassium cations, the potassium-free 4Å sieves[216] were used instead (Table **3.10**, entry 6). The only significant change was an increase in aromatic ring hydrogenation. Thus, the reaction does not require potassium cations and the molecular sieves function only as a water scavenger.

3.2.2.4 Preliminary assessment of the reaction conditions

During the assessment of turnover as a function of reaction time, inconsistent results were noted for minor changes in hydrogen pressure, a consequence of irreproducible low pressure adjustment between the reactors and high-pressure tank gauges. Anomalous results were observed in the 1.5 – 2 h time frame, leading us to briefly examine the effects of hydrogen pressure on conversion.

The effect of hydrogen pressure was investigated at three reaction temperatures (Fig. **3.5**). At 200 °C, comparable conversion is observed at both 1–2 and 7 atm H_2. At higher pressure, traces of 1-(4-biphenylyl)-1-ethanol **43** and slightly higher yield of over-hydrogenation by-products are obtained. At 150 °C, the reaction affords 57% conversion to mixtures of benzylic alcohol and deoxygenated hydrocarbon at 1–2 atm H_2 but substantially higher conversion and a 67% yield of deoxygenation at 7 atm. Unexpectedly, completely different catalyst behavior was observed at 100 °C. In this case, higher H_2 pressure *decreases* conversion at short reaction time. However, the higher-pressure reaction proceeds nearly to completion overnight, giving 1-(4-biphenylyl)-1-ethanol **43** (50%) and 4-ethylbiphenyl **44** (42%), while only 64% conversion to mostly alcohol is observed at low pressure. Minor aromatic ring hydrogenation occurs at all temperatures but is most pronounced at 200 °C.
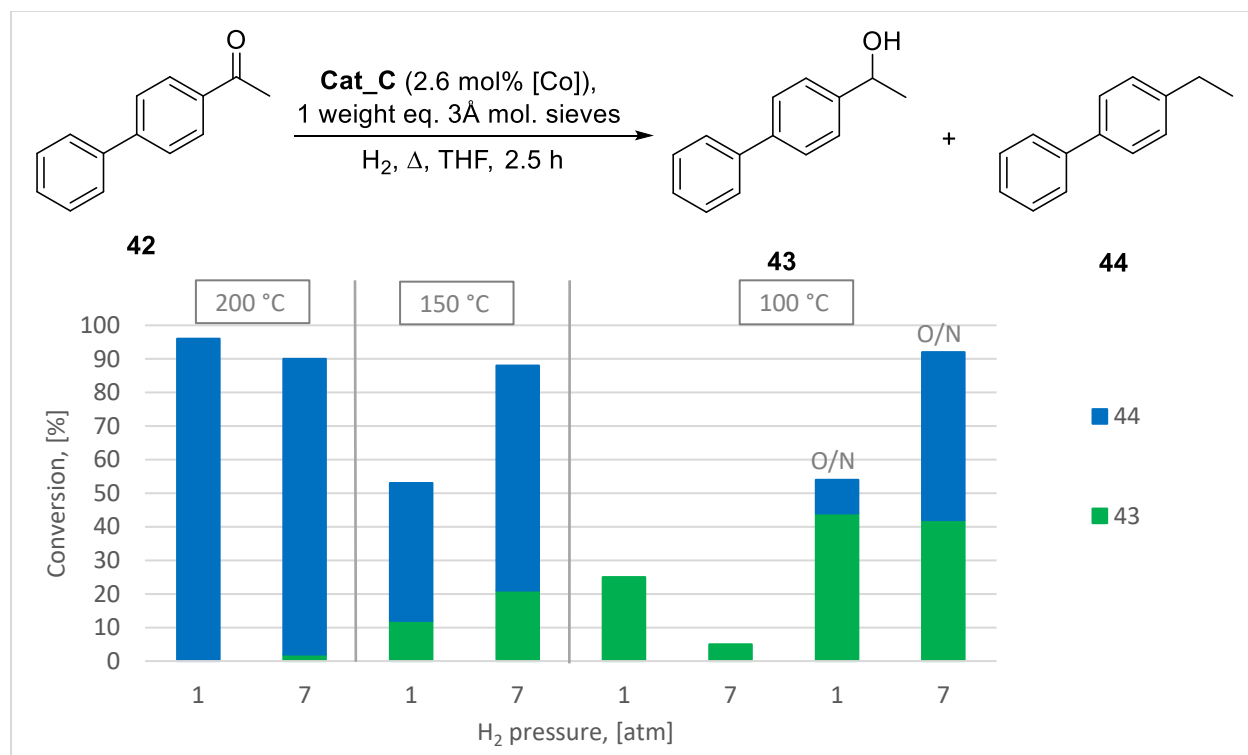
O/N = 17 h.

Figure 3.5 Pressure and temperature effects in the deoxygenation of 4-acetylbiphenyl **42** by *Cat_3C*.

Our results thus show that the reaction is strongly dependent on temperature, hydrogen pressure and reaction time. At this point, the data do not present any mechanistically logical trends and is insufficient to draw definitive conclusions. Nevertheless, reproducible and highly efficient deoxygenation of 4-acetylbiphenyl **42** is catalyzed by supported heterogeneous cobalt at 200 °C and 7 atm H_2 – unprecedented reactivity for cobalt nanoparticles.

3.2.2.5 Preliminary substrate scope
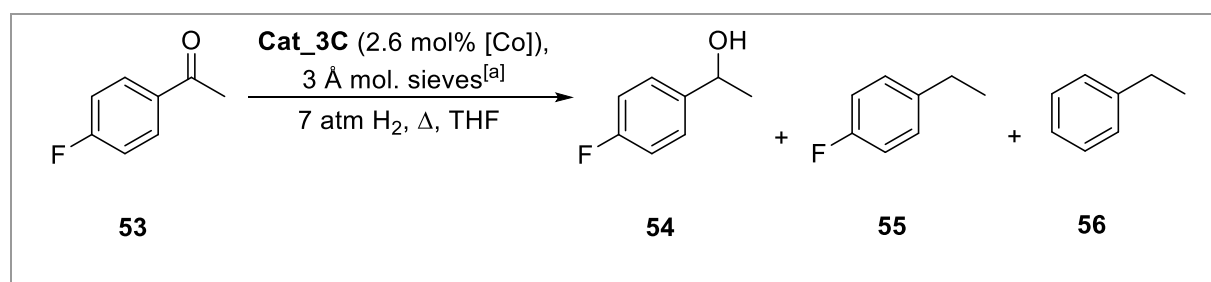
Functional group tolerance is paramount in fine chemical and pharmaceutical synthesis.[115, 122] As discussed, many deoxygenation processes are disadvantageous because of unintended reduction

of other functionalities, including halogen and *nitro* groups.[122] Strongly electron-withdrawing/deactivating substituents on the phenyl ring also inhibit many reactions.

The hydrodeoxygenation of deactivated 4-fluoroacetophenone **53** was investigated at two temperatures. At 150 °C, minimal reduction to 1-(4-fluorophenyl)ethanol **54** is observed after 2.5 h (Table **3.11**, entry 1). The substrate is fully consumed after reaction overnight, but only 22% 1-ethyl-4-fluorobenzene **55** is obtained (Table **3.11**, entry 2). Increasing the reaction temperature to

Table 3.11 Deoxygenation of 4-fluoroacetophenone **52** by *Cat_3C*.

Entry	Temperature, [°C]	Time[b]	Conversion, [%]	Conversion, [%]		
				54	55	56
1	150	2.5 h	22	20	0.4	0
2	150	O/N	99	72	22	4
3	200	2.5 h	28	21	5	0
4	200	O/N	100	0	94	5

Determined by GC-MS. [a] One weight equivalent per substrate. [b] O/N = 17 h

200 °C does not affect the conversion after 2.5 h (Table **3.11**, entry 3), the reaction proceeds to completion overnight, giving a 94% yield of 1-ethyl-4-fluorobenzene **55**, accompanied by just 5% yield of defluorination to ethylbenzene **56** (Table **3.11**, entry 4). Deoxygenation of 4-fluoroacetophenone **53** requires high reaction temperature, presumably because the inductively

deactivating *fluoro* substituent inhibits the carbonyl reduction. Defluorination, either before or after deoxygenation is not competitive.

One aliphatic ketone was explored, despite the absence of benzylic activation. However, 4-*tert*-butylcyclohexanone **57** is hydrogenated only to the corresponding alcohol, giving a mixture of *cis*- **58** and *trans*-4-*tert*-butylcyclohexanol **59** (Eqn. **3.2**). The reaction temperature is largely unimportant; nearly identical results were obtained at 150 °C and 200 °C.
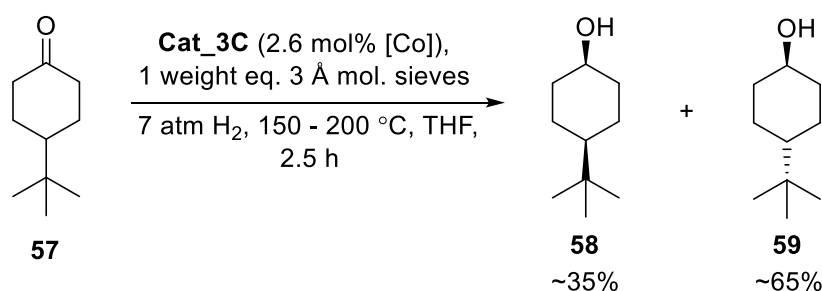
Equation 3.2 Reduction of 4-*tert*-butylcyclohexanone **55** by *Cat_3C*.

Finally, potential applications to aromatic ether cleavage were evaluated by subjecting diphenyl ether **60** to the catalytic conditions (150 °C, 7 atm H_2, 2.5 h). This reaction returns unchanged substrate.

Overall, the heterogeneous cobalt catalyst deoxygenates aromatic ketones in high yields and demonstrates great potential for selective HDO. Unactivated carbonyl substrates such as aliphatic ketones are hydrogenated only to the alcohols; the catalyst is inactive towards other C–O functionalities. Harsher reaction conditions and prolonged reaction times are required for electronically deactivated aromatic ketones.

Compared to other 1ˢᵗ row transition metal deoxygenation catalysts, this cobalt catalyst exhibits remarkable reactivity. No reduction of deactivated substrates was reported for the heterogeneous Cu/SiO_2 system or the initially homogeneous bis(phosphine)nickel catalyst **1**.[84, 87] In the reactions catalyzed by $FeCl_3$ under hydrosilylation conditions, 4-chlorobenzaldehyde was deoxygenated in only 62% yield, indicating that deoxygenation of 4-chloroacetophenone would be challenging even using silane rather than hydrogen.[102]

3.3 Conclusions and future work

3.3.1 Conclusions

After discovering that the active catalyst was insoluble, effective protocols were developed for the preparation of *base-free heterogeneous cobalt catalysts for the hydrodeoxygenation of aromatic ketones at low pressure*. The only significant side reaction, hydrogenation of aromatic ring, produces mixtures of over-hydrogenation byproducts. The reaction is sensitive to hydrogen pressure and strongly dependent on temperature, with optimal activity observed at 200 °C and 7 atm H_2. Long reaction times are required to deoxygenate substrates with deactivating substituents, but ketone deoxygenation is preferential to the reduction of fluoro substituents, potentially giving our catalyst significant advantages over current alternatives.

Importantly, base-free catalysts exploiting activated molecular sieves for water scavenging significantly suppress by-product formation, leading to quantitative hydrodeoxygenation. When KO^tBu (2 equiv) is used to scavenge water, aldol condensation and dimerization of benzylic radicals takes place to yield mixtures of dimers. Further radical additions then result in large molecular weight oligomers. When the base is replaced by activated molecular sieves, only small

amount of dimers, arising from radical coupling, is obtained. The side reactions are effectively suppressed if thermally labile, phosphoranimide-free cobalt precursor is used to prepare the active catalyst.

3.3.2 Future work

The nature of the active catalyst and the influence of the decomposition conditions is unclear. To confirm that the *tert*-butoxide ligands do not act as templating agents, a ligand-free precursor should be investigated. Readily available metal nitrates are commonly used as precursors in the production of heterogeneous catalysts.[133] Using $Co(NO_3)_2$ as a starting material would allow for facile cobalt immobilization on commercial supports such as silica or alumina, improving catalyst synthesis, recyclability and product purification. Decomposition/calcination temperature has a significant effect on the catalyst reactivity, therefore, its optimization is also imperative.[121, 133, 211]

Further optimization of the reaction conditions is paramount as evidenced by our preliminary results. Investigation of different H_2 pressures as a function of the reaction temperature at incremental time points is needed to determine the influence of these factors on the reaction rates, and to identify the optimal reaction conditions. Our cobalt catalyst exhibits extraordinary behavior; lower reaction temperature and an optimized H_2 pressure would make it an attractive candidate for industrial and academic applications. For this purpose, further substrate scope exploration is also needed. While the catalyst is inactive towards the *halo* substituents, its tolerance towards other common functionalities containing the carbonyl moiety (such as amides, ethers, carboxylic acids etc.) and chemo-, regio- and stereo-selectivity must be investigated.

Chapter 4. Experimental

4.1 General procedures (adapted from previous theses in the Stryker group)

All manipulations were performed using standard inert atmosphere techniques. Air sensitive reactions were carried out using standard Schlenk techniques on a vacuum/Ar (or N_2) double manifold or using a Labmaster sp Braun glovebox under N_2 atmosphere.

All solvents were thoroughly dried in a Grubbs-type solvent purification systems manufactured by Pure Process Technology (hexane, pentane, benzene, toluene) or Innovative Technologies, Inc. (THF, diethyl ether) or distilled from Na/benzophenone (THF) under N_2 when dark blue (benzophenone ketyl exhibits a dark blue color if water/oxygen are not present). All solvents in the glovebox were tested for residual moisture or oxygen gas using a dilute Na/benzophenone solution in THF. The low concentration benzophenone ketyl was prepared by mixing 100 mg Na, 17 mg benzophenone and 20 mL of THF in a 12-dram screw-cap vial.

Liquid reagents were degassed three times via 'freeze-pump-thaw' method and subsequently passed through Activity I neutral alumina inside of the glovebox. Volatile liquids were brought into the glovebox and stored in Teflon-sealing glass reactors under Ar or N_2 atmosphere. Non air-sensitive solids were pumped into the glovebox in the original containers or vials covered with a kimwipe. All glassware was a) flame-dried, b) oven-dried at 150 °C overnight or c) oven-dried at 200 °C for at least 2 hours prior use. Teflon stir bars used in air sensitive reactions were oven dried at 150 °C overnight. Oven-dried metal cannulas were used for liquid transfers.

Air sensitive IR sample preparation was carried out in the glovebox. Cast film samples were sealed under N_2 atmosphere with O-Rings. Elemental analysis samples were prepared in the

glovebox using two pre-weighed tin boats. Materials were dried on a high vacuum line with a three-stage diffusion pump ($<10^{-5}$ Torr). Approximately 1-2 mg of sample was loaded into one boat which was then folded into a cube and placed into the outer boat. The outer boat was folded several times, loaded into a one-dram vial, sealed with a cap, and submitted for analysis. Duplicate samples were run to ensure the accuracy of our results. NMR spectroscopy was carried out in standard NMR tubes sealed with plastic caps and wrapped with parafilm for air sensitive compounds. Hydrogen decoupled ^{31}P NMR and phosphorus decoupled ^{1}H NMR was recorded. Second order perturbations were observed for the phenyl substituents in the synthesis of triphenylphosphoranimide ligand but they were treated as single order perturbations.

Reactions that required heating and high pressures were carried out using Ika stir plates with digital temperature control and silicon oil baths. Stainless steel Parr reactors with Teflon seals and Swagelok® Quick Connect hydrogen inlets were used for high pressure catalytic reactions (referred to as 'high pressure bombs'). The reactors were fitted with pressure gauges capable of measuring pressured from 100 to 2000 psi. Glass inserts were used to separate materials in the reaction from the influence of the metals in the stainless steel.

4.2 Instrumentation (adapted from previous theses in Stryker group)

Bruker PLATFORM diffractometer equipped with a SMART APEX II CCD area detector was used to perform X-Ray Crystallography. Diffraction data collection and crystal structure determination was performed by Dr. Robert McDonald and Dr. Michael Ferguson, Chemistry X-Ray Crystallography Laboratory, University of Alberta.

CHNS elemental analyses were determined using Thermo Scientific FLASH 2000 Elemental Analyzer. Combustion analysis of triphenylphosphoranimide clusters often produces data that deviates from the expected carbon content.[188-193] Given that organometallic compounds, especially those containing phosphorus, can exhibit low carbon values,[187] nitrogen and hydrogen have been used to interpret our data as values are they more consistent with anticipated elemental composition.

FT-IR spectroscopy was carried out using Nicolet 8700 FT-IR Spectrometer operating with OMNIC spectra software. Gas chromatography-mass spectrometry was performed using Hewlett Packard GCD series G1800A GC-MS or Hewlett Packard 5890 GC with a 5970 MSD mass detector. NIST/EPA/NIH v. 2.0 Mass Spectral Library was used for structure determination. CHNS, FT-IR and GC-MS data was determined by the analytical staff at the Analytical and Instrumentation Laboratory in the Department of Chemistry at the University of Alberta. Agilent/Varian 400 MHz spectrometer at 26 °C was used to acquire ^{1}H and ^{31}P NMR spectra. Residual protium signals from the deuterated solvents were used to reference chemical shifts in ^{1}H NMR spectra. 85 % phosphoric acid was assigned a value of 0 ppm and was used as an external reference for ^{31}P NMR signals.

4.3 Chemical materials (adapted from previous theses in Stryker group)

All commercially available compounds were purchased from Sigma Aldrich, Strem or Alfa Aesar. Reagent purification was performed when necessary. Potassium *tert*-butoxide used for catalyst synthesis was sublimed according to the literature procedure.[184] Potassium trimethylsilanolate was sublimed according to the same procedure. Experimental procedures used to synthesize other reagents or precatalysts are noted down in the sections below.

4.4 Synthetic Procedures

4.4.1 Synthesis of dibromotriphenyl-phosphorane (Br$_2$PPh$_3$)

$$PPh_3 \xrightarrow[\substack{0\ °C\ \rightarrow\ RT, \\ CH_2Cl_2,\ \text{overnight}}]{Br_2} Br_2PPh_3$$
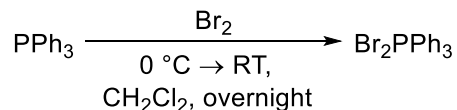
The procedure was adapted from literature.[161-162] A 500 mL round bottom flask was charged with PPh$_3$ (20.00 g, 76.25 mmol, 1 eq.), 200 mL dichloromethane and a large bar-shaped Teflon stir bar. The flask was placed in an ice bath and was cooled to 0 °C. An addition funnel was fitted onto the round bottom flask and charged with Br$_2$ (12.18 g, 76.25 mmol, 1 eq.) in 24 mL dichloromethane. The bromine solution was added dropwise within 1 hour at 0 °C. The resulting off-white slurry was stirred overnight while warming up to room temperature. The solvent was then removed *in vacuo* and the precipitate was washed with dry hexane (2x20 mL) and dry THF (2x20 mL). The compound was dried *in high vacuo* overnight. The product (30.21 g, 71.57 mmol, 93%) was spectroscopically confirmed with ^{31}P and ^{1}H NMR. The reaction yield can vary between 80 – 95%. ^{31}P{^{1}H} NMR (400 MHz, CD$_2$Cl$_2$): 51.25 ppm (s). ^{1}H{^{31}P} NMR (400 MHz, CD$_2$Cl$_2$): 7.63 ppm (t, 6H, $J = 7.6$ Hz), 7.75 ppm (tt, 3H, $J = 7.6$, 1.2 Hz), 7.80 ppm (t, 6H, $J = 7.6$, 1.2 Hz).

4.4.2 Synthesis of triphenylphosphoraniminium bromide ([H$_2$NPPh$_3$]Br)

$$Br_2PPh_3 \xrightarrow[\substack{THF,\ RT, \\ \text{overnight}}]{LiNH_2} Br[H_2NPPh_3]$$

A 100 mL round bottom flask was charged with Ph_3PBr_2 (5.50 g, 13.0 mmol, 1 eq.), 60 mL dry THF and a medium octagonal Teflon stir bar in the glovebox. Lithium amide (0.27 g, 11.7 mmol, 0.9 eq.) was added as a solid in one portion and reaction stirred overnight at room temperature. The resulting white slurry was vacuum filtered and the solid product was washed with THF (2x10 mL). The product was dried overnight *in high vacuo* and obtained as a white powder (2.89 g, 8.07 mmol, 62%). Reaction yields vary between 50 – 70%. $^{31}P\{^1H\}$ NMR (400 MHz, CDCl$_3$): 37.08 ppm (s). $^1H\{^{31}P\}$ NMR (400 MHz, CDCl$_3$): 6.90 ppm (s, broad, 2H), 7.57 ppm (dd (at), 6H, 8.4, 7.2 Hz), 7.69 ppm (tt, 3H, J = 7.6, 1.2 Hz), 7.84 ppm (dd, 6H, J = 8.4, 1.2 Hz).

4.4.3 Synthesis of sodium triphenylphosphoranimide (NaNPPh$_3$)

$$[H_2NPPh_3]Br \ + \ 6 \ NaH \ + \ 3 \ NaNH_2 \ \xrightarrow{\text{THF, RT, overnight}} \ Ph_3PNNa \cdot THF$$
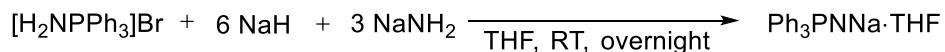
A 100 mL round bottom flask was charged with $[Ph_3PNH_2]Br$ (5.58 g, 15.6 mmol, 1 eq.), 60 mL of THF and a medium octagonal Teflon stir bar. NaH (2.32 g, 96.6 mmol, 6.2 eq.) was added as a solid in one portion and the white slurry was stirred at room temperature for 30 minutes. Sodium amide (1.95 g, 49.9 mmol, 3.2 eq.) was added in one portion and the resulting mixture stirred overnight at RT. The resulting beige slurry was vacuum filtered over a Celite layer and a yellow mother liquor solution was obtained. THF was removed *in vacuo* and the product was dried overnight *in high vacuo*. The product was obtained as a beige solid (5.30 g, 14.3 mmol, 91%) and was confirmed to be pure by NMR and elemental analysis. THF coordination is usually observed and reaction yields may vary between 75 – 91%. $^{31}P\{^1H\}$ NMR (400 MHz, C$_6$D$_6$): -10.06 ppm (s). $^1H\{^{31}P\}$ NMR (400 MHz, C$_6$D$_6$): 6.90 ppm (dd (at), 6H, J = 8.4, 7.2 Hz),

7.02 ppm (tt, 3H, J = 7.2, 1.2 Hz), 7.65 ppm (dd, 6H, J = 8.4, 1.6 Hz). Elemental analysis: C: 70.68 (71.15), N: 3.73 (3.77), H: 6.60 (6.24).

4.4.4 Synthesis of triisopropylphosphine (^{i}Pr₃P)

$$PCl_3 \quad + \quad 4^i PrMgCl \quad \xrightarrow[\text{Et}_2\text{O, overnight}]{0\ °C \rightarrow RT,} \quad iPr_3P$$
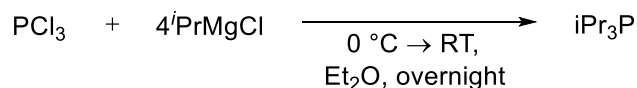
A 250 mL three-neck round bottom flask was charged with 150 mL of dry Et₂O and a large bar shaped Teflon stir bar in the glovebox. Degassed PCl₃ (2.18 mL, 0.03 mol, 1 eq.) was cannula transferred into the flask and the mixture was cooled down to 0 °C with an ice bath. An ^{i}PrMgCl solution (10.29 g, 0.100 mol, 4 eq.) was added to the PCl₃ solution in small portions *via* a large bore cannula (formation of white MgCl₂ precipitate was observed within five minutes). The reaction was stirred overnight while warming to room temperature. The reaction (thick white slurry) was quenched with degassed saturated NH₄Cl (aq) and the organic layer was cannula transferred into a 500 mL Schlenk flask (purged with Ar). The phosphine solution was washed with degassed NH₄OH (aq), H₂O and saturated NaCl (aq). The organic layer was transferred to a 250 mL Schlenk flask charged with anhydrous MgSO₄ (purged with Ar). The dried phosphine solution was canula filtered into a glass 'bomb'. Diethyl ether was removed *in vacuo* to yield a clear yellow liquid which was filtered through a kimwipe in the glovebox for further purification (3.49 g, 0.022 mol, 87%). ^{31}P NMR analysis indicated 95% purity. ^{31}P{^{1}H} NMR (400 MHz, C₆D₆): 19.56 ppm (s). ^{1}H{^{31}P} NMR (400 MHz, C₆D₆): 1.01 ppm (d, 18H, J = 7.2 Hz), 1.64 ppm (m, 3H).

4.4.5 Synthesis of dibromotriisopropyl-phosphorane (Br$_2$P^{i}Pr$_3$)

$$P^iPr_3 \xrightarrow[\substack{0\ ^\circ C\ \to\ RT, \\ Et_2O,\ overnight}]{Br_2} Br_2P^iPr_3$$
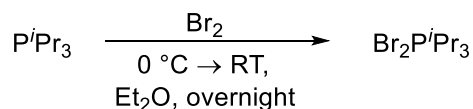
A 100 mL Schlenk flask was charged with P^{i}Pr$_3$ (3.30 g, 20.5 mmol, 1 eq.), 35 mL of dry Et$_2$O and a small octagonal Teflon stir bar in the glovebox. An addition funnel was charged with 10 mL of dry Et$_2$O and fitted onto the Schlenk flask. The setup was taken out of the glovebox, connected to the Schlenk line and the phosphine solution was cooled to 0 °C using an ice bath. Bromine (3.28 g, 20.5 mmol, 1 eq.) was transferred to the addition funnel under Ar flow and added dropwise to the Schlenk flask in 10 mins (immediate formation of white precipitate). After the addition was complete, the resulting yellow slurry was stirred overnight at room temperature. The solvent was removed *in vacuo* and the resulting off white precipitate was dried *in high vacuo* overnight (6.51 g, 20.3 mmol, 81%). Purity was confirmed by elemental analysis. NMR spectroscopy indicated inner and outer sphere bromine coordination in a 3 : 1 ratio (unknown which is which). ^{31}P{^{1}H} NMR (400 MHz, CD$_2$Cl$_2$): 89.94 (s) (68%), 37.91 ppm (s) (26%). ^{1}H{^{31}P} NMR (400 MHz, CD$_2$Cl$_2$): 18H: 1.41 ppm (d, J = 7.2 Hz), 1.52 ppm (d, J = 7.6 Hz), 3H: 2.67 ppm (m), 2.89 ppm (m). Elemental analysis: C: 34.19 (33.78), H: 6.63 (6.61).

4.4.6 Synthesis of triisopropylphosphoraniminium bromide (Br[H$_2$NP^{i}Pr$_3$])

$$Br_2P^iPr_3 \xrightarrow[\substack{THF,\ RT, \\ overnight}]{LiNH_2} Br[H_2NP^iPr_3]$$

A 100 mL round bottom flask was charged with ^{i}Pr$_3$PBr$_2$ (2.66 g, 8.32 mmol, 1 eq.), 25 mL of dry THF and a small octagonal Teflon stir bar in the glovebox. Lithium amide (0.18 g, 7.91

mmol, 0.95 eq.) was added as a solid in one portion and the reaction stirred overnight at room temperature. The resulting white slurry was vacuum filtered and the solid product was washed with THF (2x10 mL), dissolved in DCM and vacuum filtered over Celite. The product was dried overnight *in vacuo* and obtained as beige powder (1.12 g, 4.37 mmol, 56%). The product can be obtained as a white or beige powder; yield varies between 50 – 60%. Purity was confirmed by NMR. $^{31}P\{^1H\}$ NMR (400 MHz, CDCl$_3$): 64.73 ppm (s). $^1H\{^{31}P\}$ NMR (400 MHz, CDCl$_3$): 1.42 ppm (d, 18H, J = 7.6 Hz), 2.74 ppm (m, 3H), 5.31 ppm (s, 2H). Elemental analysis: C: 42.32 (42.20), N: 5.32 (5.47), H: 9.35 (9.05).

4.4.7 Synthesis of sodium triisopropylphosphoranimide (NaNP^{i}Pr$_3$)

$$Br[H_2N^iPr_3] \quad + \quad 6\ NaH \quad + \quad 3\ NaNH_2 \xrightarrow{\text{THF, RT, overnight}} {}^iPr_3PNNa\cdot THF$$
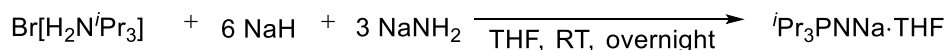
A 100 mL round bottom flask was charged with [^{i}Pr$_3$PNH$_2$]Br (0.50 g, 1.95 mmol, 1 eq.), 10 mL of THF and a small octagonal Teflon stir bar. Sodium hydride (0.28 g, 11.7 mmol, 6 eq.) was added as a solid in one portion and the white slurry was stirred at room temperature for 30 minutes. Sodium amide (0.23 g, 5.86 mmol, 3 eq.) was added in one portion and the resulting mixture stirred overnight at RT. The resulting beige slurry was vacuum filtered over a Celite layer and a yellow mother liquor solution was obtained. THF was removed *in vacuo* and the product was further dried overnight *in high vacuo*. The product was obtained as a beige solid (0.44 g, 14.3 mmol, 91%) and was confirmed to be pure by NMR and elemental analysis. Reaction yields may vary between 75 – 91%. THF coordination can be observed; clusters of different nuclearity are formed affecting NMR results. $^{31}P\{^1H\}$ NMR (400 MHz, CDCl$_3$): 12.23

ppm (s). ^{1}H{^{31}P} NMR (400 MHz, CDCl$_3$): 1.09 ppm (d, 18H, J = 7.6 Hz), 1.68 ppm (m, 3H). Elemental analysis: C: 54.69 (54.81), N: 7.14 (7.10), H: 10.37 (10.73).

4.4.8 Synthesis of [Co(NPPh$_3$)(OSiMe$_3$)(THF)]$_2$ 37 by salt metathesis
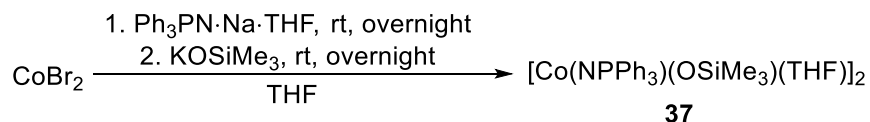
$$\text{CoBr}_2 \xrightarrow[\text{THF}]{\substack{\text{1. Ph}_3\text{PN·Na·THF, rt, overnight} \\ \text{2. KOSiMe}_3\text{, rt, overnight}}} \text{[Co(NPPh}_3\text{)(OSiMe}_3\text{)(THF)]}_2$$
$$\textbf{37}$$

Inside the glovebox, a 12-dram screw-cap vial was charged with a bar-shaped, small stir bar, CoBr$_2$ (240 mg, 1.10 mmol, 1.02 eq.) and approximately 25 mL of dry THF. The solution was stirred for ~15 minutes until all CoBr$_2$ was dissolved to give a clear, blue solution. A Ph$_3$PNNa·THF ligand (400 mg, 1.08 mmol, 1 eq.) was added all at once resulting in an immediate change to a teal slurry which was stirred overnight at room temperature. *In situ* addition of a sublimed KOSiMe$_3$ (148 mg, 1.12 mmol, 1.04 eq.) resulted in an immediate colour change to deep blue and significantly increased product solubility. The solution was stirred overnight at room temperature and filtered through a Celite plugged pipet (~2 cm Celite). Solvent removal *in vacuo* affords a blue precipitate. A concentrated solution of the precipitate in THF was filtered through a Celite plugged pipet. The solvent was removed *in vacuo*, and the extraction was repeated twice. The product was dried *in high vacuo* overnight to give a blue, crystalline solid with retained THF coordination (422 mg, 0.449 mmol). The reaction yield is 85 % and can vary between 50 – 85 %. FT-IR: ν/cm^{-1} cast film from THF = 482 w, 529 s, 549 s, 693 s, 719 s, 746 s, 825 s, 900 m, 930 m, 967 m, 997 s, 1013 s, 1035 s, 1113 s, 1161 w, 1185 w, 1235 m, 1311 w, 1427 s, 1484 m, 1574 w, 1590 w, 1679 w, 1820 w, 1907 w, 1967 w, 2891 m,

2947 m, 3013 w, 3055 m. Elemental analysis calculated for $C_{50}H_{64}Co_2N_2O_4P_2Si_2$: C: 57.26 (60.47), N: 2.98 (2.82), H: 5.92 (6.50).

4.4.9 Synthesis of [Co(NPPh₃)(OᵗBu)(THF)]₂ 39 by salt metathesis
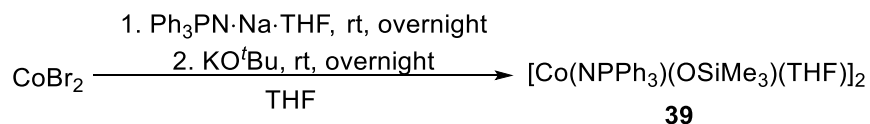
$$CoBr_2 \xrightarrow[\text{THF}]{\substack{\text{1. Ph}_3\text{PN·Na·THF, rt, overnight} \\ \text{2. KO}^t\text{Bu, rt, overnight}}} \underset{\textbf{39}}{[\text{Co(NPPh}_3)(\text{OSiMe}_3)(\text{THF})]_2}$$

Inside the glovebox, a 12-dram screw-cap vial was charged with a bar-shaped small stir bar, CoBr₂ (179 mg, 0.82 mmol, 1.01 eq.) and approximately 20 mL of dry THF. The solution was stirred for ~15 minutes until all CoBr₂ was dissolved to give a clear, blue solution. A Ph₃PNNa·THF ligand (300 mg, 0.81 mmol, 1 eq.) was added all at once affording an immediate change to a teal slurry which was stirred overnight at room temperature. Sublimed KOᵗBu (93 mg., 0.82 mmol, 1.02 eq.) was added *in situ* and the solution was stirred overnight at room temperature. Next day, the solution was filtered through a Celite plugged pipet (~2 cm Celite) and the solvent was removed *in vacuo* giving a dark green precipitate with lilac bands. A concentrated solution of the precipitate in THF was filtered through a Celite plugged pipette affording a green solution while the lilac impurity remained on top of the Celite. The solvent was removed *in vacuo* and the extraction was repeated. Drying the product *in high vacuo* overnight results in a dark green, crystalline solid with retained THF coordination (270 mg, 0.304 mmol). Reaction yield is 75 % and can vary between 40 -75 %. FT-IR: v/cm^{-1} cast film from THF = 529 s, 564 w, 593 s, 619 w, 694 s, 711 s, 747 m, 932 w, 998 m, 1025 m, 1068 s, 1114 s, 1186 m, 1212 s, 1308 w, 1394 w, 1424 s, 1482 m, 1572 w, 15888 w, 1820 w, 1899 w, 1959 w, 2855 m,

2925 m, 2959 m, 3050 m. Elemental analysis calculated for $C_{50}H_{64}Co_2N_2O_4P_2$: C: 62.41 (65.00), N: 3.19 (2.92), H: 6.30 (6.71).

4.4.10 Synthesis of $[Co(NP^iPr_3)_2]_3$ 40 by salt metathesis

$$CoBr_2 \xrightarrow[\text{THF, rt, overnight}]{\text{2 eq. } ^iPr_3PNNa} [Co(P^iPr_3)_2]_3$$

40
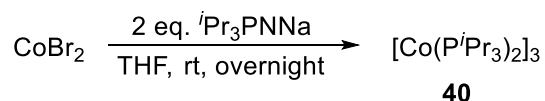
Inside the glovebox, a 5-dram vial was charged with a bar-shaped small stir bar, $CoBr_2$ (117 mg., 0.532 mmol, 1 eq.) and approximately 10 mL of dry THF. The solution was stirred for ~15 minutes until all $CoBr_2$ was dissolved to give a clear, blue solution. Sodium triisopropylphosphoranimide (210 mg., 1.065 mmol, 2 eq.) was added all at once resulting in an immediate change to a dark green slurry. The reaction was stirred overnight at room temperature and the solution was filtered through a Celite plugged pipet (~2 cm Celite). Solvent removal *in vacuo* resulted in a dark green solid which was dissolved in 10 mL hexane. The solution was filtered through a Celite plug and the solvent was removed *in vacuo*. Drying the product *in high vacuo* overnight gives a dark green, oily solid (188 mg., 0.154 mmol). Reaction yield of 87 % was obtained. FT-IR: v/cm^{-1} cast film from THF = 401 w, 523 m, 661 s, 694 s, 760 w, 885 m, 927 w, 1017 m, 1054 s, 1093 s, 1159 m, 1204 m, 1257 w, 1275 w, 1394 m, 1464 s, 2870 s, 2925 s, 2955 s. Elemental analysis calculated for $C_{50}H_{126}Co_3N_6P_6$: C: 54.42 (53.06), N: 6.48 (6.88), H: 10.39 (10.39).

4.5 Catalytic procedures

The catalytic results are reported in percent conversion and percent yields. The reactions were quantified by ^1H NMR with a hexamethyldisiloxane standard. The NMR standard was added to

each reaction upon the reaction work-up in a 6 : 1 ratio of 4-acetylbiphenyl : hexamethyldisiloxane. The substrate (4-acetylbiphenyl **42**) and the anticipated products (1-(4-biphenylyl)-1-ethanol **43** and 4-ethylbiphenyl **44**) contain distinct methyl groups that can be used to distinguish the compounds and quantify the reaction yields (Fig. **4.1**). The reaction mixture was dissolved in CDCl$_3$ and analyzed by ^{1}H NMR (Appendix **C1.1**, representative ^{1}H NMR spectrum). Upon peak integration, peak of the standard was set to 1.0 (100%) giving the exact conversion and yields.

	Shift, [ppm]	Signal	J, [Hz]
A	**2.66**	**s**	**-**
B	**1.59**	**d**	**6.4**
C	**1.35**	**t**	**7.6**
D	4.99	q	6.4
E	var.	s, br	-
F	2.74	q	7.6
X	**0.19**	**s**	**-**

Hexamethyldisiloxane
Six equivalent methyl groups:
- add 1/6 mol compared to **43**
- set the peak integration to
1.0 (100 %)
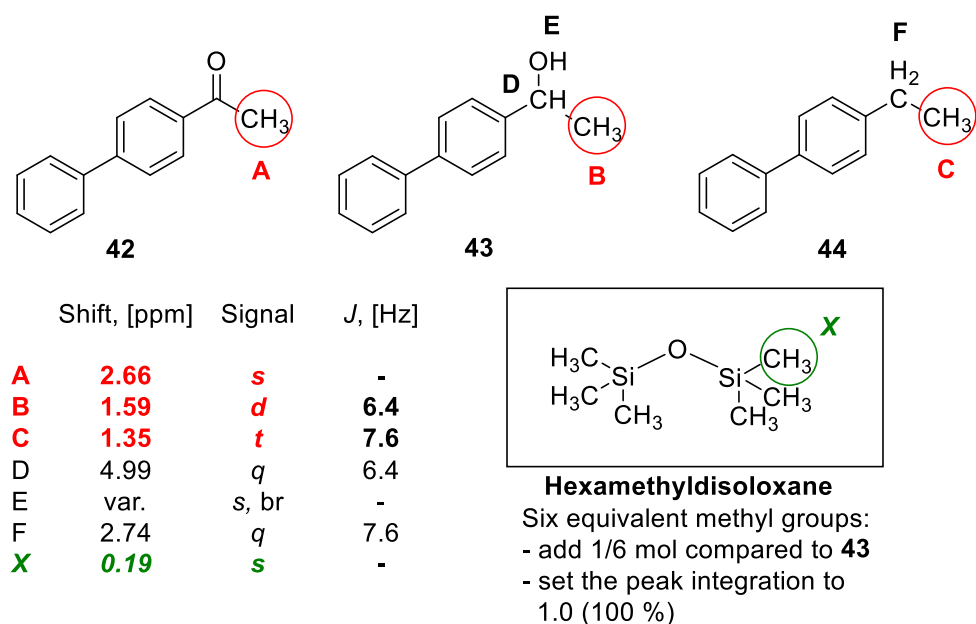
Figure 4.1 ^{1}H NMR quantification of catalytic results with hexamethyldisiloxane as an internal standard.

If the reactions were analyzed by GC-MS, the yields were approximated from the peak area percentage due to the lack of calibration.

Clusters [Co(NPPh$_3$)(OSiMe$_3$)(THF)]$_2$ **37** and [Co(NPPh$_3$)(O^{t}Bu)(THF)]$_2$ **39** were considered to be dimeric and cluster [Co(NP^{i}Pr$_3$)$_2$]$_3$ **40** was considered to be trimeric for the purpose of calculating catalyst loading.

4.5.1 A general procedure for hydrodeoxygenation of 4-acetylbiphenyl 42 by [Co(NPPh₃)(OʹBu)(THF)]₂ 39 and KOʹBu

In a glovebox, a stainless steel high-pressure reaction vessel was charged with a small bar-shaped stir bar, 4-acetylbiphenyl **42** (123 mg., 0.622 mmol), **39** (3.4 mg., 0.0042 mmol), 9-BBN (2.1 mg., 0.0082 mmol), KOʹBu (142 mg., 1.24 mmol) and 5 mL THF. The reactor was sealed, removed from the glovebox, connected to a hydrogen line and charged with 34 atm H_2 (500 psi). The reactor was then immersed into an oil bath at 150 °C and stirred overnight at 1200 rpm. Next day, the reactor was removed from the heating source and immersed into a room-temperature bath. Once cooled, the reactor was slowly depressurized and opened to air. The resulting mixture was transferred into a 5-dram vial. The reactor was washed twice with 5 mL toluene portions which were added to the 5-dram vial. The reaction was quenched with ~3 M HCl solution and the organic compounds were extracted thrice with toluene/THF mixture. The extract was dried with $MgSO_4$, filtered through a silica plugged pipet (~2 cm silica) and a Florisil® plugged pipet (~2 cm Florisil®). The solution has a slight yellowish/tan shade if the solution consists largely of 4-acetylbiphenyl **42**. Hydrogenation and deoxygenation products 1-(4-biphenylyl)-1-ethanol **43** and 4-ethylbiphenyl **44** give a clear, colorless solution. The solvents were removed *in vacuo* affording a) a slightly yellow solid (4-acetylbiphenyl **42**), b) white precipitate (significant portion of 1-(4-biphenylyl)-1-ethanol **43**), or c) a semi-liquid, yellowish solid if considerable deoxygenation takes place. The reaction products were dissolved in $CDCl_3$, 20 μL of hexamethyldisiloxane (0.103 mmol) was added to the solution and the sample was analyzed by ^{1}H NMR (95 % conversion, 69 % of **43** and 12 % of **44**).

4.5.1.1 Hydrodeoxygenation of 4-acetylbiphenyl 42 by [Co(NPPh₃)(OᵗBu)(THF)]₂ 39 and KOᵗBu without 9-BBN

The general procedure was applied to 4-acetylbiphenyl **42** (123 mg., 0.622 mmol), **39** (3.4 mg., 0.0042 mmol) and KOᵗBu (142 mg., 1.24 mmol). The reaction was quantified by ^{1}H NMR: 95 % conversion, 40 % of 4-biphenylyl)-1-ethanol **43,** 23 % of 4-ethylbiphenyl **44**. GC-MS: 94 % conversion, 49 % of 4-biphenylyl)-1-ethanol **43,** 29 % of 4-ethylbiphenyl **44**, 15 % of biphenyl **45.**

4.5.1.2 Hydrodeoxygenation of 4-acetylbiphenyl 42 by [Co(NPPh₃)(OᵗBu)(THF)]₂ 39 and KOᵗBu with alumina support (4 wt% of 39)

The general procedure was applied to 4-acetylbiphenyl **42** (123 mg., 0.622 mmol), **39** (3.4 mg., 0.0042 mmol), 9-BBN (2.1 mg., 0.0082 mmol) and KOᵗBu (142 mg., 1.24 mmol). Basic Al_2O_3 (75 mg., 0.75 mmol) was added to the reactor before sealing it. The reaction was quantified by ^{1}H NMR: 94 % conversion, 55 % of 4-biphenylyl)-1-ethanol **43,** 21 % of 4-ethylbiphenyl **44**. GC-MS: 94 % conversion, 65 % of 4-biphenylyl)-1-ethanol **43,** 22 % of 4-ethylbiphenyl **44**, 4 % of biphenyl **45.**

4.5.1.3 Hydrodeoxygenation of 4-acetylbiphenyl 42 by [Co(NPPh₃)(OᵗBu)(THF)]₂ 39 and KOᵗBu at 175 °C

The general procedure was applied to 4-acetylbiphenyl **42** (123 mg., 0.622 mmol), **39** (3.4 mg., 0.0042 mmol), 9-BBN (2.1 mg., 0.0082 mmol) and KOᵗBu (142 mg., 1.24 mmol). The reactor was placed in an oil bath at 175 °C after adding H_2. The reaction was quantified by ^{1}H NMR: 95 % conversion, 49 % of 4-biphenylyl)-1-ethanol **43,** 16 % of 4-ethylbiphenyl **44**. GC-MS:

92 % conversion, 59 % of 4-biphenylyl)-1-ethanol **43,** 18 % of 4-ethylbiphenyl **44**, 8.5 % of biphenyl **45** and 5 % of dimerization**.**

4.5.1.4 Hydrodeoxygenation of 4-acetylbiphenyl 42 by [Co(NPPh₃)(OᵗBu)(THF)]₂ 39 and KOᵗBu at 175 °C without 9-BBN

The general procedure was applied to 4-acetylbiphenyl **42** (123 mg., 0.622 mmol), **39** (3.4 mg., 0.0042 mmol) and KOᵗBu (142 mg., 1.24 mmol). The reactor was placed in an oil bath at 175 °C after adding H_2. The reaction was quantified by ^{1}H NMR: 73 % conversion, 40 % of 4-biphenylyl)-1-ethanol **43,** 16 % of 4-ethylbiphenyl **44**.

4.5.1.5 Hydrodeoxygenation of 4-acetylbiphenyl 42 by [Co(NPPh₃)(OᵗBu)(THF)]₂ 39 and KOᵗBu (3 eq. base)

The general procedure was applied to 4-acetylbiphenyl **42** (123 mg., 0.622 mmol), **39** (3.4 mg., 0.0042 mmol), 9-BBN (2.1 mg., 0.0082 mmol) and KOᵗBu (222 mg., 1.88 mmol). The reaction was quantified by ^{1}H NMR: 94 % conversion, 48 % of 4-biphenylyl)-1-ethanol **43,** 17 % of 4-ethylbiphenyl **44**. GC-MS: 68 % conversion, 29 % of 4-biphenylyl)-1-ethanol **43,** 12 % of 4-ethylbiphenyl **44**, 14 % of biphenyl **45** and 2 % of dimerization**.**

4.5.1.6 Hydrodeoxygenation of 4-acetylbiphenyl 42 by [Co(NPPh₃)(OᵗBu)(THF)]₂ 39 and KOᵗBu (3 eq. base) without 9-BBN

The general procedure was applied to 4-acetylbiphenyl **42** (123 mg., 0.62 mmol), **39** (3.4 mg., 0.0042 mmol) and KOᵗBu (222 mg., 1.88 mmol). The reaction was quantified by ^{1}H NMR:

76 % conversion, 27 % of 4-biphenylyl)-1-ethanol **43,** 12 % of 4-ethylbiphenyl **44**. GC-MS indicates 11 % of biphenyl **45.**

4.5.1.7 Hydrodeoxygenation of 4-acetylbiphenyl 42 by [Co(NPPh₃)(OᵗBu)(THF)]₂ 39 and KOᵗBu at 110 – 140 °C

The general procedure was applied to 4-acetylbiphenyl **42** (123 mg., 0.622 mmol), **39** (3.4 mg., 0.0042 mmol), 9-BBN (2.1 mg., 0.0082 mmol) and KOᵗBu (142 mg., 1.24 mmol). The reactor was placed in an oil bath at an indicated temperature after adding H_2. The samples were analyzed and quantified by ^{1}H NMR.

Table 4.1 Low temperature studies in the hydrodeoxygenation of 4-acetylbiphenyl **42** by **39**.

Entry	Temperature, [°C]	Conversion, [%]	Yield, [%]
			43
1	110	97	85
2	120	85	83
3	130	77	76
4	140	80	79

* Stoichiometric conversion to 4-ethylbiphenyl was detected at 120 – 140 °C.

4.5.1.8 Hydrodeoxygenation of 4-acetylbiphenyl 42 by [Co(NPPh₃)(OᵗBu)(THF)]₂ 39 and KOᵗBu at 110 – 140 °C without 9-BBN

The general procedure was applied to 4-acetylbiphenyl **42** (123 mg., 0.622 mmol), **39** (3.4 mg., 0.0042 mmol) and KO^{t}Bu (142 mg., 1.24 mmol). The reactor was placed in an oil bath at an indicated temperature after adding H$_2$. The samples were analyzed and quantified by ^{1}H NMR.

Table 4.2 Low temperature studies in the hydrodeoxygenation of 4-acetylbiphenyl **42** by **39** without 9-BBN.

Entry	Temperature, [°C]	Conversion, [%]	Yield, [%]
			43
1	110	15	13
2	120	39	37
3	130	44	43
4	140	31	30

4.5.1.9 Hydrodeoxygenation of 4-acetylbiphenyl 42 by [Co(NPPh₃)(O^{t}Bu)(THF)]₂ 39 and KO^{t}Bu at 1 – 2 atm H₂

The general procedure was applied to 4-acetylbiphenyl **42** (123 mg., 0.622 mmol), **39** (3.4 mg., 0.0042 mmol), 9-BBN (2.1 mg., 0.0082 mmol) and KO^{t}Bu (142 mg., 1.24 mmol). The reactor was pressurized to 7 atm H$_2$ (100 psi) and depressurized to ~1 – 2 atm twice H$_2$ before placing it in an oil bath at 150 °C. Analysis by ^{1}H NMR shows 43 % conversion, 1 % of 4-biphenylyl)-1-ethanol **43** and 5 % of 4-ethylbiphenyl **44**. GC-MS: 18 % conversion, 1 % of 4-biphenylyl)-1-ethanol **43,** 4 % of 4-ethylbiphenyl **44**, 4 % of biphenyl **45** and 5 % of dimerization**.**

4.5.1.9 Hydrodeoxygenation of 4-acetylbiphenyl 42 by [Co(NPPh₃)(OᵗBu)(THF)]₂ 39 and KOᵗBu at 1 – 2 atm H₂ without 9-BBN

The general procedure was applied to 4-acetylbiphenyl **42** (123 mg., 0.622 mmol), **39** (3.4 mg., 0.0042 mmol) and KOᵗBu (142 mg., 1.24 mmol). The reactor was pressurized to 7 atm H₂ (100 psi) and depressurized to ~1 – 2 atm twice H₂ before placing it in an oil bath at 150 °C. Analysis by ¹H NMR shows 37 % conversion with 6 % of 4-biphenylyl)-1-ethanol **43**. GC-MS: 2 % conversion, 0 % of 4-biphenylyl)-1-ethanol **43,** 0 % of 4-ethylbiphenyl **44**, 4 % of biphenyl **45.**

4.5.2 A general procedure for hydrodeoxygenation of 4-acetylbiphenyl 42 by [Co(NPPh₃)(OSiMe₃)(THF)]₂ 37 and KOᵗBu

In a glovebox, a stainless steel high pressure reaction vessel with glass lining was charged with a small bar-shaped stir bar, 4-acetylbiphenyl **42** (123 mg., 0.622 mmol), **37** (3.8 mg., 0.0042 mmol), 9-BBN (2.1 mg., 0.0082 mmol), KOᵗBu (142 mg., 1.24 mmol) and 5 mL THF. The reactor was sealed, removed from the glovebox and charged with 34 atm H₂ (500 psi) on the hydrogen line, immersed into an oil bath at 150 °C, and stirred overnight at 1200 rpm. Next day, the reactor was removed from the heating source and immersed into a room-temperature bath. Once cooled, the reactor was slowly depressurized and opened to air. The resulting mixture was transferred into a 5-dram vial. The reactor was washed twice with 5 mL toluene portions which were added to the 5-dram vial. The reaction was quenched with ~3 M HCl solution and the organic compounds were extracted thrice with toluene/THF mixture. The extract was dried with MgSO₄, filtered through a silica plugged pipet (~2 cm silica) and a Florisil® plugged pipet (~2 cm Florisil®). The solution has a slight yellowish/tan shade if the solution consists largely of

4-acetylbiphenyl **42**. Hydrogenation and deoxygenation products **43** and **44** give a clear, colorless solution. The solvents were removed *in vacuo* to give a) a slightly yellow solid (4-acetylbiphenyl **42**), b) white precipitate (significant portion of 1-(4-biphenylyl)-1-ethanol **43**), or c) a semi-liquid, yellowish solid if considerable deoxygenation takes place. The reaction products were dissolved in CDCl$_3$, 20 μL of hexamethyldisiloxane (0.103 mmol) was added and the sample was analyzed by ^{1}H NMR (97 % conversion, 48 % of **43** and 15 % of **44**).

4.5.2.1 Hydrodeoxygenation of 4-acetylbiphenyl 42 by [Co(NPPh₃)(OSiMe₃)(THF)]₂ 37 and KO*t*Bu without 9-BBN

The general procedure was applied to 4-acetylbiphenyl **42** (123 mg., 0.622 mmol), **37** (3.8 mg., 0.0042 mmol) and KO*t*Bu (142 mg., 1.24 mmol). The reaction was quantified by ^{1}H NMR: 89 % conversion, 43 % of 4-biphenylyl)-1-ethanol **43,** 11 % of 4-ethylbiphenyl **44**. GC-MS: 91 % conversion, 52 % of 4-biphenylyl)-1-ethanol **43,** 16 % of 4-ethylbiphenyl **44**, 17 % of biphenyl **45** and 14 % of dimerization**.**

4.5.2.2 Hydrodeoxygenation of 4-acetylbiphenyl 42 by [Co(NPPh₃)(OSiMe₃)(THF)]₂ 37 and KO*t*Bu at 0.3 mol% catalyst

The general procedure was applied to 4-acetylbiphenyl **42** (123 mg., 0.622 mmol), **39** (1.7 mg., 0.0021 mmol), 9-BBN (1 mg., 0.0041 mmol) and KO*t*Bu (142 mg., 1.24 mmol). Analysis by ^{1}H NMR shows 94 % conversion, 48 % of 4-biphenylyl)-1-ethanol **43** and 25 % of 4-ethylbiphenyl **44**.

4.5.2.3 Hydrodeoxygenation of 4-acetylbiphenyl 42 by [Co(NPPh₃)(OSiMe₃)(THF)]₂ 37 and KO*t*Bu at 2.0 mol% catalyst

The general procedure was applied to 4-acetylbiphenyl **42** (123 mg., 0.622 mmol), **39** (11 mg., 0.0125 mmol), 9-BBN (1 mg., 0.0250 mmol) and KO^{t}Bu (142 mg., 1.24 mmol). Analysis by ^{1}H NMR shows 91 % conversion, 64 % of 4-biphenylyl)-1-ethanol **43** and 20 % of 4-ethylbiphenyl **44**.

4.5.2.4 Hydrodeoxygenation of 4-acetylbiphenyl 42 by [Co(NPPh$_3$)(OSiMe$_3$)(THF)]$_2$ 37 and KO^{t}Bu at 6.0 mol% 9-BBN

The general procedure was applied to 4-acetylbiphenyl **42** (123 mg., 0.622 mmol), **37** (3.8 mg., 0.0042 mmol), 9-BBN (9 mg., 0.0322 mmol) and KO^{t}Bu (142 mg., 1.24 mmol). Analysis by ^{1}H NMR shows 96 % conversion, 60 % of 4-biphenylyl)-1-ethanol **43** and 10 % of 4-ethylbiphenyl **44**.

4.5.2.5 Hydrodeoxygenation of 4-acetylbiphenyl 42 by [Co(NPPh$_3$)(OSiMe$_3$)(THF)]$_2$ 37 and KO^{t}Bu in toluene

The general procedure was applied to 4-acetylbiphenyl **42** (123 mg., 0.622 mmol), **37** (3.8 mg., 0.0042 mmol), 9-BBN (9 mg., 0.0322 mmol), KO^{t}Bu (142 mg., 1.24 mmol) and 5 mL toluene. The products were analyzed by ^{1}H NMR: 97 % conversion, 83 % of 4-biphenylyl)-1-ethanol **43** and 3 % of 4-ethylbiphenyl **44**.

4.5.2.6 Hydrodeoxygenation of 4-acetylbiphenyl 42 by [Co(NPPh$_3$)(OSiMe$_3$)(THF)]$_2$ 37 and KO^{t}Bu (1 eq. base)

The general procedure was applied to 4-acetylbiphenyl **42** (123 mg., 0.622 mmol), **37** (3.8 mg., 0.0042 mmol), 9-BBN (9 mg., 0.0322 mmol) and KO^{t}Bu (71 mg., 0.622 mmol). The products

were analyzed by ^{1}H NMR: 97 % conversion, 14 % of 4-biphenylyl)-1-ethanol **43** and 9 % of 4-ethylbiphenyl **44**. GC-MS: 93 % conversion, 7 % of 4-biphenylyl)-1-ethanol **43,** 30 % of 4-ethylbiphenyl **44**, 5.5 % of biphenyl **45** and 35 % of dimerization**.**

4.5.2.7 Base screening in the hydrodeoxygenation of 4-acetylbiphenyl 42 by [Co(NPPh₃)(OSiMe₃)(THF)]₂ 37

The general procedure was applied to 4-acetylbiphenyl **42** (123 mg., 0.622 mmol), **37** (3.8 mg., 0.0042 mmol), 9-BBN (9 mg., 0.0322 mmol) and a base (1.24 mmol). The samples were analyzed and quantified by ^{1}H NMR. Dimerization was determined by GC-MS.

Table 4.3 Base screening in the deoxygenation of 4-acetylbiphenyl **42** by **37**.
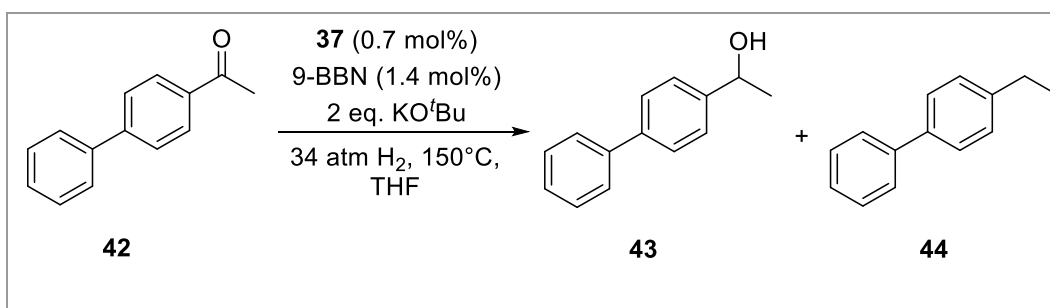
Entry	Base	Conversion, [%][a]	Yield, [%][a]		Dimerization products, [%][b]
			43	**44**	
1	KO^{t}Bu	97	48	15	-
2	NaO^{t}Bu	98	16	15	50
3	LiO^{t}Bu	100	-	-	100
4	Ti(O^{i}Pr)₄	48	22	-	N/A
5	KOSiMe₃	100	-	-	100

[a] Quantified by ^{1}H NMR using hexamethyldisiloxane as an internal standard. [b] Detected by Gas Chromatography – Mass Spectrometry.

4.5.2.8 Hydrodeoxygenation of 4-acetylbiphenyl 42 by [Co(NPPh₃)(OSiMe₃)(THF)]₂ 37 and KO^{t}Bu over 4 hours at 150 °C

The general procedure was applied to 4-acetylbiphenyl **42** (123 mg., 0.622 mmol), **37** (3.8 mg., 0.0042 mmol), 9-BBN (9 mg., 0.0322 mmol) and KO^{t}Bu (142 mg., 1.24 mmol). The reactions were pressurized to 34 atm H$_2$ and immersed into pre-heated oil baths at 150 °C for a described period of time. The samples were analyzed and quantified by ^{1}H NMR.

Table 4.4 Deoxygenation of 4-acetylbiphenyl **42** by **37** over 4 hours.

Entry	Time	Conversion, [%]	Yield, [%]	
			43	**44**
1	15 mins	11	3	0
2	30 mins	50	41	0
3	45 mins	73	63	0
4	1 h	94	87	1
5	2 h	94	73	4
6	3 h	93	74	6
7	4 h	93	75	9

4.5.2.9 Hydrodeoxygenation of 4-acetylbiphenyl 42 by [Co(NPPh₃)(OSiMe₃)(THF)]₂ 37 and KO^{t}Bu for 4 days

The general procedure was applied to 4-acetylbiphenyl **42** (123 mg., 0.622 mmol), **37** (3.8 mg., 0.0042 mmol), 9-BBN (9 mg., 0.0322 mmol) and KO^{t}Bu (142 mg., 1.24 mmol). The reaction was pressurized to 34 atm H$_2$ and immersed into an oil bath at 150 °C for four days. The sample was analyzed and quantified by ^{1}H NMR: 96 % conversion, 11 % of 4-biphenylyl)-1-ethanol **43** and 30 % of 4-ethylbiphenyl **44**.
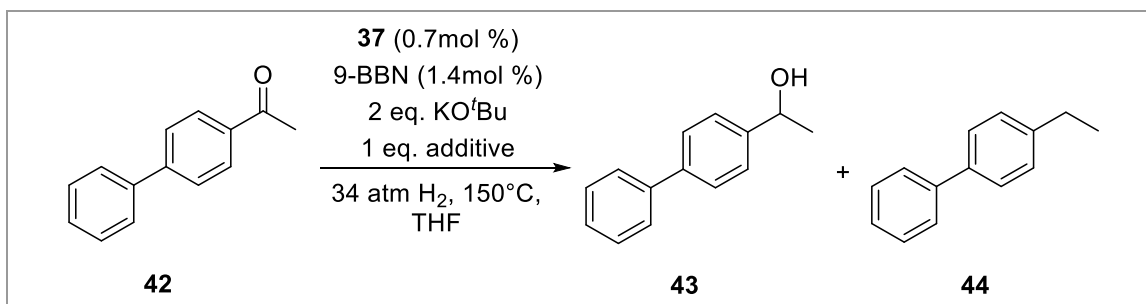
4.5.2.10 Hydrodeoxygenation of 4-acetylbiphenyl 42 by [Co(NPPh₃)(OSiMe₃)(THF)]₂ 37 and KOʹBu for 4 days without 9-BBN

The general procedure was applied to 4-acetylbiphenyl **42** (123 mg., 0.622 mmol), **37** (3.8 mg., 0.0042 mmol) and KOʹBu (142 mg., 1.24 mmol). The reaction was pressurized to 34 atm H_2 and immersed into an oil bath at 150 °C for four days. The sample was analyzed and quantified by ^{1}H NMR: 94 % conversion, 43 % of 4-biphenylyl)-1-ethanol **43** and 11 % of 4-ethylbiphenyl **44**.

4.5.2.11 Additional scavenger screening in the hydrodeoxygenation of 4-acetylbiphenyl 42 by [Co(NPPh₃)(OSiMe₃)(THF)]₂ 37 and KOʹBu

The general procedure was applied to 4-acetylbiphenyl **42** (123 mg., 0.622 mmol), **37** (3.8 mg., 0.0042 mmol), 9-BBN (9 mg., 0.0322 mmol), KOʹBu (142 mg., 1.24 mmol) and one equivalent of an additional scavenger. The reactions were pressurized to 34 atm H_2 and immersed into pre-heated oil baths at 150 °C for a described period of time. The results quantified by ^{1}H NMR. The samples were submitted for GC-MS to determine the dimerization content.

Table 4.5 Additional scavenger screening in the deoxygenation of 4-acetylbiphenyl **42** by **37**.

Reaction scheme: **42** → **43** + **44**, with conditions: **37** (0.7 mol %), 9-BBN (1.4 mol %), 2 eq. KO^{t}Bu, 1 eq. additive, 34 atm H$_2$, 150 °C, THF.
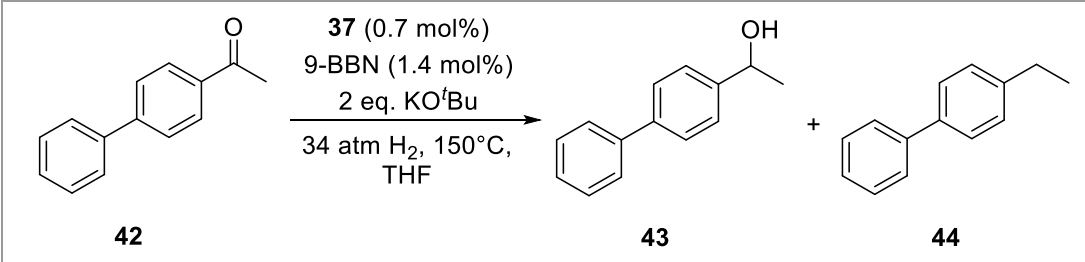
Entry	Time	Conversion, [%]	Yield, [%][d]		Aldol adducts, [%][e]
			43	**44**	
1ᵃ	AlMe$_3$	97	81	9	0
2	VCl$_3$	72	-	-	70
3ᵇ	Ti(O^{i}Pr)$_4$	100	-	-	100
4ᶜ	Mol. sieves, 3Å	96	68	9	0

[a] 0.33 eq. of AlMe$_3$ was used. [b] 1 eq. of KO^{t}Bu and 1 eq. of Ti(O^{i}Pr)$_4$ were used. [c] One mass eq. of molecular sieves was used. [d] Quantified by ^{1}H NMR using hexamethyldisiloxane as an internal standard. [e] Detected by GC-MS.

4.5.2.12 Hydrodeoxygenation of 4-acetylbiphenyl 42 by [Co(NPPh₃)(OSiMe₃)(THF)]₂ 37 and KO^{t}Bu at 200 °C over 4 hours

The general procedure was applied to 4-acetylbiphenyl **42** (123 mg., 0.622 mmol), **37** (3.8 mg., 0.0042 mmol), 9-BBN (9 mg., 0.0322 mmol) and KO^{t}Bu (142 mg., 1.24 mmol). The reactions were pressurized to 34 atm H$_2$ and immersed into pre-heated oil baths at 200 °C for a described period of time. The samples were analyzed and quantified by ^{1}H NMR (Table **4.6**) and GC-MS (Table **4.7**).

Table 4.6 Deoxygenation of 4-acetylbiphenyl **42** by **37** over 4 hours at 200 °C.

Entry	Time	Conversion, [%]	Yield[a], [%]	
			43	**44**
1	30 mins	80	75	75
2	1 h	87	71	71
3	2 h	94	37	37
4	4 h	98	22	22

[a] Quantified by ^{1}H NMR. [b] Analyzed by GC-MS.

Table 4.7 Deoxygenation of 4-acetylbiphenyl **42** by **37** over 4 hours at 200 °C.

Entry	Time	Conversion, [%]	Yield[a], [%]				
			43	**44**	**Dimers**	**4-vinylbiphenyl 47**	**Biphenyl 45**
1	30 mins	69	3	57	5	3	0.5
2	1 h	86	81	2	1.5	1.5	0.5
3	2 h	92	55	35	5	0.5	3.5
4	4 h	99	45	20	21	3	4

[a] Analyzed by GC-MS.

4.5.2.13 Hydrodeoxygenation of 1-(4-biphenylyl)-1-ethanol 43 by [Co(NPPh₃)(OSiMe₃)(THF)]₂ 37 and KO*t*Bu at 200 °C for 2 h

The general procedure was applied to 1-(4-biphenylyl)-1-ethanol **43** (124 mg., 0.622 mmol), **37** (3.8 mg., 0.0042 mmol), 9-BBN (9 mg., 0.0322 mmol) and KO*t*Bu (142 mg., 1.24 mmol). The

125

reaction was pressurized to 34 atm H_2 and immersed into pre-heated oil baths at 200 °C for 2 h. The sample was analyzed and quantified by ^{1}H NMR: 85% conversion, 32% of 4-ethylbiphenyl. GC-MS: 93% conversion, 63% of 4-ethylbiphenyl **44**, 14% of biphenyl **45**, 0.5% of 4-vinylbiphenyl **47**, 9% of 4-acetylbiphenyl **42**, 5% of dimerization and traces of impurities.

4.5.2.14 Hydrodeoxygenation of 1-(4-biphenylyl)-1-ethanol 43 by [Co(NPPh₃)(OSiMe₃)(THF)]₂ 37 and KOʳBu at 200 °C overnight

The general procedure was applied to 1-(4-biphenylyl)-1-ethanol **43** (124 mg., 0.622 mmol), **37** (3.8 mg., 0.0042 mmol), 9-BBN (9 mg., 0.0322 mmol) and KOʳBu (142 mg., 1.24 mmol). The reaction was pressurized to 34 atm H_2 and immersed into pre-heated oil baths at 200 °C overnight. The sample was analyzed and quantified by ^{1}H NMR: 100% conversion, 39% of 4-ethylbiphenyl. GC-MS: 100 % conversion, 89 % of 4-ethylbiphenyl **44**, 11% of biphenyl **45**.
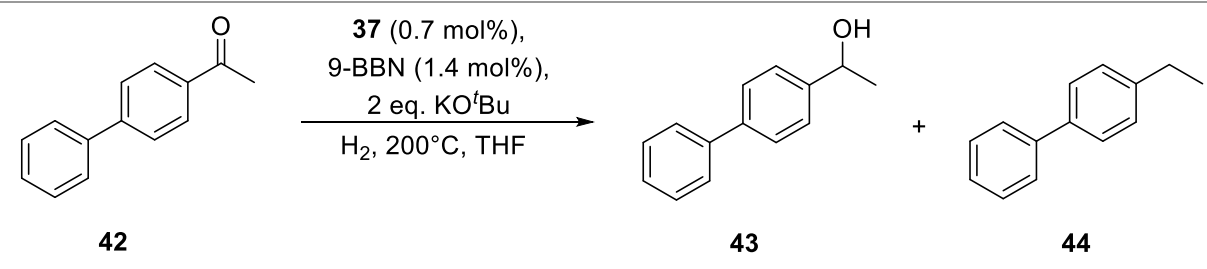
4.5.2.15 Hydrodeoxygenation of 4-acetylbiphenyl 42 by [Co(NPPh₃)(OSiMe₃)(THF)]₂ 37 and KOʳBu at 200 °C overnight

The general procedure was applied to 4-acetylbiphenyl **42** (123 mg., 0.622 mmol), **37** (3.8 mg., 0.0042 mmol), 9-BBN (9 mg., 0.0322 mmol) and KOʳBu (142 mg., 1.24 mmol). The reaction was pressurized to 34 atm H_2 and immersed into pre-heated oil baths at 200 °C overnight. The sample was analyzed and quantified by ^{1}H NMR: 100% conversion, 38% of 4-ethylbiphenyl. GC-MS: 100 % conversion, 86 % of 4-ethylbiphenyl **44**, 14% of biphenyl **45**.

4.5.2.16 Optimization of H₂ pressure in hydrodeoxygenation of 4-acetylbiphenyl 42 by [Co(NPPh₃)(OSiMe₃)(THF)]₂ 37 and KOʳBu at 200 °C

The general procedure was applied to 4-acetylbiphenyl **42** (123 mg., 0.622 mmol), **37** (3.8 mg., 0.0042 mmol), 9-BBN (9 mg., 0.0322 mmol) and KO^{t}Bu (142 mg., 1.24 mmol). The reactions were pressurized to a described hydrogen pressure and immersed into pre-heated oil baths at 200 °C for a described period of time. The samples were analyzed and quantified by ^{1}H NMR. GC-MS: 100 % conversion, 84 % of 4-ethylbiphenyl **44**, 13% of biphenyl **45** and minor impurities.

Table 4.8 Pressure effect in the deoxygenation of 4-acetybiphenyl **42** by precatalyst **37** at 200 °C.

Entry	Pressure, [atm]	Time	Conversion, [%]	Yield, [%]	
				43	44
1	34	overnight	100	0	39
2	27	overnight	96	15	40
3	20	overnight	84	8	26
4	7	overnight	69	0	22
5	34	4 h	97	22	24
6	27	4 h	92	49	22
7	20	4 h	94	8	42

4.5.2.17 Optimization of H$_2$ pressure in hydrodeoxygenation of 4-acetylbiphenyl 42 by [Co(NPPh$_3$)(OSiMe$_3$)(THF)]$_2$ 37 and KO^{t}Bu at 150 °C

The general procedure was applied to 4-acetylbiphenyl **42** (123 mg., 0.622 mmol), **37** (3.8 mg., 0.0042 mmol), 9-BBN (9 mg., 0.0322 mmol) and KO^{t}Bu (142 mg., 1.24 mmol). The reactions were pressurized to a described hydrogen pressure and immersed into pre-heated oil baths at 150 °C for a described period of time. The samples were analyzed and quantified by ^{1}H NMR.

Table 4.9 Pressure effect in the deoxygenation of 4-acetybiphenyl **42** by precatalyst **37** at 150 °C.

Entry	Pressure, [atm]	Time	Conversion, [%]	Yield, [%]	
				43	**44**
1	34	overnight	97	48	15
2	27	overnight	93	52	19
3	20	overnight	92	56	13
4	20	4 h	84	62	6
5	34	4 h	93	75	9
6	14	overnight	88	72	2
7	7	overnight	52	42	s*

* s = stoichiometric.

4.5.2.18 Optimization of H_2 pressure in hydrodeoxygenation of 4-acetylbiphenyl 42 by [Co(NPPh₃)(OSiMe₃)(THF)]₂ 37 and KO^{t}Bu at 110 °C

The general procedure was applied to 4-acetylbiphenyl **42** (123 mg., 0.622 mmol), **37** (3.8 mg., 0.0042 mmol), 9-BBN (9 mg., 0.0322 mmol) and KO^{t}Bu (142 mg., 1.24 mmol). The reactions were pressurized to a described hydrogen pressure and immersed into pre-heated oil baths at 110 °C for a described period of time. The samples were analyzed and quantified by ^{1}H NMR.
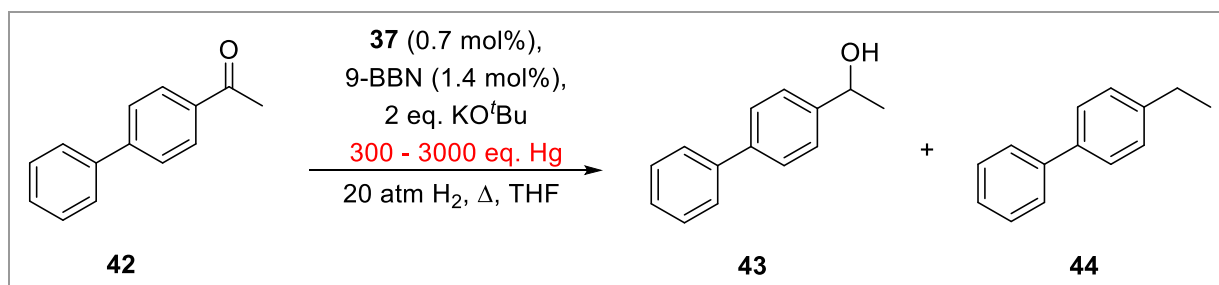
Table 4.10 Pressure effect in the deoxygenation of 4-acetybiphenyl **42** by precatalyst **37** at 110 °C.

Entry	Pressure, [atm]	Time	Conversion, [%]	Yield, [%]	
				43	**44**
1	34	overnight	96	96	0
2	20	overnight	84	80	0
3	34	4 h	32	31	0
4	20	4 h	8	2	0

4.5.2.19 Mercury tests for catalyst [Co(NPPh₃)(OSiMe₃)(THF)]2ₓ 37 at 110 °C, 150 °C and 200 °C
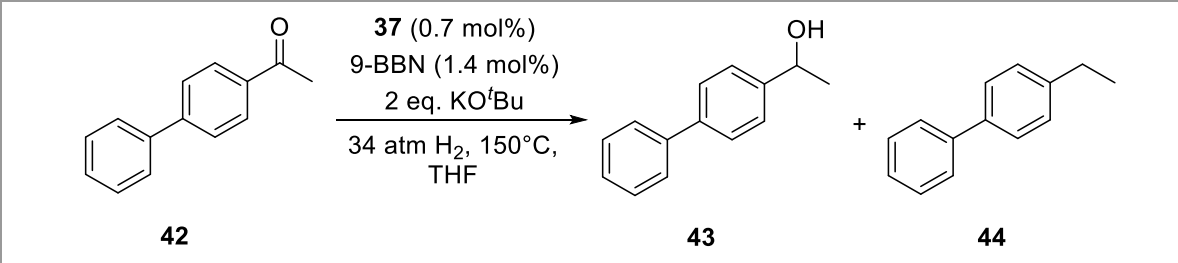
The general procedure was applied to 4-acetylbiphenyl **42** (123 mg., 0.622 mmol), **37** (3.8 mg., 0.0042 mmol), 9-BBN (9 mg., 0.0322 mmol), KO^{t}Bu (142 mg., 1.24 mmol) and 300 or 3000 equivalents of Hg per catalyst (0.247 g. and 2.47 g., respectively). The reactions were pressurized to 20 atm H$_2$ and immersed into preheated oil baths at a set temperature for a described amount of time. The results were quantified by ^{1}H NMR.

Table 4.11 Mercury poisoning tests at 110 °C, 150 °C and 200 °C.

37 (0.7 mol%), 9-BBN (1.4 mol%), 2 eq. KO^{t}Bu, 300 - 3000 eq. Hg, 20 atm H$_2$, Δ, THF

42 → 43 + 44

Entry	Temperature, [°C]	Time	Hg, [eq.]	Conversion, [%]	Yield, [%] 43	Yield, [%] 44
1	110	overnight	-	84	80	0
2	110	overnight	300	11	3	0
3	150	overnight	-	92	56	13
4	150	overnight	300	62	30	13
5	150	4 h	-	84	62	6
6	150	4 h	300	19	17	0
7	150	4 h	3000	9	4	0
8	200	4 h	-	98	22	24
9	200	4 h	300	88	13	28
10	200	4 h	3000	22	4	7

4.5.3 A general procedure for hydrodeoxygenation of 4-acetylbiphenyl 42 by [Co(NP^{i}Pr$_3$)$_2$]$_3$ 40 and KO^{t}Bu

In a glovebox, a stainless steel high pressure reaction vessel with glass lining was charged with a small bar-shaped stir bar, 4-acetylbiphenyl **42** (123 mg., 0.622 mmol), **40** (5.0 mg., 0.0042 mmol), 9-BBN (2.1 mg., 0.0082 mmol), KO^{t}Bu (142 mg., 1.24 mmol) and 5 mL THF. The reactor was sealed, removed from the glovebox, connected to a hydrogen line and charged with 34 atm H$_2$ (500 psi). The reaction vessel was immersed into an oil bath at 150 °C and stirred overnight at 1200 rpm. Next day, the reactor was removed from the heating source and immersed into a room-temperature bath. Once cooled, the reactor was slowly depressurized and opened to

air. The resulting mixture was transferred into a 5-dram vial. The reactor was washed twice with 5 mL toluene portions which were added to the 5-dram vial. The reaction was quenched with ~3 M HCl solution and the organic compounds were extracted thrice with toluene/THF. The extract was dried with MgSO$_4$, filtered through a silica plugged pipet (~2 cm silica) and a Florisil® plugged pipet (~2 cm Florisil®). The solution has a slight yellowish/tan shade if the solution consists largely of 4-acetylbiphenyl **42**, whereas a hydrogenation and deoxygenation products **43** and **44** give a clear, colorless solution. The solvents were removed *in vacuo* affording a) a slightly yellow solid (4-acetylbiphenyl **42**), b) white precipitate (significant portion of 1-(4-biphenylyl)-1-ethanol **43**), or c) a semi-liquid, yellowish solid if considerable deoxygenation takes place. The reaction products were dissolved in CDCl$_3$, 20 µL of hexamethyldisiloxane (0.103 mmol) was added to the solution and the sample was analyzed by ^{1}H NMR (96 % conversion, 91 % of **43** and 3 % of **44**).

4.5.3.1 Hydrodeoxygenation of 4-acetylbiphenyl 42 by [Co(NP^{i}Pr$_3$)$_2$]$_3$ 40 and KO^{t}Bu in hexane

The general procedure was applied to 4-acetylbiphenyl **42** (123 mg., 0.622 mmol), **40** (5.0 mg., 0.0042 mmol), 9-BBN (2.1 mg., 0.0082 mmol), KO^{t}Bu (142 mg., 1.24 mmol) and 5 mL hexane. The sample was analyzed and quantified by ^{1}H NMR: 46 % conversion, 37 % of 4-biphenylyl)-1-ethanol **43** and 1 % of 4-ethylbiphenyl **44**.

4.5.3.2 Hydrodeoxygenation of 4-acetylbiphenyl 42 by [Co(NP^{i}Pr$_3$)$_2$]$_3$ 40 and KO^{t}Bu in hexane with alumina support (4 wt% 39)

The general procedure was applied to 4-acetylbiphenyl **42** (123 mg., 0.622 mmol), **40** (5.0 mg., 0.0042 mmol), 9-BBN (2.1 mg., 0.0082 mmol), KO^{t}Bu (142 mg., 1.24 mmol) and 5 mL hexane. Basic Al$_2$O$_3$ (75 mg., 0.75 mmol) was added to the reactor before sealing it. The reaction was quantified by ^{1}H NMR: 86 % conversion, 72 % of 4-biphenylyl)-1-ethanol **43,** 3 % of 4-ethylbiphenyl **44**.

4.5.3.3 Hydrodeoxygenation of 4-acetylbiphenyl 42 by [Co(NP^{i}Pr$_3$)$_2$]$_3$ 40 and KO^{t}Bu at 200 °C for 4 h

The general procedure was applied to 4-acetylbiphenyl **42** (123 mg., 0.622 mmol), **40** (5.0 mg., 0.0042 mmol), 9-BBN (2.1 mg., 0.0082 mmol) and KO^{t}Bu (142 mg., 1.24 mmol). The reactor was pressurized to 34 atm H$_2$ and immersed into a pre-heated oil bath at 200 °C for 4 h. The sample was analyzed and quantified by ^{1}H NMR: 90 % conversion, 24 % of 4-biphenylyl)-1-ethanol **43** and 34 % of 4-ethylbiphenyl **44**.

4.5.3.4 Hydrodeoxygenation of 4-acetylbiphenyl 42 by [Co(NP^{i}Pr$_3$)$_2$]$_3$ 40 and KO^{t}Bu at 110 °C and 1 atm H$_2$

The general procedure was applied to 4-acetylbiphenyl **42** (123 mg., 0.622 mmol), **40** (5.0 mg., 0.0042 mmol), 9-BBN (2.1 mg., 0.0082 mmol) and KO^{t}Bu (142 mg., 1.24 mmol). The reactor was pressurized to 7 atm H$_2$ and slowly depressurized to atmospheric pressure twice, and immersed into a pre-heated oil bath at 110 °C for 4 h. The sample was analyzed and quantified by ^{1}H NMR: 15 % conversion and 8 % of 4-biphenylyl)-1-ethanol **43**.

4.5.4 A general procedure for control reactions with KO^{t}Bu

In a glovebox, a stainless steel high pressure reaction vessel with glass lining was charged with a small bar-shaped stir bar, 4-acetylbiphenyl **42** (123 mg., 0.622 mmol), KO*t*Bu (142 mg., 1.24 mmol) and 5 mL THF. The reactor was sealed, removed from the glovebox and connected to a hydrogen line. The reactor was charged with 34 atm H_2 (500 psi), immersed into an oil bath at 150 °C and stirred overnight at 1200 rpm. Next day, the reactor was removed from the heating source and immersed into a room-temperature bath. Once cooled, the reactor was slowly depressurized and opened to the atmosphere. The resulting mixture was transferred into a 5-dram vial. The reactor was washed twice with 5 mL toluene portions which were added to the 5-dram vial. The reaction was quenched with ~3 M HCl solution and the organic compounds were extracted thrice with toluene/THF. The extract was dried with $MgSO_4$, filtered through a silica plugged pipet (~2 cm) and a Florisil® plugged pipet (~2 cm Florisil). The solution has a slight yellowish/tan shade if the solution consists largely of 4-acetylbiphenyl **42**, whereas a hydrogenation and deoxygenation products **43** and **44** give a clear, colorless solution. The solvents were removed *in vacuo* to give a) a slightly yellow solid (4-acetylbiphenyl **42**), b) white precipitate (significant portion of 1-(4-biphenylyl)-1-ethanol **43**), or c) a semi-liquid, yellowish solid if considerable deoxygenation takes place. The reaction products were dissolved in $CDCl_3$, 20 μL of hexamethyldisiloxane (0.103 mmol) was added to the solution and the sample was analyzed by ^1H NMR (4 % conversion, 0 % of 4-biphenylyl)-1-ethanol **43** and 0 % of 4-ethylbiphenyl **44**).

4.5.4.1 Control reaction with KO*t*Bu and 9-BBN at 20 atm H_2 for 4 h

The general procedure was applied to 4-acetylbiphenyl **42** (123 mg., 0.622 mmol), 9-BBN (2.1 mg., 0.0082 mmol) and KO*t*Bu (142 mg., 1.24 mmol). The reaction was pressurized to 20 atm H_2

and immersed into a pre-heated oil bath at 150 °C for 4 h. The sample was analyzed by ^{1}H NMR: 1 % conversion and 1 % of 4-biphenylyl)-1-ethanol **43.**

4.5.4.2 Control reaction with KO^{t}Bu and 9-BBN at 20 atm H$_2$ and 200 °C for 4 h

The general procedure was applied to 4-acetylbiphenyl **42** (123 mg., 0.622 mmol), 9-BBN (2.1 mg., 0.0082 mmol) and KO^{t}Bu (142 mg., 1.24 mmol). The reaction was pressurized to 20 atm H$_2$ and immersed into a pre-heated oil bath at 200 °C for 4 h. The sample was analyzed by ^{1}H NMR: 14 % conversion and 0 % of 4-biphenylyl)-1-ethanol **43** and 1 % of 4-ethylbiphenyl **44.**
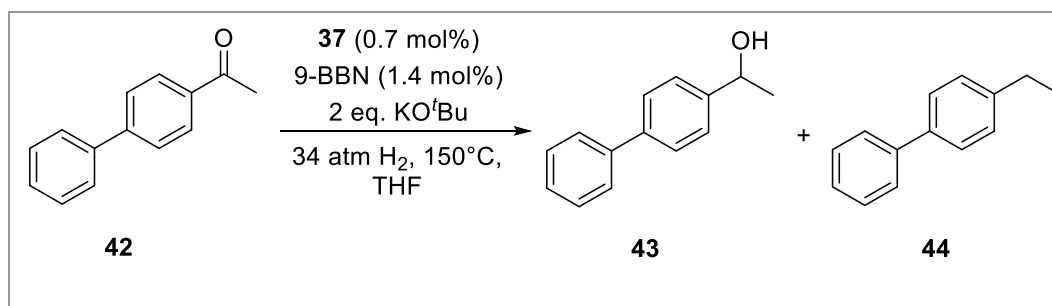
4.5.4.3 Control reaction with KO^{t}Bu and 9-BBN at 34 atm H$_2$ and 200 °C for 4 h

The general procedure was applied to 4-acetylbiphenyl **42** (123 mg., 0.622 mmol), 9-BBN (2.1 mg., 0.0082 mmol) and KO^{t}Bu (142 mg., 1.24 mmol). The reaction was pressurized to 20 atm H$_2$ and immersed into a pre-heated oil bath at 200 °C for 4 h. The sample was analyzed by ^{1}H NMR: 12 % conversion and 0.5 % of 4-biphenylyl)-1-ethanol **43** and 2 % of 4-ethylbiphenyl **44.**

4.5.4.4 Control reactions with KO^{t}Bu and 9-BBN without H$_2$

The general procedure was applied to 4-acetylbiphenyl **42** (123 mg., 0.622 mmol), 9-BBN (2.1 mg., 0.0082 mmol) and KO^{t}Bu (142 mg., 1.24 mmol). The reactions were immersed into oil baths at a described temperature and stirred overnight. The results were quantified by ^{1}H NMR.

Table 4.12 Control reactions at 110 °C, 150 °C and 200 °C without hydrogen.

Entry	Temperature, [°C]	Conversion, [%]	Yield, [%]	
			43	**44**
1	110	10	1	0
2	150	8	0	0
3	200	12	0	0

4.5.5 General procedure for pre-decomposition of [Co(NPPh₃)(OSiMe₃)(THF)]₂ 37 and [Co(NPPh₃)₂]₃ 23 into *Cat_1A-E* and *Cat_2A*

In a glovebox, a stainless steel high pressure reaction vessel with glass lining was charged with a small bar-shaped stirbar, **37** (3.8 mg., 0.0041 mmol), other additives and 4 mL THF. The reactor was sealed, removed from the glovebox and connected to a hydrogen line. The reaction vessel charged with 34 atm H₂ (500 psi), immersed into an oil bath at 200 °C and stirred for a set amount of time at 1200 rpm. The reactor was then removed from the heating source and immersed into a room-temperature bath. Once cooled, the reactor was slowly depressurized to release the hydrogen and transferred back into the glovebox.

4.5.5.1 Pre-decomposition of [Co(NPPh₃)(OSiMe₃)(THF)]₂ 37 into *Cat_1A*

The general procedure was applied to **37** (3.8 mg., 0.0041 mmol), 9-BBN (2.1 mg., 0.0082 mmol) and KO*t*Bu (142 mg., 1.24 mmol). The reactor was pressurized to 34 atm H₂ and stirred at

200 °C for 2 h. A colorless THF solution and a black film deposit on the glass insert was observed upon opening the reactor.

4.5.5.2 Pre-decomposition of [Co(NPPh₃)(OSiMe₃)(THF)]₂ 37 into *Cat_1B*

The general procedure was applied to **37** (3.8 mg., 0.0041 mmol), 9-BBN (2.1 mg., 0.0082 mmol) and KO^{t}Bu (142 mg., 1.24 mmol). The reactor was pressurized to 34 atm H_2 and stirred at 200 °C for 1 h. A colorless THF solution and a black film deposit on the glass insert was observed upon opening the reactor.

4.5.5.3 Pre-decomposition of [Co(NPPh₃)(OSiMe₃)(THF)]₂ 37 into *Cat_1C*

The general procedure was applied to **37** (3.8 mg., 0.0041 mmol) and 9-BBN (2.1 mg., 0.0082 mmol). The reactor was pressurized to 34 atm H_2 and stirred at 200 °C for 1 h. A colorless THF solution and a black film deposit on the glass insert was observed upon opening the reactor.

4.5.5.4 Pre-decomposition of [Co(NPPh₃)(OSiMe₃)(THF)]₂ 37 into *Cat_1D*

The general procedure was applied to **37** (3.8 mg., 0.0041 mmol). The reactor was pressurized to 34 atm H_2 and stirred at 200 °C for 1 h. A colorless THF solution and a black film deposit on the glass insert was observed upon opening the reactor.

4.5.5.5 Pre-decomposition of [Co(NPPh₃)(OSiMe₃)(THF)]₂ 37 into *Cat_1E*

The general procedure was applied to **37** (3.8 mg., 0.0041 mmol), 9-BBN (2.1 mg., 0.0082 mmol) and 3Å activated molecular sieves (123 mg.). The reactor was pressurized to 34 atm H_2 and stirred at 200 °C for 1 h. A colorless THF solution and a black film deposit on the glass insert was observed upon opening the reactor.

4.5.5.6 Pre-decomposition of [Co(NPPh₃)₂]₃ 23 into *Cat_2A*

The general procedure was applied to **23** (7.5 mg., 0.0041 mmol) and 9-BBN (2.1 mg., 0.0082 mmol). The reactor was pressurized to 34 atm H₂ and stirred at 200 °C for 1 h. A brown THF solution and a black film deposit on the glass insert was observed upon opening the reactor.

4.5.6 General procedure for catalysis reactions by pre-decomposed *Cat_1A-D* and KO^t^Bu

The reaction was conducted immediately upon the pre-decomposition procedure. Once the reactor with *Cat_1A-D* was opened in the glovebox, 4-acetylbiphenyl **42** (123 mg., 0.622 mmol) and 1 mL THF were added to the reaction vessel. The reactor was sealed, removed from the glovebox and connected to a hydrogen line. The reactor was pressurized to a described H₂ pressure, immersed into a pre-heated oil bath at a described temperature, and stirred for a set amount of time at 1200 rpm. The reactor was then removed from the heating source and immersed into a room-temperature bath. Once cooled, the reactor was slowly depressurized and opened to the atmosphere. The resulting mixture was transferred into a 5-dram vial. The reactor was washed twice with 5 mL toluene portions which were added to the 5-dram vial. The reaction was quenched with ~3 M HCl solution and the organic compounds were extracted thrice with toluene/THF. The extract was dried with MgSO₄, filtered through a silica plugged pipet (~2 cm silica) and a Florisil® plugged pipet (~2 cm Florisil®). The solution has a slight yellowish/tan shade if the solution consists largely of 4-acetylbiphenyl **42**, whereas a hydrogenation and deoxygenation products **43** and **44** give a clear, colorless solution. The solvents were removed *in vacuo* to give a) slightly yellow solid (4-acetylbiphenyl **42**), b) white precipitate (significant portion of 1-(4-biphenylyl)-1-ethanol **43**), or c) a semi-liquid, yellowish solid if considerable

deoxygenation takes place. The reaction products were dissolved in CDCl$_3$, 20 μL of hexamethyldisiloxane (0.103 mmol) was added and the sample was analyzed by ^{1}H NMR.

4.5.6.1 Deoxygenation of 4-acetylbiphenyl 42 by *Cat_1A-B*

The general procedure was applied to 4-acetylbiphenyl **42** (123 mg., 0.622 mmol). The reactor was pressurized to 34 atm H$_2$, immersed into preheated oil bath at 150 °C and stirred for a described amount of time. The results were quantified by ^{1}H NMR.

Table 4.13 Deoxygenation of 4-acetylbiphenyl **42** by *Cat_1A-B*.

Entry	Time, [h]	Conversion, [%]	Yield, [%]	
			43	44
1	1	4	2	0
2	2	7	6	s*

* s = stoichiometric.

4.5.6.2 Deoxygenation of 4-acetylbiphenyl 42 by *Cat_1C-D*

The general procedure was applied to 4-acetylbiphenyl **42** (123 mg., 0.622 mmol) and KO^{t}Bu (142 mg., 1.24 mmol). The reactor was pressurized to a described pressure, immersed into a preheated oil bath at a described temperature and stirred for a described amount of time. The results were quantified by ^{1}H NMR.

Table 4.14 Deoxygenation of 4-acetylbiphenyl **42** by *Cat_1C-D*.

Entry	Cat.	Pressure, [atm]	T, [°C]	Time	Conversion, [%]	Yield, [%] 43	Yield, [%] 44
1	*Cat_1C*	34	150	1 h	86	78	s*
2	*Cat_1C*	1-2	150	overnight	55	31	8
3	*Cat_1C*	34	200	1 h	88	47	19
4	*Cat_1C*	34	200	1 h	98	28	1
5	*Cat_1C*	1-2	200	1 h	36	10	8
6	*Cat_1C*	1-2	200	overnight	19	0	7
7	*Cat_1C*	20	200	overnight	91	37	25
8	*Cat_1D*	34	200	1 h	4	2	2

4.5.6.3 Deoxygenation of 4-acetylbiphenyl 42 by *Cat_1C* and 1 eq. of KOtBu at 200 °C and 34 atm H$_2$

The general procedure was applied to 4-acetylbiphenyl **42** (123 mg., 0.622 mmol) and KO^{t}Bu (142 mg., 1.24 mmol). The reactor was pressurized to 34 atm H$_2$, immersed into a preheated oil bath at 200 °C and stirred for a 1 h. The sample was analyzed by GC-MS: 97 % conversion, 39% of 4-biphenylyl)-1-ethanol **43,** 0.5 % of 4-ethylbiphenyl **44**, 0.5% of 4-vinylbiphenyl **47** and 57% aldol condensation.

4.5.7 General procedure for catalysis reactions by pre-decomposed *Cat_1C-E* and *Cat_2A* in the presence of activated molecular sieves as water scavenger

The reaction was conducted immediately upon the pre-decomposition procedure. Once the reactor with *Cat_1C* was opened in the glovebox, 4-acetylbiphenyl **42** (123 mg., 0.622 mmol), activated 3Å molecular sieves (123 mg., 1 wt. equivalent) and 1 mL THF were added to the reaction vessel. The reactor was sealed, removed from the glovebox and connected to a hydrogen line. The reactor was charged with 7 atm H_2 and slowly depressurized to 1 – 2 atm twice, immersed into a preheated oil bath at 200 °C and stirred overnight at 1200 rpm. The reactor was then removed from the heating source and immersed into a room-temperature bath. Once cooled, the reactor was slowly depressurized and opened to the atmosphere. The resulting mixture was transferred into a 5-dram vial and the reactor was washed twice with 5 mL THF/Et_2O portions which were added to the 5-dram vial. The mixture was filtered through a silica plugged pipet (~2 cm silica) and a Florisil® plugged pipet (~2 cm Florisil®). The solution has a slight yellowish/tan shade if the solution consists largely of 4-acetylbiphenyl **42**, whereas a hydrogenation and deoxygenation products **43** and **44** give a clear, colorless solution. The solvents were removed *in vacuo*. The reaction products were dissolved in $CDCl_3$, 20 μL of hexamethyldisiloxane (0.103 mmol) was added to the solution and the sample was analyzed by ^{1}H NMR: 100 % conversion, 0 % of 4-biphenylyl)-1-ethanol **43** and 79 % of 4-ethylbiphenyl **44**. GC-MS: 100% conversion, 0.5 % of 4-biphenylyl)-1-ethanol **43,** 86% of 4-ethylbiphenyl 44, 0.5% of 4-vinylbiphenyl **47** and 13% dimerization.

4.5.7.1 Preparation of activated 3Å molecular sieves

Five grams of 3Å molecular sieves were ground to powder using a mortar and pestle. The sieves powder was transferred into a 100 mL beaker and heated in air at 500 °C for 3 h. The oven was turned off and the container was allowed to cool for 30 mins. The beaker was then transferred into the drybox and sieves were stored in a sealed 5-dram vial.

4.5.7.2 Deoxygenation of 4-acetylbiphenyl 42 by *Cat_1C-D*

The general procedure was applied to 4-acetylbiphenyl **42** (123 mg., 0.622 mmol) and activated 3Å molecular sieves (123 mg., 1 wt. equivalent). The reaction was immersed into a preheated oil bath at the indicated temperature after adding H_2 and stirred for a described amount of time. The results were quantified by ^1H NMR.

Table 4.15 Deoxygenation of 4-acetylbiphenyl **42** by *Cat_1C-D*.

Entry	Cat.	Temperature, [°C]	Time	Conversion, [%]	Yield, [%] 43	44
1	*Cat_1C*	200	overnight	100	0	79
2	*Cat_1C*	200	2.5 h	4	2	0
3	*Cat_1C*	150	overnight	22	18	s*
4	*Cat_1C*	110	overnight	8	3	0
5	*Cat_1D*	200	overnight	79	55	24

4.5.7.3 Deoxygenation of 4-acetylbiphenyl 42 by *Cat_1E*

The general procedure was applied to 4-acetylbiphenyl **42** (123 mg., 0.622 mmol). The reaction was immersed into a preheated oil bath at 200 °C after adding H_2 and stirred overnight. The results were quantified by ^{1}H NMR: 41 % conversion, 18 % of of 4-biphenylyl)-1-ethanol **43** and 14 % of 4-ethylbiphenyl **44**.

4.5.7.4 Deoxygenation of 4-acetylbiphenyl 42 by *Cat_2A*

The general procedure was applied to 4-acetylbiphenyl **42** (123 mg., 0.622 mmol) and activated 3Å molecular sieves (123 mg., 1 wt. equivalent). The reaction was immersed into a preheated oil bath at 200 °C after adding H_2 and stirred for an indicated time. The results were quantified by ^{1}H NMR.

Table 4.16 Deoxygenation of 4-acetylbiphenyl **42** by *Cat_2A*.

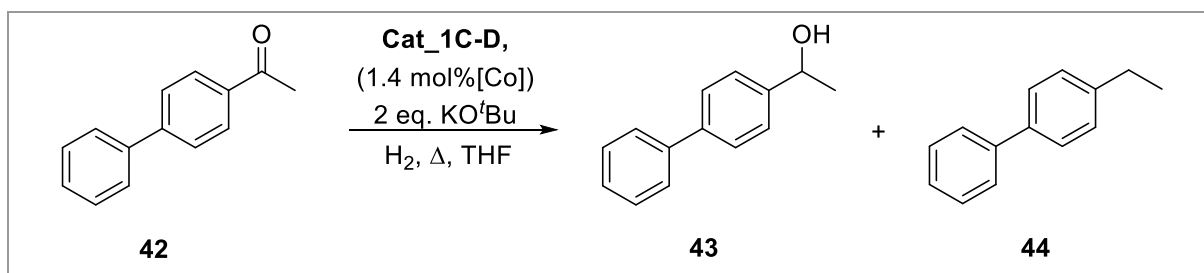| Entry	Time	Conversion, [%]	Yield, [%]	
			43	44
1	overnight	100	0	100
2	2.5 h	2	2	0

4.5.7.5 Deoxygenation of 4-acetylbiphenyl 42 by *Cat_1C-solid* at 200 °C

The general procedure was applied to 4-acetylbiphenyl **42** (123 mg., 0.622 mmol) and activated 3Å molecular sieves (123 mg., 1 wt. equivalent). The solid cobalt film was washed thrice with 5

mL THF portions and 5 mL of fresh THF was added to the glass liner. The substrate and sieves were added to the reaction mixture and the reactor was sealed. Hydrogen was added to the reactor and the reactor was immersed into a preheated oil bath at 200 °C and stirred overnight. The results were quantified by ^{1}H NMR: 88 % conversion, 32 % of 4-biphenylyl)-1-ethanol **43** and 55 % of 4-ethylbiphenyl **44**.

4.5.7.6 Deoxygenation of 4-acetylbiphenyl 42 by *Cat_1C-liquid* at 200 °C

The general procedure was applied to 4-acetylbiphenyl **42** (123 mg., 0.622 mmol) and activated 3Å molecular sieves (123 mg., 1 wt. equivalent). The colorless THF solution was decanted from the solid cobalt particles and filtered through a Celite plug (~2 cm Celite in a Pasteur pipet) into a 5-dram vial. The solid layer was washed thrice with 5 mL THF portions which were filtered through the Celite plug and added to the THF filtrate. The colorless THF solution was transferred to a new high-pressure reactor with a glass insert. The substrate, sieves and a small stir bar were added to the reaction mixture and the reactor was sealed. The reactor was immersed into a preheated oil bath at 200 °C upon adding H_2 and stirred overnight. The results were quantified by ^{1}H NMR: 0 % conversion.

4.5.7.7 Deoxygenation of 4-acetylbiphenyl 42 by *Cat_2A-solid* at 200 °C

The general procedure was applied to 4-acetylbiphenyl **42** (123 mg., 0.622 mmol) and activated 3Å molecular sieves (123 mg., 1 wt. equivalent). The solid cobalt film was washed thrice with 5 mL THF portions and 5 mL of fresh THF was added to the glass liner. The substrate and sieves were added to the reaction mixture and the reactor was sealed. The reactor was immersed into a

preheated oil bath at 200 °C upon adding H$_2$ and stirred overnight. The results were quantified by ^{1}H NMR: 85 % conversion, 27 % of 4-biphenylyl)-1-ethanol **43** and 58 % of 4-ethylbiphenyl **44**.
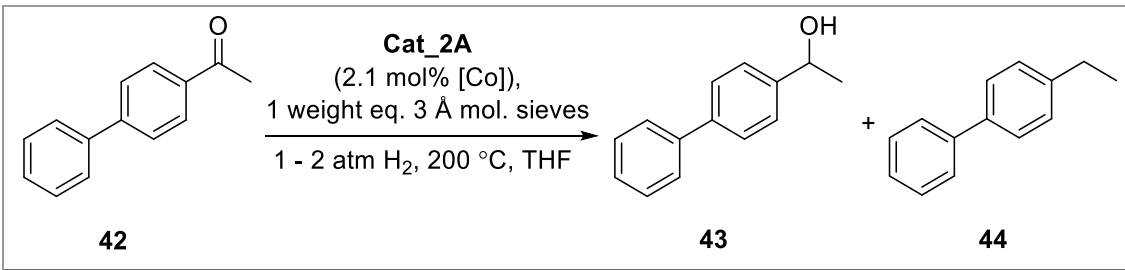
4.5.7.8 Deoxygenation of 4-acetylbiphenyl 42 by *Cat_2A-liquid* at 200 °C

The general procedure was applied to 4-acetylbiphenyl **42** (123 mg., 0.622 mmol) and activated 3Å molecular sieves (123 mg., 1 wt. equivalent). The brown THF solution was decanted from the solid cobalt particles and filtered through a Celite plug (~2 cm Celite in a Pasteur pipet) into a 5-dram vial. The solid layer was washed thrice with 5 mL THF portions which were filtered through the Celite plug and added to the THF filtrate. The brown THF solution was transferred to a new high-pressure reactor with a glass insert. The substrate, sieves and a small stir bar were added to the reaction mixture and the reactor was sealed. The reactor was immersed into a preheated oil bath at 200 °C upon adding H$_2$ and stirred overnight. The results were quantified by ^{1}H NMR: 86 % conversion, 52 % of of 4-biphenylyl)-1-ethanol **43** and 32 % of 4-ethylbiphenyl **44**.

4.5.7.9 Control reaction with 9-BBN and activated 3Å molecular sieves at 200 °C

In a glovebox, a stainless steel high pressure reaction vessel with glass lining was charged with a small bar-shaped stir bar, 9-BBN (2.1 mg., 0.0082 mmol) and 4 mL THF. The reactor was sealed, removed from the glovebox and attached to a 'high pressure' hydrogen line. The reaction vessel was pressurized to 34 atm H$_2$ (500 psi), immersed into a pre-heated oil bath at 200 °C, and stirred for a set amount of time at 1200 rpm. The reactor was then removed from the heating source and immersed into a room-temperature bath. Once cooled, the reactor was slowly depressurized to release the hydrogen and transferred back into the glovebox. The general

catalytic procedure was then applied to 4-acetylbiphenyl **42** (123 mg., 0.622 mmol) and activated 3Å molecular sieves (123 mg., 1 wt. equivalent). The reaction was immersed into a preheated oil bath at 200 °C upon adding H_2 and stirred overnight. The results were quantified by ^{1}H NMR: 0 % conversion, 100 % of 4-acetylbiphenyl **42**.

4.5.8 General procedure for pre-decomposition of CoBr₂ into *Cat_3A-D*

In a glovebox, a stainless steel high pressure reaction vessel with glass lining was charged with a small bar-shaped stir bar, CoBr₂ (3.5 mg., 0.016 mmol), other additives and 4 mL THF. The reactor was sealed, removed from the glovebox and attached to a 'high pressure' hydrogen line. The reaction vessel was pressurized to 34 atm H_2 (500 psi), immersed into an oil bath at 200 °C, and stirred for 1 h at 1200 rpm. The reactor was then removed from the heating source and immersed into a room-temperature bath. Once cooled, the reactor was slowly depressurized to release the hydrogen and transferred back into the glovebox.

4.5.8.1 Pre-decomposition of CoBr₂ into *Cat_3A*

The general procedure was applied to CoBr₂ (3.5 mg., 0.016 mmol) and 9-BBN (4.2 mg., 0.016 mmol). A light blue solution was observed upon opening the reactor.

4.5.8.2 Pre-decomposition of CoBr₂ into *Cat_3B*

The general procedure was applied to CoBr₂ (3.5 mg., 0.016 mmol), 9-BBN (4.2 mg., 0.016 mmol) and KO^{t}Bu (4.0 mg., 0.036 mmol). A colorless THF solution and a black film deposit on the glass insert was observed upon opening the reactor.

4.5.8.3 Pre-decomposition of CoBr₂ into *Cat_3C*

The general procedure was applied to CoBr$_2$ (3.5 mg., 0.016 mmol) and KO^{t}Bu (4.0 mg., 0.036 mmol). A colorless THF solution and a black film deposit on the glass insert was observed upon opening the reactor.

4.5.8.4 Pre-decomposition of CoBr$_2$ into *Cat_3D*
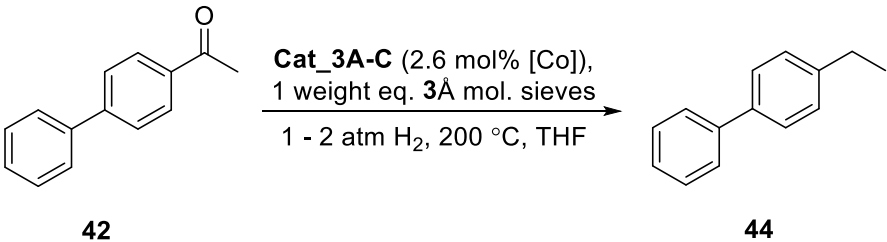
The general procedure was applied to CoBr$_2$ (3.5 mg., 0.016 mmol) and NaO^{t}Bu (3.5 mg., 0.036 mmol). A colorless THF solution and a black film deposit on the glass insert was observed upon opening the reactor.

4.5.9 General procedure for catalysis reactions by pre-decomposed *Cat_3A-D* in the presence of activated molecular sieves as water scavenger

The reaction was conducted immediately upon the pre-decomposition procedure. Once the reactor with *Cat_3A-D* was opened in the glovebox, 4-acetylbiphenyl **42** (123 mg., 0.622 mmol), activated 3Å molecular sieves (123 mg., 1 wt. equivalent) and 1 mL THF were added to the reaction vessel. The reactor was sealed, removed from the glovebox and connected to a hydrogen line. The reactor was charged with 7 atm H$_2$ and slowly depressurized to 1 – 2 atm twice, immersed into a preheated oil bath at 200 °C and stirred for an indicated time at 1200 rpm. The reactor was then removed from the heating source and immersed into a room-temperature bath. Once cooled, the reactor was slowly depressurized and opened to the atmosphere. The resulting mixture was transferred into a 5-dram vial. The reactor was washed twice with 5 mL THF/Et$_2$O portions which were added to the 5-dram vial. The mixture was filtered through a silica plugged pipet (~2 cm silica) and a Florisil® plugged pipet (~2 cm Florisil®). The solvents were removed *in vacuo* to give a semi-liquid solid. The reaction products were dissolved in CDCl$_3$, 20 μL of

hexamethyldisiloxane (0.103 mmol) was added to the solution and the sample was analyzed by ^{1}H NMR.
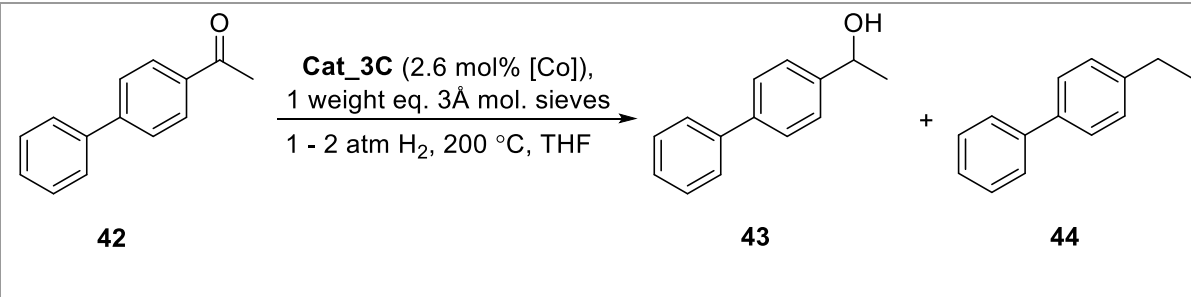
Table 4.17 Deoxygenation of 4-acetylbiphenyl **42** by *Cat_3A-D*.

Entry	Cat.	Mol. sieves	Time	Conversion, [%]	Yield, [%]
					44
1	*Cat_3A*	3 Å	overnight	0	0
2	*Cat_3B*	3 Å	overnight	100	100
3	*Cat_3C*	3 Å	overnight	100	83[a]
4	*Cat_3C*	3 Å	2.5 h	100	96
5	*Cat_3D*	3 Å	2.5 h	100	99
6	*Cat_3D*	4 Å	2.5 h	100	88[b]

4.5.9.1 Hydrodeoxygenation of 4-acetylbiphenyl by *Cat_3C* over 2.5 h

Once the reactor containing *Cat_3C* was opened in the glovebox, the general procedure was applied to 4-acetylbiphenyl **42** (123 mg., 0.622 mmol) and activated 3Å molecular sieves (123 mg., 1 wt. equivalent). The reactor was immersed into a preheated oil bath at 200 °C and stirred for an indicated amount of time after adding H_2. The results were quantified by ^{1}H NMR.

Table 4.18 Deoxygenation of 4-acetylbiphenyl **42** by *Cat_3C* over 2.5 h.

Entry	Time, [h]	Conversion, [%]	Yield, [%]	
			43	**44**
1	0.5	22	9	9
2	1.0	43	14	22
3	1.5	3	2	0
4	1.5	99	5	92
5	2.0	55	0	54
6	2.5	100	0	96

4.5.9.2 Temperature and pressure optimization in hydrodeoxygenation of 4-acetylbiphenyl by *Cat_3C*

The general procedure was applied to 4-acetylbiphenyl **42** (123 mg., 0.622 mmol) and activated 3Å molecular sieves (123 mg., 1 wt. equivalent). The reactor was pressurized to an indicated pressure and the reactor was immersed into a preheated oil bath at an indicated temperature and stirred for 2.5 h after adding H_2. The results were quantified by ^{1}H NMR and GC-MS.

Table 4.19 Deoxygenation of 4-acetylbiphenyl **42** by *Cat_3C* at 100 – 200 °C.

Entry	Temperature, [°C]	H$_2$ pressure, [atm]	Conversion, [%]	Yield, [%]		
				43	**44**	By-products[b]
1	200	1	100	0	96	4
2	200	7	100	0	88	11
3	200	7	100	0	84	13
4	200	7	98	6	84	5
5	150	1	57	12	41	4
6	150	7	100	0	92	6
7	150	7	88	42	41	4
8	100	1	29	25	0	0
9	100	1	35	25	4	4
10	100	1	29	25	0	2
11	100	7	7	4	0	3
12	100	7	7	5	0	2
13[a]	100	1	54	39	10	4
14[a]	100	1	78	67	8	2
15[a]	100	7	100	42	50	6

Determined by GC-MS. [a] Carried out overnight. [b] Over-hydrogenation of an aromatic ring.

4.5.10 General procedure for substrate scope investigation with *Cat_3C*
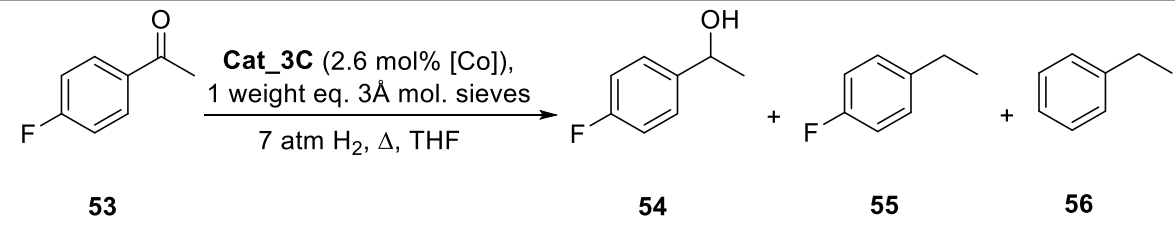
The reaction was conducted immediately upon the pre-decomposition procedure. Once the reactor with *Cat_3C* was opened in the glovebox, a substrate (0.622 mmol), activated 3Å molecular sieves (1 weight equivalent) and 1 mL THF were added to the reaction vessel. The reactor was sealed, removed from the glovebox and connected to a hydrogen line. The reactor was pressurized to 7 atm H$_2$, slowly depressurized to ~1 atm H$_2$ and pressurized to 7 atm H$_2$

again. The reaction was immersed into a preheated oil bath at 200 °C and stirred for an indicated time at 1200 rpm. The reactor was then removed from the heating source and immersed into a room-temperature bath. Once cooled, the reactor was slowly depressurized and opened to the atmosphere. The resulting mixture was transferred into a 5-dram vial. The reactor was washed twice with 5 mL THF/Et$_2$O portions which were added to the 5-dram vial. The mixture was filtered through a silica plugged pipet (~2 cm silica) and a Florisil® plugged pipet (~2 cm Florisil®). The sample was submitted for GC-MS analysis.

4.5.10.1 Deoxygenation of 4-fluoroacetophenone 53

The general procedure was applied to 4-fluoroacetophenone **53** (85 mg., 75 mL, 0.622 mmol) and activated 3Å molecular sieves (85 mg., 1 wt. equivalent). The reactor was immersed into a preheated oil bath at an indicated temperature and stirred for an indicated time. The results were analyzed by GC-MS.
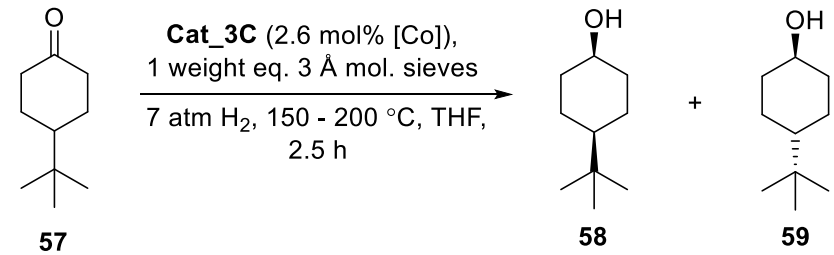
Table 4.20 Deoxygenation of 4-fluoroacetophenone **53** by *Cat_3C*.

Entry	Temperature, [°C]	Time	Conversion, [%]	Yield, [%]		
				53	54	55
1	150	2.5 h	22	20	0.4	0
2	200	2.5 h	28	21	4.9	0
3	150	overnight	99	72	22	4
4	200	overnight	100	0	94	5

4.5.10.2 Deoxygenation of 4-*tert*-butylcyclohexanone 57

The general procedure was applied to 4-*tert*-butylcyclohexanone **57** (92 mg., 0.622 mmol) and activated 3Å molecular sieves (92 mg., 1 wt. equivalent). The reactor was immersed into a preheated oil bath at an indicated temperature and stirred for 2.5 h. The results were analyzed by GC-MS.

Table 4.21 Deoxygenation of 4-*tert*-butylcyclohexanone **57** by *Cat_3C*.

Entry	Temperature, [°C]	Time	Conversion, [%]	Yield, [%]	
				58	**59**
1	150	2.5 h	100	37	63
2	200	2.5 h	100	33	67

4.5.10.3 Deoxygenation of diphenyl ether 60

The general procedure was applied to diphenyl ether **60** (106 mg., 0.622 mmol) and activated 3Å molecular sieves (106 mg., 1 wt. equivalent). The reactor was immersed into a preheated oil bath at 150 °C and stirred for 2.5 h. The results were analyzed by GC-MS: 0 % conversion.

References

(1)   Bosch, C. Process of producing ammonia. US990191A, **1911**.

(2)   Smil, V., *Enriching the Earth: Fritz Haber, Carl Bosch, and the Transformation of World Food Production*. The MIT Press: **2004**.

(3)   Goodall, B. L., Cycloaliphatic Polymers via Late Transition Metal Catalysis. In *Late Transition Metal Polymerization Catalysis*, Wiley-VCH Verlag GmbH & Co. KGaA: **2005**; pp 101-154.

(4)   Bailey, A. E., *Industrial & Engineering Chemistry* **1952,** *44*, 990-994.

(5)   Jovanovic, D., *Catal. Today* **1998**, *43*, 21-28.

(6)   Statista. Revenue of the worldwide pharmaceutical market from 2001 to 2015. https://www.statista.com/statistics/263102/pharmaceutical-market-worldwide-revenue-since-2001/ (accessed 2017.03.29).

(7)   Robles, O.; Romo, D., *Natural product reports* **2014,** *31*, 318-334.

(8)   Bellus, D.; Castedo, L.; Chen, J.; Chiu, C. K. F.; Collins, S. G.; Craig, D.; Fernández, I.; Fravel, B.; Gerster, M.; González-Bello, C.; Kataoka, T.; Khiar, N.; Low, C. M. R.; Maguire, A. R.; Marsini, M. A.; Metzner, P.; Murugan, R.; Nakamura, S.; Perrio, S.; Pettus, T. R. R.; Rakitin, O. A.; Reboul, V.; Sandford, G.; Scriven, E. F. V.; Shcherbakova, I.; Stanforth, S. P.; Thomas, A. W.; Toru, T.; Waldvogel, S. R.; Watanabe, S.; Wehming, K. M.; Zhdankin, V. V., Science of Synthesis: Houben-Weyl Methods of Molecular Transformations Vol. 31a. In *Arene-X (X=Hal, O, S, Se, Te)*, 1st Edition ed.; Georg Thieme Verlag: Stuttgart, New York, **2007**.

(9)   Blay, G.; Montesinos-Magraner, M.; Pedro, J. R., Friedel–Crafts Alkylation of Arenes in Total Synthesis. In *Arene Chemistry*, John Wiley & Sons, Inc: **2015**; pp 33-58.

(10)   Sartori, G.; Maggi, R.; Santacroce, V., Catalytic Friedel–Crafts Acylation Reactions. In *Arene Chemistry*, John Wiley & Sons, Inc: **2015**; pp 59-82.

(11)   Röper, M.; Gehrer, E.; Narbeshuber, T.; Siegel, W., Acylation and Alkylation. In *Ullmann's Encyclopedia of Industrial Chemistry*, Wiley-VCH Verlag GmbH & Co. KGaA: **2000**.

(12)   Baumann, K.; Knapp, H.; Strnadt, G.; Schulz, G.; Grassberger, M. A., *Tetrahedron Lett.* **1999,** *40*, 7761-7764.

(13)   Luo, Y.-R., Comprehensive Handbook of Chemical Bond Energies. CRC Press: **2007**.

(14)   Glockler, G., *J. Phys. Chem.* **1958,** *62*, 1049-1054.

(15)   Magano, J.; Dunetz, J. R., *Org. Process Res. Dev.* **2012,** *16*, 1156-1184.

(16)   Mitchell, R. H.; Lai, Y.-H., *Tetrahedron Lett.* **1980**, *21*, 2637-2638.

(17)   Zhang, C.-Z.; Yang, H.; Wu, D.-L.; Lu, G.-Y., *Chin. J. Chem .* **2007,** *25*, 653-660.

(18)   Gribble, G. W.; Kelly, W. J.; Emery, S. E., *Synthesis* **1978,** *1978*, 763-765.

(19)   Choi, J.-W.; Kang, Y.-H., *Bull. Korean Chem. Soc.* **2005,** *26*, 343-344.

(20)   Rahaim, R. J., Jr.; Maleczka, R. E., Jr., *Org. Lett.* **2011,** *13*, 584-587.

(21)   Kishner, N., *Russ. J. Phys. Chem.* **1911,** *43*, 582.

(22)   Wolff, L., *Justus Liebigs Annalen der Chemie* **1912,** *394*, 86-108.

(23)   Clemmensen, E., *Ber. Dtsch. Chem. Ges.* **1913,** *46*, 1837-1843.

(24)   Clemmensen, E., *Ber. Dtsch. Chem. Ges.* **1914,** *47*, 51-63.

(25)   Wolfrom, M. L.; Karabinos, J. V., *JACS* **1944,** *66*, 909-911.

(26)   Mozingo, R.; Wolf, D. E.; Harris, S. A.; Folkers, K., *JACS* **1943,** *65*, 1013-1016.

(27)   Lin, S. D.; Sanders, D. K.; Albert Vannice, M., *Appl. Cat., A* **1994,** *113*, 59-73.

(28)   W. Gribble, G., *Chem. Soc. Rev.* **1998,** *27*, 395.

(29)   Herr, C. H.; Whitmore, F. C.; Schiessler, R. W., *JACS* **1945,** *67*, 2061-2063.

(30)   Soffer, M. D.; Soffer, M. B.; Sherk, K. W., *JACS* **1945,** *67*, 1435-1436.

(31)   Huang, M., *JACS* **1946,** *68*, 2487-2488.

(32)   Barton, D. H. R.; Ives, D. A. J.; Thomas, B. R., *J. Chem. Soc.* **1955**, 2038.

(33)   Cram, D. J.; Sahyun, M. R. V., *JACS* **1962,** *84*, 1734-1735.

(34)   Grundon, M. F.; Henbest, H. B.; Scott, M. D., *J. Chem. Soc.* **1963**, 1855-1858.

(35)   Caglioti, L.; Magi, M., *Tetrahedron* **1963,** *19*, 1127-1131.

(36)   Furrow, M. E.; Myers, A. G., *JACS* **2004,** *126*, 5436-45.

(37)   Schlosser, M.; Kampmann, D.; Stuhlmüller, G.; Simon, R.; Cottet, F.; Leroux, F., *Synthesis* **2005,** *2005*, 1028-1029.

(38)   Eisenbraun, E. J.; Payne, K. W.; Bymaster, J. S., *Industrial & Engineering Chemistry Research* **2000,** *39*, 1119-1123.

(39)   Kuethe, J. T.; Childers, K. G.; Peng, Z.; Journet, M.; Humphrey, G. R.; Vickery, T.; Bachert, D.; Lam, T. T., *Org. Process Res. Dev.* **2009,** *13*, 576-580.

(40)   Brewster, J. H., *Journal of the American Chemical Society* **1954,** *76*, 6364-6368.

(41)   Nakabayashi, T., *JACS* **1960,** *82*, 3900-3906.

(42)   Martin, E. L., The Clemmensen Reduction. In *Org. React.*, John Wiley & Sons, Inc.: **2004**.

(43)   Talapatra, S. K.; Chakrabarti, S.; Mallik, A. K.; Talapatra, B., *Tetrahedron* **1990,** *46*, 6047-6052.

(44)   Yamamura, S.; Ueda, S.; Hirata, Y., *Chem. Commun. (London)* **1967**, 1049-1050.

(45)   Hiegel, G. A.; Carney, J. R., *Synth. Commun.* **1996,** *26*, 2625-2631.

(46)   Xu, S.; Toyama, T.; Nakamura, J.; Arimoto, H., *Tetrahedron Lett.* **2010,** *51*, 4534-4537.

(47)   Raney, M. Method of producing finely-divided nickel. US1628190A, **1927**.

(48)   Wainwright, M. S., Skeletal Metal Catalysts. In *Preparation of Solid Catalysts*, Wiley-VCH Verlag GmbH: **2008**; pp 28-43.

(49)   Papa, D.; Schwenk, E.; Whitman, B., *JOC* **1942,** *7*, 587-590.

(50)   Koscielski, T.; Bonnier, J. M.; Damon, J. P.; Masson, J., *Appl. Cat.* **1989,** *49*, 91-99.

(51)   Masson, J.; Vidal, S.; Cividino, P.; Fouilloux, P.; Court, J., *Appl. Cat., A* **1993,** *99*, 147-159.

(52)   Ishimoto, K.; Mitoma, Y.; Nagashima, S.; Tashiro, H.; Prakash, G. K. S.; Olah, G. A.; Tashiro, M., *Chem. Commun.* **2003**, 514-515.

(53)   Liu, G. B.; Zhao, H. Y.; Zhu, J. D.; He, H. J.; Yang, H. J.; Thiemann, T.; Tashiro, H.; Tashiro, M., *Synth. Commun.* **2008,** *38*, 1651-1661.

(54)   Zuidema, D. R.; Williams, S. L.; Wert, K. J.; Bosma, K. J.; Smith, A. L.; Mebane, R. C., *Synth. Commun.* **2011,** *41*, 2927-2931.

(55)   Schlesinger, H. I.; Brown, H. C.; Abraham, B.; Bond, A. C.; Davidson, N.; Finholt, A. E.; Gilbreath, J. R.; Hoekstra, H.; Horvitz, L.; Hyde, E. K.; Katz, J. J.; Knight, J.; Lad, R. A.; Mayfield, D. L.; Rapp, L.; Ritter, D. M.; Schwartz, A. M.; Sheft, I.; Tuck, L. D.; Walker, A. O., *JACS* **1953,** *75*, 186-190.

(56)   Banfi, L.; Narisano, E.; Riva, R., Sodium Borohydride. In *Encyclopedia of Reagents for Organic Synthesis*, John Wiley & Sons, Ltd: **2001**.

(57)   Ketcha, D. M.; Lieurance, B. A.; Homan, D. F. J.; Gribble, G. W., *JOC* **1989,** *54*, 4350-4356.

(58)   Ono, A.; Suzuki, N.; Kamimura, J., *Synthesis* **1987**, 736-738.

(59)   Lau, C. K.; Tardif, S.; Dufresne, C.; Scheigetz, J., *JOC* **1989,** *54*, 491-494.

(60)   Lau, C. K.; Dufresne, C.; Belanger, P. C.; Pietre, S.; Scheigetz, J., *JOC* **1986,** *51*, 3038-3043.

(61)   Uddin, J.; Morales, C. M.; Maynard, J. H.; Landis, C. R., *Organometallics* **2006,** *25*, 5566-5581.

(62)   Maier, W. F.; Bergmann, K.; Bleicher, W.; Schleyer, P. v. R., *Tetrahedron Lett.* **1981,** *22*, 4227-4230.

(63)   Rao, A. V. R.; Mehendale, A. R.; Reddy, K. B., *Tetrahedron Lett.* **1982,** *23*, 2415-2418.

(64)   Sutton, A. D.; Waldie, F. D.; Wu, R.; Schlaf, M.; Silks, L. A.; Gordon, J. C., *Nat Chem* **2013,** *5*, 428-432.

(65)   Vannice, M. A.; Poondi, D., *J. Catal.* **1997,** *169*, 166-175.

(66)   Poondi, D.; Vannice, M. A., *J. Mol. Catal. A: Chem.* **1997,** *124*, 79-89.

(67)   Lin, S. D.; Sanders, D. K.; Vannice, M. A., *J. Catal.* **1994,** *147*, 370-374.

(68)   Faba, L.; Díaz, E.; Ordóñez, S., *Catal. Sci. Technol.* **2015,** *5*, 1473-1484.

(69)   McManus, I.; Daly, H.; Thompson, J. M.; Connor, E.; Hardacre, C.; Wilkinson, S. K.; Sedaie Bonab, N.; ten Dam, J.; Simmons, M. J. H.; Stitt, E. H.; D'Agostino, C.; McGregor, J.; Gladden, L. F.; Delgado, J. J., *J. Catal.* **2015**, *330*, 344-353.

(70)   Bertero, N. M.; Trasarti, A. F.; Apesteguía, C. R.; Marchi, A. J., *Appl. Cat., A* **2011,** *394*, 228-238.

(71)   Ramos, R.; Tišler, Z.; Kikhtyanin, O.; Kubička, D., *Appl. Cat., A* **2017,** *530*, 174-183.

(72)   Santori, G. F.; Moglioni, A. G.; Vetere, V.; Iglesias, G. Y. M.; Casella, M. L.; Ferretti, O. A., *Appl. Cat., A* **2004,** *269*, 215-223.

(73)   Bejblová, M.; Zámostný, P.; Červený, L.; Čejka, J., *Appl. Catal., A* **2005,** *296*, 169-175.

(74)   Mäki-Arvela, P.; Hájek, J.; Salmi, T.; Murzin, D. Y., *Appl. Catal., A* **2005,** *292*, 1-49.

(75)   Lenarda, M.; Casagrande, M.; Moretti, E.; Storaro, L.; Frattini, R.; Polizzi, S., *Catal. Lett.* **2007,** *114*, 79-84.

(76)   Falcone, D. D.; Hack, J. H.; Davis, R. J., *ChemCatChem* **2016,** *8*, 1074-1083.

(77)   Chen, M.; Maeda, N.; Baiker, A.; Huang, J., *ACS Catalysis* **2012,** *2*, 2007-2013.

(78)   Gong, S. W.; He, H. F.; Zhao, C. Q.; Liu, L. J.; Cui, Q. X., *Synth. Commun.* **2012,** *42*, 574-581.

(79)   Kogan, V.; Aizenshtat, Z.; Neumann, R., *Angew. Chem. Int. Ed.* **1999,** *38*, 3331-3334.

(80)   Wang, W.; Yang, Y.; Luo, H.; Hu, T.; Liu, W., *Catal. Commun.* **2011,** *12*, 436-440.

(81)   Wang, W.-Y.; Yang, Y.-Q.; Bao, J.-G.; Luo, H.-A., *Catal. Commun.* **2009,** *11*, 100-105.

(82)   Wang, W.-Y.; Yang, Y.-Q.; Luo, H.-A.; Liu, W.-Y., *Catal. Commun.* **2010,** *11*, 803-807.

(83)   Wang, W.; Yang, Y.; Luo, H.; Peng, H.; He, B.; Liu, W., *Catal. Commun.* **2011,** *12*, 1275-1279.

(84)   Zaccheria, F.; Ravasio, N.; Ercoli, M.; Allegrini, P., *Tetrahedron Lett.* **2005,** *46*, 7743-7745.

(85)   Bertero, N. M.; Apesteguía, C. R.; Marchi, A. J., *Appl. Catal., A* **2008,** *349*, 100-109.

(86)   Ma, J.; Liu, S.; Kong, X.; Fan, X.; Yan, X.; Chen, L., *Res. Chem. Intermed.* **2011,** *38*, 1341-1349.

(87)   Flores-Gaspar, A.; Pinedo-González, P.; Crestani, M. G.; Muñoz-Hernández, M.; Morales-Morales, D.; Warsop, B. A.; Jones, W. D.; García, J. J., *J. Mol. Catal. A: Chem.* **2009,** *309*, 1-11.

(88)   Kalutharage, N.; Yi, C. S., *JACS* **2015,** *137*, 11105-11114.

(89)   Stephan, D. W.; Erker, G., *Angew. Chem. Int. Ed.* **2010,** *49*, 46-76.

(90)   Stephan, D. W., *Acc. Chem. Res.* **2015,** *48*, 306-316.

(91)   Paradies, J., *Angew. Chem. Int. Ed.* **2014,** *53*, 3552-3557.

(92)   Lindqvist, M.; Sarnela, N.; Sumerin, V.; Chernichenko, K.; Leskela, M.; Repo, T., *Dalton Trans* **2012,** *41*, 4310-2.

(93)   Mahdi, T.; Stephan, D. W., *Angew. Chem. Int. Ed. Engl.* **2015,** *54*, 8511-8514.

(94)   Marciniec, B., Hydrosilylation of Unsaturated Carbon—Heteroatom Bonds. In *Hydrosilylation: A Comprehensive Review on Recent Advances*, Marciniec, B., Ed. Springer Netherlands: Dordrecht, **2009**; pp 289-339.

(95)   West, C. T.; Donnelly, S. J.; Kooistra, D. A.; Doyle, M. P., *JOC* **1973,** *38*, 2675-2681.

(96)   Fry, J. L.; Orfanopoulos, M.; Adlington, M. G.; Dittman, W. P.; Silverman, S. B., *JOC* **1978,** *43*, 374-375.

(97)   Fry, J. L.; Silverman, S. B.; Orfanopoulos, M., *Organic Syntheses* **1981,** *60*, 108.

(98)   Jaxa-Chamiec, A.; Shah, V. P.; Kruse, L. I., *J. Chem. Soc., Perkin Trans. 1* **1989**, 1705-1706.

(99)   Miyai, T.; Ueba, M.; Baba, A., *Synlett* **1999**, 182-184.

(100)   Sakai, N.; Nagasawa, K.; Ikeda, R.; Nakaike, Y.; Konakahara, T., *Tetrahedron Lett.* **2011,** *52*, 3133-3136.

(101)   Chandrasekhar, S.; Reddy, C. R.; Babu, B. N., *JOC* **2002,** *67*, 9080-9082.

(102)   Campagne, J.-M.; Dal Zotto, C.; Virieux, D., *Synlett* **2009**, 0276-0278.

(103)   Wang, H.; Li, L.; Bai, X.-F.; Shang, J.-Y.; Yang, K.-F.; Xu, L.-W., *Adv. Synth. Catal.* **2013**, 341-347.

(104)   Volkov, A.; Gustafson, K. P.; Tai, C. W.; Verho, O.; Backvall, J. E.; Adolfsson, H., *Angew. Chem. Int. Ed. Engl.* **2015,** *54*, 5122-6.

(105)   Kennedy-Smith, J. J.; Nolin, K. A.; Gunterman, H. P.; Toste, F. D., *J. Am. Chem. Soc.* **2003,** *125*, 4056-7.

(106)   Bernardo, J. R.; Fernandes, A. C., *Green Chem.* **2016,** *18*, 2675-2681.

(107)   Fernandes, T. A.; Fernandes, A. C., *ChemCatChem* **2015,** *7*, 3503-3507.

(108)   Fernandes, T. A.; Bernardo, J. R.; Fernandes, A. C., *ChemCatChem* **2015,** *7*, 1177-1183.

(109)   Sousa, S. C. A.; Fernandes, T. A.; Fernandes, A. C., *Eur. J. Org. Chem.* **2016,** *2016*, 3109-3112.

(110)   Mao, Z.; Gregg, B. T.; Cutler, A. R., *JACS* **1995,** *117*, 10139-10140.

(111)   Mehta, M.; Holthausen, M. H.; Mallov, I.; Perez, M.; Qu, Z. W.; Grimme, S.; Stephan, D. W., *Angew. Chem. Int. Ed. Engl.* **2015,** *54*, 8250-8254.

(112)   Yuan, L. Z.; Renko, D.; Khelifi, I.; Provot, O.; Brion, J. D.; Hamze, A.; Alami, M., *Org. Lett.* **2016,** *18*, 3238-3241.

(113)   Kamochi, Y.; Kudo, T.; Masuda, T.; Takadate, A., *Chem. Pharm. Bull.* **2005,** *53*, 1017-1020.

(114)   Hicks, L. D.; Han, J. K.; Fry, A. J., *Tetrahedron Lett.* **2000,** *41*, 7817-7820.

(115)   Hagen, J., Heterogeneously Catalyzed Processes in Industry. In *Industrial Catalysis*, Wiley-VCH Verlag GmbH & Co. KGaA: **2015**; pp 261-298.

(116)   Hagen, J., Homogeneously Catalyzed Industrial Processes. In *Industrial Catalysis*, Wiley-VCH Verlag GmbH & Co. KGaA: **2015**; pp 47-80.

(117)   Hagen, J., Planning, Development, and Testing of Catalysts. In *Industrial Catalysis*, Wiley-VCH Verlag GmbH & Co. KGaA: **2015**; pp 395-432.

(118)   Hagen, J., Homogeneous Catalysis with Transition Metal Catalysts. In *Industrial Catalysis*, Wiley-VCH Verlag GmbH & Co. KGaA: **2015**; pp 17-46.

(119)   Chakraborty, S.; Guan, H., *Dalton Trans* **2010,** *39*, 7427-36.

(120)   Hagen, J., Introduction. In *Industrial Catalysis*, Wiley-VCH Verlag GmbH & Co. KGaA: **2015**; pp 1-16.

(121)   Hagen, J., Heterogeneous Catalysis: Fundamentals. In *Industrial Catalysis*, Wiley-VCH Verlag GmbH & Co. KGaA: **2015**; pp 99-210.

(122)   Raghunath, V. C., *Platinum Met. Rev.* **2011,** *55*, 180-185.

(123)   van Leeuwen, P. W. N. M.; Chadwick, J. C., Elementary Steps. In *Homogeneous Catalysts*, Wiley-VCH Verlag GmbH & Co. KGaA: **2011**; pp 1-49.

(124)   Grubbs, R. H., Introduction. In *Handbook of Metathesis*, Wiley-VCH Verlag GmbH: **2008**; pp 1-3.

(125)   Schrock, R. R., The Discovery and Development of High Oxidation State Mo and W Imido Alkylidene Complexes for Alkene Metathesis. In *Handbook of Metathesis*, Wiley-VCH Verlag GmbH: **2008**; pp 8-32.

(126)   Nguyen, S. T.; Trnka, T. M., The Discovery and Development of Well-Defined, Ruthenium-Based Olefin Metathesis Catalysts. In *Handbook of Metathesis*, Wiley-VCH Verlag GmbH: **2008**; pp 61-85.

(127)   Katz, T. J., Fischer Metal Carbenes and Olefin Metathesis. In *Handbook of Metathesis*, Wiley-VCH Verlag GmbH: **2008**; pp 47-60.

(128)   Copéret, C.; Lefebvre, F.; Basset, J.-M.; Leconte, M., From Ill-Defined to Well-Defined W Alkylidene Complexes. In *Handbook of Metathesis*, Wiley-VCH Verlag GmbH: **2008**; pp 33-46.

(129)   Werner, H.; Wolf, J., Synthesis of Rhodium and Ruthenium Carbene Complexes with a 16-Electron Count. In *Handbook of Metathesis*, Wiley-VCH Verlag GmbH: **2008**; pp 95-111.

(130)   Roper, W. R., Synthesis of Ruthenium Carbene Complexes. In *Handbook of Metathesis*, Wiley-VCH Verlag GmbH: **2008**; pp 86-94.

(131)   Tolman, C. A., *Chem. Rev.* **1977,** *77*, 313-348.

(132)   Catlow, C. R.; French, S. A.; Sokol, A. A.; Thomas, J. M., *Philos Trans A Math Phys Eng Sci* **2005,** *363*, 913-36; discussion 1035-40.

157

(133)   Hagen, J., Catalyst Shapes and Production of Heterogeneous Catalysts. In *Industrial Catalysis*, Wiley-VCH Verlag GmbH & Co. KGaA: **2015**; pp 211-238.

(134)   Low, P. J., *Annual Reports Section "A" (Inorganic Chemistry)* **2005,** *101*, 375-393.

(135)   Tolman, C. A., *JACS* **1970,** *92*, 2956-2965.

(136)   Gillespie, J. A.; Zuidema, E.; van Leeuwen, P. W. N. M.; Kamer, P. C. J., Phosphorus Ligand Effects in Homogeneous Catalysis and Rational Catalyst Design. In *Phosphorus(III) Ligands in Homogeneous Catalysis: Design and Synthesis*, John Wiley & Sons, Ltd: **2012**; pp 1-26.

(137)   Li, W.; Zhang, X., Chiral Phosphines and Diphosphines. In *Phosphorus(III) Ligands in Homogeneous Catalysis: Design and Synthesis*, John Wiley & Sons, Ltd: **2012**; pp 27-80.

(138)   Staudinger, H.; Meyer, J., *Helv. Chim. Acta* **1919,** *2*, 635-646.

(139)   Schmidbaur, H.; Jonas, G., *Chem. Ber.* **1968,** *101*, 1271-1285.

(140)   Dehnicke, K.; Strähle, J., *Polyhedron* **1989,** *8*, 707-726.

(141)   Dehnicke, K.; Krieger, M.; Massa, W., *Coord. Chem. Rev.* **1999,** *182*, 19-65.

(142)   Batsanov, A. S.; Davidson, M. G.; Howard, J. A. K.; Lamb, S.; Lustig, C.; Price, R. D., *Chem. Commun.* **1997**, 1211-1212.

(143)   Anfang, S.; Seybert, G.; Harms, K.; Geiseler, G.; Massa, W.; Dehnicke, K., *Z. Anorg. Allg. Chem.* **1998,** *624*, 1187-1192.

(144)   Gröb, T.; Chitsaz, S.; Harms, K.; Dehnicke, K., *Z. Anorg. Allg. Chem.* **2002,** *628*, 473-479.

(145)   Gröb, T.; Harms, K.; Dehnicke, K., *Z. Anorg. Allg. Chem.* **2000,** *626*, 1065-1072.

(146)   Schlecht, S.; Deubel, D. V.; Frenking, G.; Geiseler, G.; Harms, K.; Magull, J.; Dehnicke, K., *Z. Anorg. Allg. Chem.* **1999,** *625*, 887-891.

(147)   Honeyman, C. H.; Lough, A. J.; Manners, I., *Inorg. Chem.* **1994,** *33*, 2988-2993.

(148)   Nußhär, D.; Weller, F.; Dehnicke, K., *Z. Anorg. Allg. Chem.* **1993,** *619*, 507-512.

(149)   Stahl, M. M.; Faza, N.; Massa, W.; Dehnicke, K., *Z. Anorg. Allg. Chem.* **1998,** *624*, 209-214.

(150)   Mai, H. J.; Wocadlo, S.; Kang, H. C.; Massa, W.; Dehnicke, K.; Maichle-Mössmer, C.; Strähle, J.; Fenske, D., *Z. Anorg. Allg. Chem.* **1995,** *621*, 705-712.

(151)   Klein, H. F.; Haller, S.; Koenig, H.; Dartiguenave, M.; Dartiguenave, Y.; Menu, M. J., *JACS* **1991,** *113*, 4673-4675.

(152)   Abram, S.; Abram, U.; zu Köcker, R. M.; Dehnicke, K., *Z. Anorg. Allg. Chem.* **1996,** *622*, 867-872.

(153)   Camacho-Bunquin, J.; Ferguson, M. J.; Stryker, J. M., *J. Am. Chem. Soc.* **2013,** *135*, 5537-5540.

(154)   Hollink, E.; Wei, P.; Stephan, D. W., *Can. J. Chem.* **2005,** *83*, 430-434.

(155)   Stephan, D. W.; Stewart, J. C.; Guérin, F.; Courtenay, S.; Kickham, J.; Hollink, E.; Beddie, C.; Hoskin, A.; Graham, T.; Wei, P.; Spence, R. E. v. H.; Xu, W.; Koch, L.; Gao, X.; Harrison, D. G., *Organometallics* **2003,** *22*, 1937-1947.

(156)   Dehnicke, K.; Weller, F., *Coord. Chem. Rev.* **1997,** *158*, 103-169.

(157)   Ravi, P.; Gröb, T.; Dehnicke, K.; Greiner, A., *Macromol. Chem. Phys.* **2001,** *202*, 2641-2647.

(158)   Neumüller, B.; Dehnicke, K., *Z. Anorg. Allg. Chem.* **2004,** *630*, 799-805.

(159)   Luinstra, G. A.; Queisser, J.; Bildstein, B.; Görtz, H.-H.; Amort, C.; Malaun, M.; Krajete, A.; Werne, G.; Kristen, M. O.; Huber, N.; Gernert, C., Highly Active Ethene Polymerization Catalysts with Unusual Imine Ligands. In *Late Transition Metal Polymerization Catalysis*, Wiley-VCH Verlag GmbH & Co. KGaA: **2005**; pp 59-99.

(160)   LePichon, L.; Stephan, D. W.; Gao, X.; Wang, Q., *Organometallics* **2002,** *21*, 1362-1366.

(161)   Hamilton, R.; Zhao, T.; Brown, H. J. S.; Gauthier, J. M. A., University of Alberta, Edmonton, Unpublished Work, 2010.

(162)   Zimmer, H.; Jayawant, M.; Gutsch, P., *JOC* **1970,** *35*, 2826-2828.

(163)   Zhao, T. Phosphoranimide-supported Nickel Clusters for Hydrotreatment. University of Edmonton, Edmonton, **2016**.

(164)   Hamilton, R., University of Alberta, Edmonton, Unpublished Work, 2011.

(165)   Brown, H. J. S. Mixed-Valence First-Row Metal Clusters for Catalytic Hydrodesulfurization and Hydrodeoxygenation. University of Alberta, Edmonton, **2013**.

(166)   Camacho-Bunquin, J. Empowering the Base Metals: Rational Design of High-Activity Homogeneous Catalysts for Reduction of Organic Unsaturates and Mild-Condition Hydrotreatment. PhD, University of Alberta, Edmonton, **2013**.

(167)   Triphenylphosphine.   http://www.chemspider.com/Chemical-Structure.11283.html   (accessed 2017.05.07).

(168)   Triisopropylphosphine.   http://www.chemspider.com/Chemical-Structure.73055.html   (accessed 2017.05.07).

(169)   Robinson, T. P.; Price, R. D.; Davidson, M. G.; Fox, M. A.; Johnson, A. L., *Dalton Trans* **2015,** *44*, 5611-5619.

(170)   Mitton, S., University of Alberta, Edmonton, Unpublished Work, 2015.

(171)   Kubo, R.; Tomita, K., *J. Phys. Soc. Jpn.* **1954,** *9*, 888-919.

(172)   Roesky, H. W.; Seseke, U.; Noltemeyer, M.; Sheldrick, G. M., *Z. Naturforsch., B: Chem. Sci.* **1988,** *43*, 1130-1136.

(173)   Gauthier, J. M. A. Titanacyclobutene and Cobalt(II) Phosphinimide Complexes. PhD, University of Alberta, Edmonton, **2012**.

(174)   Vorapattanapong, A., University of Alberta, Edmonton, Unpublished Work, 2016.

(175)   Holthausen, M. H.; Mallov, I.; Stephan, D. W., *Dalton Transactions* **2014,** *43*, 15201-15211.

(176)   Lundgren, R. J.; Stradiotto, M., Key Concepts in Ligand Design. In *Ligand Design in Metal Chemistry*, John Wiley & Sons, Ltd: **2016**; pp 1-14.

(177)   Birkenstock, U.; Bönnemann, H.; Bogdanovic, B.; Walter, D.; Wilke, G., **1974,** *70*, 250-265.

(178)   Hanusa, T. P.; Carlson, C. N., Transition Metal Complexes with Bulky Allyl Ligands. In *Encyclopedia of Inorganic and Bioinorganic Chemistry*, John Wiley & Sons, Ltd: **2011**.

(179)   Nkala, F., University of Alberta, Edmonton, Unpublished Work, 2017.

(180)   Mahoney, W. S.; Brestensky, D. M.; Stryker, J. M., *JACS* **1988,** *110*, 291-293.

(181)   Bezman, S. A.; Churchill, M. R.; Osborn, J. A.; Wormald, J., *JACS* **1971,** *93*, 2063-2065.

(182)   Krempner, C., *Eur. J. Inorg. Chem.* **2011,** *2011*, 1689-1698.

(183)   Van der Sluys, L. S.; Miller, M. M.; Kubas, G. J.; Caulton, K. G., *JACS* **1991,** *113*, 2513-2520.

(184)   Turova, N. Y.; Turevskaya, E. P.; Kessler, V. G.; Yanovskaya, M. I., The Chemistry of Metal Alkoxides. Springer US: **2002**.

(185)   Bradley, D. C., **1959,** *23*, 10-36.

(186)   Clark, E., *Industrial & Engineering Chemistry Analytical Edition* **1941,** *13*, 820-821.

(187)   Culmo,   R.   F.   Elemental   Analysis.   https://www.perkinelmer.com/lab-solutions/resources/docs/APP_011267_01_TheElementalAnalysisofVariousClassesofChemicalCompoundsUsingCHN.pdf (accessed 2017.06.28).

(188)   Anfang, S.; Gröb, T.; Harms, K.; Seybert, G.; Massa, W.; Greiner, A.; Dehnicke, K., *Z. Anorg. Allg. Chem.* **1999,** *625*, 1853-1859.

(189)   Grün, M.; Harms, K.; Köcker, R. M. Z.; Dehnicke, K.; Goesmann, H., *Z. Anorg. Allg. Chem.* **1996,** *622*, 1091-1096.

(190)   Li, J.-S.; Weller, F.; Schmock, F.; Dehnicke, K., *Z. Anorg. Allg. Chem.* **1995,** *621*, 2097-2103.

(191)   Neumüller, B.; Dehnicke, K., *Z. Anorg. Allg. Chem.* **2004,** *630*, 1360-1362.

(192)   Mronga, N.; Weller, F.; Dehnicke, K., *Z. Anorg. Allg. Chem.* **1983,** *502*, 35-44.

(193)   Gröb, T.; Seybert, G.; Massa, W.; Dehnicke, K., *Z. Anorg. Allg. Chem.* **2001,** *627*, 304-306.

(194)   Borisov, S. N.; Voronkov, M. G.; Lukevits, E. Y., Organosilicon Compounds of Group VIII Elements. In *Organosilicon Heteropolymers and Heterocompounds*, Springer US: Boston, MA, **1970**; pp 519-568.

(195)   Stangret, J.; Gampe, T., *J. Mol. Struct.* **2005,** *734*, 183-190.

(196)   Bowron, D. T.; Finney, J. L.; Soper, A. K., *JACS* **2006,** *128*, 5119-5126.

(197)   Burford, N.; Clyburne, J. A. C.; Silvert, D.; Warner, S.; Whitla, W. A.; Darvesh, K. V., *Inorg. Chem.* **1997,** *36*, 482-484.

(198)   Olmstead, M. M.; Power, P. P.; Sigel, G., *Inorg. Chem.* **1986,** *25*, 1027-1033.

(199)   Walling, C.; Bollyky, L., *JACS* **1964,** *86*, 3750-3752.

(200)   Berkessel, A.; Schubert, T. J. S.; Müller, T. N., *JACS* **2002,** *124*, 8693-8698.

(201)   Bäckvall, J.-E., *J. Organomet. Chem.* **2002,** *652*, 105-111.

(202)   Yamakawa, M.; Ito, H.; Noyori, R., *JACS* **2000,** *122*, 1466-1478.

(203)   Hartmann, R.; Chen, P., *Angew. Chem.* **2001,** *113*, 3693-3697.

(204)   Carey, F. A.; Sundberg, R. J., Advanced Organic Chemistry. In *Part B: Reactions and Synthesis* [Online] Springer US: **2007**.

(205)   Dyson, P. J.; Jessop, P. G., *Catal. Sci. Technol.* **2016,** *6*, 3302-3316.

(206)   Barham, J. P.; Coulthard, G.; Emery, K. J.; Doni, E.; Cumine, F.; Nocera, G.; John, M. P.; Berlouis, L. E.; McGuire, T.; Tuttle, T.; Murphy, J. A., *J. Am. Chem. Soc.* **2016,** *138*, 7402-7410.

(207)   Mohamed, R. K.; Byers, P. M.; Alabugin, I. V., Radical Reactions. In *Encyclopedia of Physical Organic Chemistry*, John Wiley & Sons, Inc.: **2016**.

(208)   Studer, A.; Curran, D. P., *Angew. Chem. Int. Ed.* **2016,** *55*, 58-102.

(209)   Sanderson, J. J.; Hauser, C. R., *JACS* **1949,** *71*, 1595-1596.

(210)   Physical Properties of Polymers Handbook. Mark, J. E., Ed. Springer-Verlag New York: New York, **2007**.

(211)   Widegren, J. A.; Bennett, M. A.; Finke, R. G., *J. Am. Chem. Soc.* **2003,** *125*, 10301-10.

(212)   Weddle, K. S.; Aiken, J. D.; Finke, R. G., *JACS* **1998,** *120*, 5653-5666.

(213)   Williams, D. B.; Lawton, M., *JOC* **2010,** *75*, 8351-8354.

(214)   Rouquerol, J.; Avnir, D.; Fairbridge, C. W.; Everett, D. H.; Haynes, J. M.; Pernicone, N.; Ramsay, J. D. F.; Sing, K. S. W.; Unger, K. K. *Recommendations for the characterization of porous solids (Technical Report)*; 1365-3075

0033-4545; **1994**.

(215)   Rouquerol, J.; Avnir, D.; Fairbridge, C. W.; Everett, D. H.; Haynes, J. M.; Pernicone, N.; Ramsay, J. D. F.; Sing, K. S. W.; Unger, K. K., *Pure Appl. Chem.* **1994,** *66*.

(216)   Aldrich, S. Molecular Sieves - Technical Information Bulletin. http://www.sigmaaldrich.com/chemistry/chemical-synthesis/learning-center/technical-bulletins/al-1430/molecular-sieves.html (accessed 2017.06.10).

(217)   Pujadó, P. R.; Rabó, J. A.; Antos, G. J.; Gembicki, S. A., *Catal. Today* **1992,** *13*, 113-141.

(218)   Gao, Y.; Klunder, J. M.; Hanson, R. M.; Masamune, H.; Ko, S. Y.; Sharpless, K. B., *JACS* **1987,** *109*, 5765-5780.

(219)   Thomas, J. M.; Raja, R.; Sankar, G.; Bell, R. G., *Acc. Chem. Res.* **2001,** *34*, 191-200.

(220)   Demel, J.; Sujandi; Park, S.-E.; Čejka, J.; Štěpnička, P., *J. Mol. Catal. A: Chem.* **2009,** *302*, 28-35.

(221)   Grunewald, G. C.; Drago, R. S., *JACS* **1991,** *113*, 1636-1639.

(222)   Odom, J. D.; Barnes, J. A.; Hudgens, B. A.; Durig, J. R., *J. Phys. Chem.* **1974,** *78*, 1503-1509.

(223)   Staubitz, A.; Robertson, A. P.; Manners, I., *Chem. Rev.* **2010,** *110*, 4079-4124.

(224)   Ignatyev, I. S.; Partal, F.; Lopez Gonzalez, J. J.; Sundius, T., *Spectrochim Acta A Mol Biomol Spectrosc* **2004,** *60*, 1169-78.

(225)   Reisz, J. A.; Klorig, E. B.; Wright, M. W.; King, S. B., *Org. Lett.* **2009,** *11*, 2719-2721.

(226)   Brown, O., University of Alberta, Edmonton, Unpublished Work, 2016.

(227)   Kaesz, H. D.; Saillant, R. B., *Chem. Rev.* **1972,** *72*, 231-281.

(228)   Muetterties, E. L.; Rakowski, M. C.; Hirsekorn, F. J.; Larson, W. D.; Basus, V. J.; Anet, F. A. L., *JACS* **1975,** *97*, 1266-1267.

(229)   Muetterties, E. L.; Hirsekorn, F. J., *JACS* **1974,** *96*, 4063-4064.

(230)   Bleeke, J. R.; Muetterties, E. L., *JACS* **1981,** *103*, 556-564.

(231)   Muetterties, E. L.; Bleeke, J. R., *Acc. Chem. Res.* **1979,** *12*, 324-331.

(232)   Stuhl, L. S.; Rakowski DuBois, M.; Hirsekorn, F. J.; Bleeke, J. R.; Stevens, A. E.; Muetterties, E. L., *JACS* **1978,** *100*, 2405-2410.

(233)   Rakowski, M. C.; Hirsekorn, F. J.; Stuhl, L. S.; Muetterties, E. L., *Inorg. Chem.* **1976,** *15*, 2379-2382.

Appendix

Appendix 1. Additional characterization data

Appendix A1.1 Signer molecular weight calculation for [Co(NPPh$_3$)(OSiMe$_3$)(THF)]$_2$ 37.

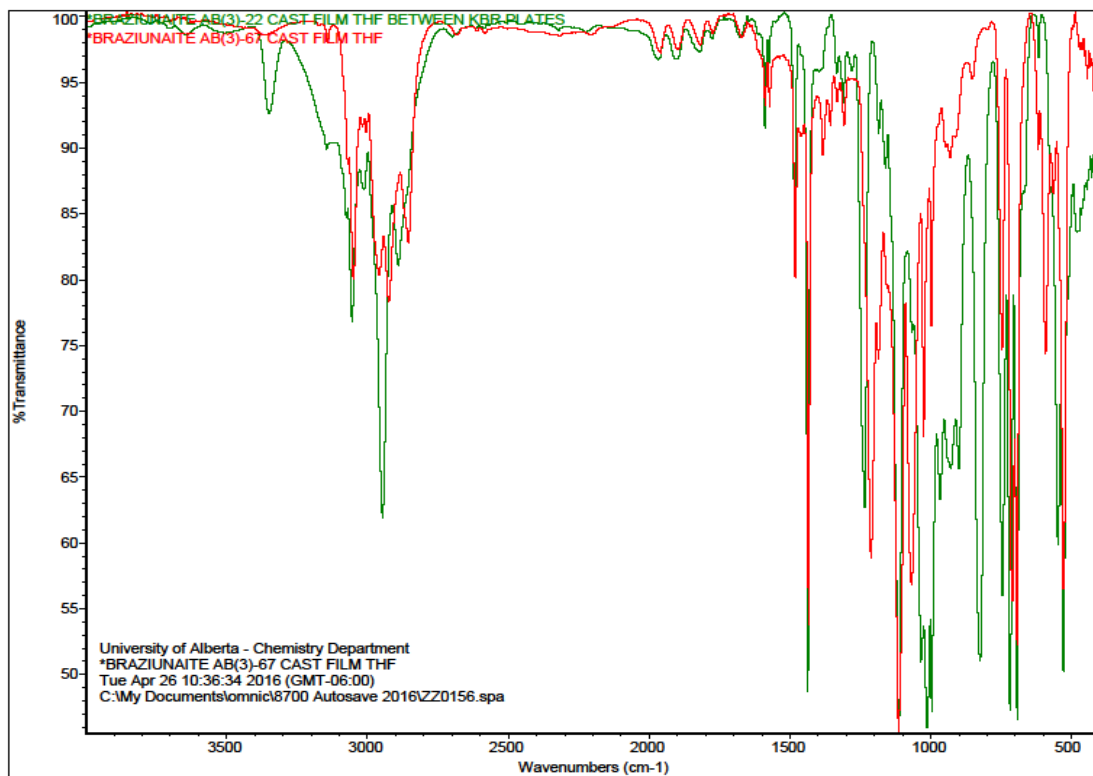Formula used for Signer method: $MW_1 = \frac{G_1 V_2 MW_2}{G_2 V_1}$

Data

Compound 1 ([Co(NPPh$_3$)(OSiMe$_3$)(THF)]$_x$ **37**): G_1 = 22.2 g, V_i (solution) = 2.30 mL, V_1 = 1.45 mL

Compound 2 (Ferrocene): G_2 = 22.2 g, V_i (solution) = 2.35 mL, V_2 = 3.10 mL, MW$_2$ = 186.04 g/mol

$$MW_1 = \frac{22.2\frac{g}{mol} \times 3.10\ mL \times 186.04\frac{g}{mol}}{22.2\frac{g}{mol} \times 1.45\ mL} = 397.75\frac{g}{mol}$$

Appendix A1.2 FT-IR overlay of [Co(NPPh$_3$)(OSiMe$_3$)(THF)]$_2$ 37 and [Co(NPPh$_3$)(O′Bu)(THF)]$_2$ 39.

Figure 1. FT-IR overlay spectrum of [Co(NPPh$_3$)(OSiMe$_3$)(THF)]$_2$ **37** (green) and [Co(NPPh$_3$)(O^{t}Bu)(THF)]$_2$ **39** (red).

Appendix A1.3 FT-IR spectrum of [Co(NP^{i}Pr$_3$)$_2$]$_3$ 40.
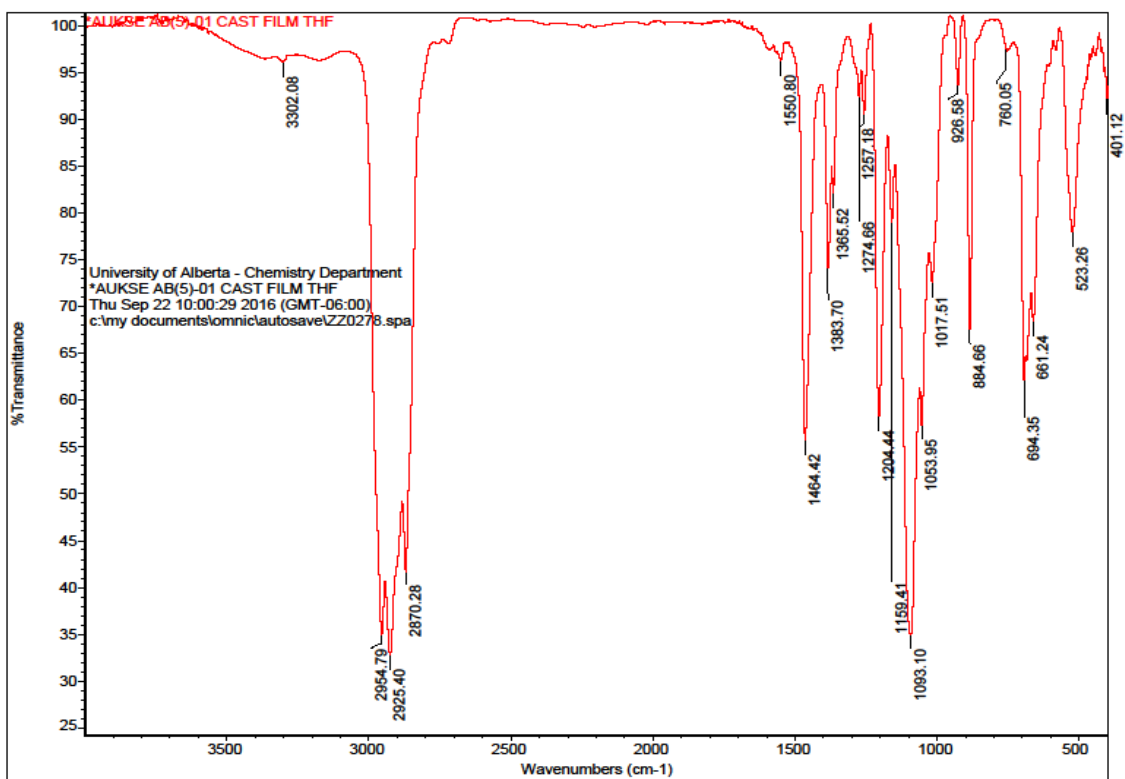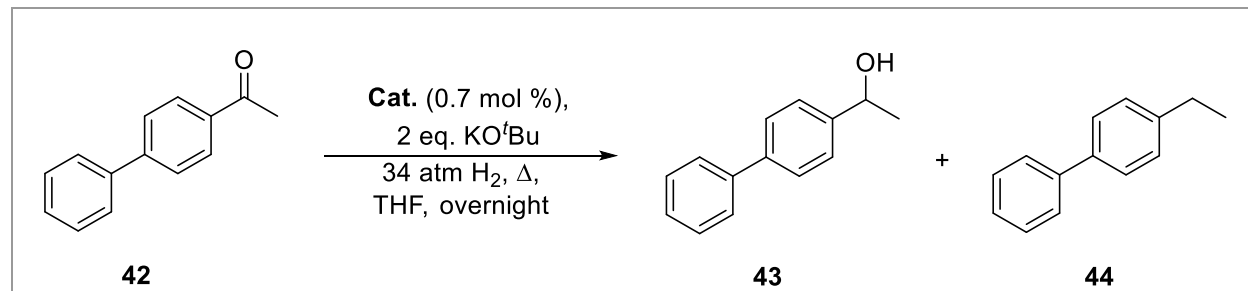
Figure 1. FT-IR spectrum of [Co(NP^{i}Pr$_3$)$_2$]$_3$ **40**.

**Appendix 2. Additional analysis data**

Appendix B1.1 Select GC-MS data

Table 1. Deoxygenation of 4-acetylbiphenyl **42** by precatalysts **37** and **39** in the absence of 9-BBN.

Entry	Catalyst	Conversion, [%]	Yield, [%]			
			43	**44**	**biphenyl 45**	**Dimerization products**
1	**39**	94	49	29	15	0
2	**37**	91	52	16	17	14

Appendix 3

Appendix C1.1 A representative ^{1}H NMR spectrum for the quantification of catalytic results.
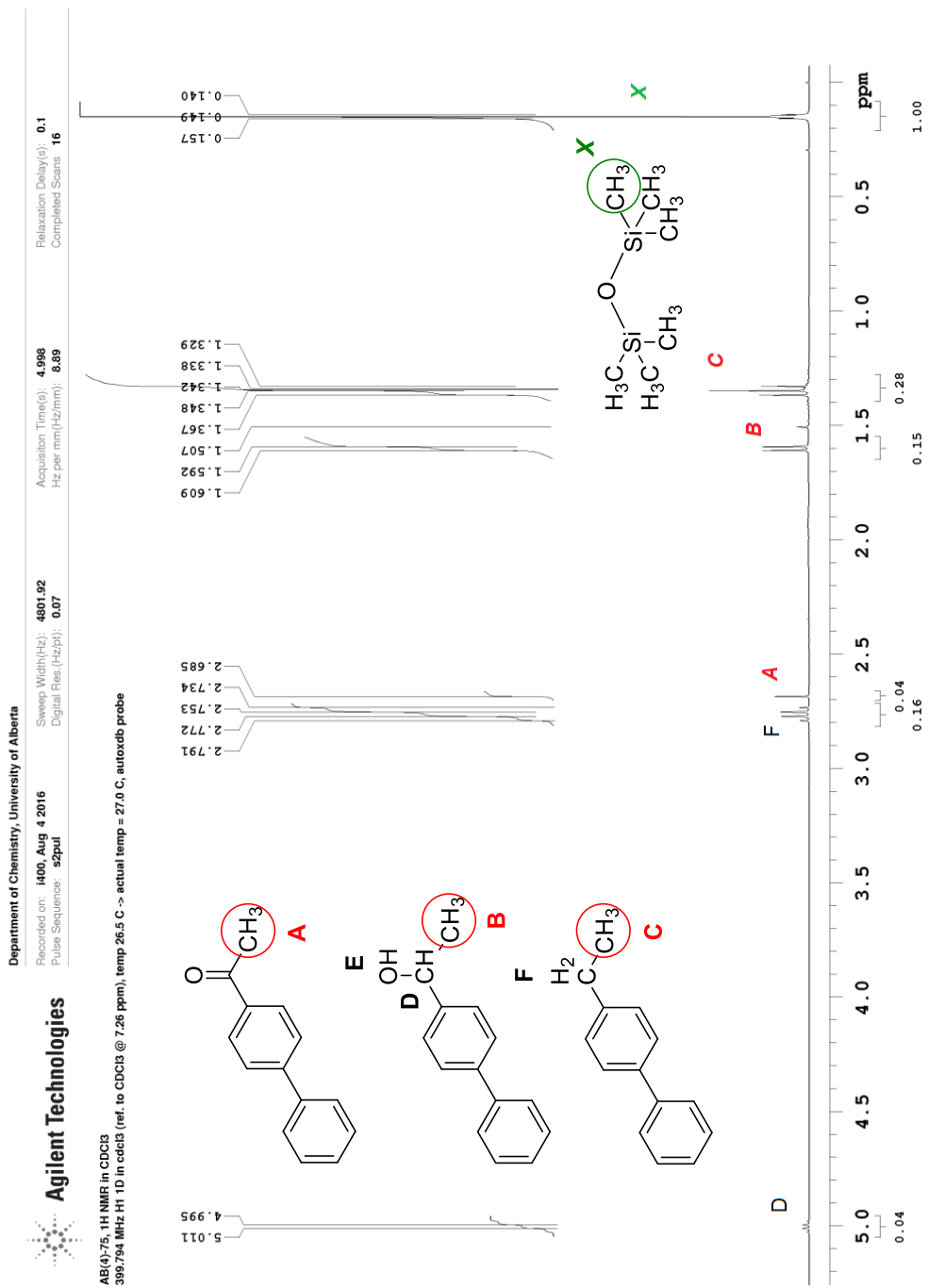
Figure 1. Representative 1H NMR spectrum of hydrodeoxygenation of 4-acetylbiphenyl by [Co]

catalysts.